Faculty Search Committee
Department of Neuroscience
Brown University

April 5, 2012

Dear Search Committee Members,

I am writing to apply for the tenure-track Assistant Professor position in Computational Neuroscience in the Department of Neuroscience at Brown University. My research interests include computational, neurophysiologic, and optogenetic approaches to the study of brain function which will qualify me to play an active role in the Interdepartmental Brown Institute for Brain Science. Enclosed please find my CV with a list of individuals who will recommend me, a summary of my research contributions, a description of my plans for future investigations, my teaching philosophy, and three selected reprints of my publications.

Over my scientific career, I have trained in medicine, psychology, neurophysiology, and systems neuroscience. A fundamental problem in Neuroscience is to understand the neuronal mechanisms of information representation in learning and memory. My long-term goal is to elucidate how neuronal ensemble activity during resting and sleep interacts with activity induced by external stimuli to encode new experience and support animal learning. Toward this end, my recent work in the hippocampus revealed that temporal firing sequences reflecting a new place cell order expressed during a novel spatial experience exist during the rest and sleep periods preceding the novel experience, even in animals that had no prior experience on linear tracks. I call these internally generated temporal sequences 'preplay'.

As an independent researcher, I intend to set up a laboratory that will benefit from the use of a combination of techniques, including: high-density tetrode electrophysiological recordings of neuronal ensembles in freely behaving rodents, computational methods of decoding spatial trajectories from the brain activity, genetic dissection of neuronal circuits with implications for models of brain disease, and optogenetic stimulation of different classes of neurons.

My research renews my personal enthusiasm for neuroscience, which in turn inspires my teaching. Teaching and mentoring students will be an important part of my career and I am committed to sharing my passion for science and research with my students and the intellectual community I participate in.

I look forward to exploring the exciting possibility of becoming a member of your department's research and teaching team. Please let me know if you require additional information and thank you for your consideration.

Yours sincerely,

George Dragoi, M.D., Ph.D.
Research Scientist
The Picower Institute for Learning and Memory at MIT
Tel.: (617) 324-3930
Email: gdragoi@mit.edu

CURRICULUM VITAE

GEORGE DRAGOI, MD, PhD
The Picower Institute for Learning and Memory
Massachusetts Institute of Technology
43 Vassar Street
Cambridge, MA 02139
Tel: (617) 324-3930
Email: gdragoi@mit.edu

Education

09/1996-04/2002	**Ph.D.** in **Neuroscience**, Rutgers University, Newark, NJ. Laboratory of Gyorgy Buzsaki. **Ph.D. Thesis**: Plasticity and neural coding in the hippocampus.
10/1990-06/1995	**B.A.** in **Psychology and Special Education**, Al. I. Cuza University of Iasi, Romania. GPA 9.6/10. **B.A. Thesis**: Influence of Psychological State on Immune Parameters.
09/1988-09/1994	**M.D.**, Gr. T. Popa University of Medicine & Pharmacy, Iasi, Romania. GPA 9.8/10. **M.D. Thesis**: Immunomodulatory Activity of a Sulphonamidic Derivative.

Professional Appointments

05/2010-present	**Research scientist**, Picower Institute for Learning and Memory, MIT. Laboratory of Susumu Tonegawa.
09/2003-04/2010	**Postdoctoral associate**, Picower Institute for Learning and Memory, MIT. Laboratory of Susumu Tonegawa.
05/2002-08/2003	**Postdoctoral fellow**, Rutgers University, Newark, NJ. Laboratory of Gyorgy Buzsaki.
01/1995-08/1996	**Resident Physician**, Sf. Spiridon University Hospital, Iasi, Romania

Summer Courses

2001	Workshop on Analysis of Neural Data, Marine Biological Laboratory, Woods Hole, MA
1999	Cold Spring Harbor Laboratory Spring Course: The Biology of Memory, Cold Spring Harbor, NY
1994	Human Memory (W. Hirst, New School for Social Research, NY)
1994	First International Summer Institute in Cognitive Science, Buffalo, NY

Awards

2002	FENS Forum Scholarship, Paris

2001	First Prize, INS Student and Postdoctoral Symposium, Rutgers University
2001	Workshop on Analysis of Neural Data Scholarship, MBL
1999	Rutgers University Graduate School Dean's Office Travel Fund
1999	Cold Spring Harbor Laboratory Spring Course Scholarship
1996-2002	Graduate Assistantship, Rutgers University
1996	Johnson and Johnson Excellence Fellowship
1996	Soros Foundation Travel Grant
1994	McDonnell-Douglas Travel Grant
1994	Institute for Cognitive Sciences Scholarship, FISI, Buffalo, NY
1992-1994	Student Honor Fellowship, Medical School

Publications

Peer Reviewed Journal Articles

Dragoi G, Tonegawa S (**in preparation**) Internal development of novel spatial representations.

Dragoi G, Tonegawa S (2011) Preplay of future place cell sequences by hippocampal cellular assemblies. **Nature.** 469:397-401.

Dragoi G, Buzsaki G (2006) Temporal encoding of place sequences by hippocampal cell assemblies**. Neuron.** 50:145-57 (featured on the **cover** of the magazine).

Dragoi G, Harris KD, Buzsaki G (2003) Place representation within hippocampal networks is modified by long-term potentiation. **Neuron.** 39:843-53.

Harris KD, Csicsvari J, Hirase H, **Dragoi G**, Buzsaki G (2003) Organization of cell assemblies in the hippocampus. **Nature.** 424:552-6.

Buzsaki G, Harris K.D., Henze D.A., Hirase H., Leinekugel X., **Dragoi G**., Czurko A. (2002) Conversion of firing rate to timing in the hippocampus. **J. Physiol** *(London).* 544:15S.

Buzsaki G, Csicsvari J, **Dragoi G**, Harris KD, Henze D, Hirase H (2002) Homeostatic maintenance of neuronal excitability by burst discharges in vivo. **Cereb Cortex.** 12:893-899.

Harris KD, Henze DA, Hirase H, Leinekugel X, **Dragoi G**, Czurko A, Buzsaki G (2002) Spike train dynamics predicts theta-related phase precession in hippocampal pyramidal cells. **Nature.** 417:738-741.

Marshall L, Henze DA, Hirase H, Leinekugel X, **Dragoi G** and Buzsaki G (2002) Hippocampal pyramidal cell-interneuron spike transmission is frequency dependent and responsible for place modulation of interneuron discharge. **J Neurosci.** 22RC197:1-5.

Dragoi G, Carpi D, Recce M, Csicsvari J and Buzsaki G (1999) Interactions between Hippocampus and Medial Septum during Sharp Waves and Theta Oscillation in the Behaving Rat. **J Neurosci.** 19:6191-6199.

Book Chapters

Dragoi G (2012) Electrophysiological approaches for studying neuronal circuits in vivo. In: **Neuronal Network Analysis** (T Fellin and M Halassa, eds). Springer.

Buzsaki G, Carpi D, Csicsvari J, **Dragoi G**, Harris KD, Henze D, Hirase H (2003) Maintenance and modification of firing rates and sequences in the hippocampus: does sleep play a role? In: **Sleep and Brain Plasticity** (P Maquet, C Smith, R Stickgold, eds). Oxford University Press.

Buzsaki G, **Dragoi G**, Csicsvari J, Hirase H, Czurko A and Henze D (2000) GABAergic Interneuronal Networks in the Hippocampus. In: **GABA in the Nervous System** (DL Martin and RW Olsen, eds). Lippincott Williams & Wilkins. 317-336.

Abstracts and Scientific Meetings

Dragoi G and Tonegawa S (2011) Internal development of novel spatial representations. Program No. 539 ***(slide presentation)***. **2011 Neuroscience Meeting Planner.** Washington, DC: Society for Neuroscience, 2011. Online.

Dragoi G and Tonegawa S (2010) Preplay and CA3 NMDAR-mediated plasticity facilitate rapid encoding in the hippocampus. Program No. 635.9 ***(slide presentation)***. **2010 Neuroscience Meeting Planner.** San Diego, CA: Society for Neuroscience, 2010. Online.

Dragoi G and Tonegawa S (2010) Preplay of future place cell sequences by hippocampal cellular assemblies. **FENS Abstract** F119, Amsterdam.

Dragoi G and Tonegawa S (2009) Temporal preplay of place sequences is associated with rapid encoding of novel information. Program No. 95.4. **2009 Neuroscience Meeting Planner.** Chicago, IL: Society for Neuroscience, 2009. Online.

Dragoi G, Wilson MA, Tonegawa S (2008) Blockade of CA3 NMDA receptors reveals differential hippocampal responses to degrees of novelty. Program No. 219.5 ***(slide presentation)***. **2008 Neuroscience Meeting Planner.** Washington, DC: Society for Neuroscience, 2008. Online.

Dragoi G, Wilson MA, Tonegawa S (2007) Impaired place field formation and high-frequency oscillations in the hippocampus of CA3 NMDA receptor-deficient mice. Program No. 640.16. **2007 Neuroscience Meeting Planner.** San Diego, CA: Society for Neuroscience, 2007. Online.

Dragoi G, Buzsaki G (2005) Episodic encoding of place sequences by hippocampal cell assemblies. Program No. 813.8 ***(slide presentation)***. **2005 Abstract Viewer/Itinerary Planner.** Washington, DC: Society for Neuroscience, 2005. Online.

Dragoi G, Buzsaki G (2005) Episodic encoding of place sequences by hippocampal cell assemblies. **Gordon Conference on Neural Circuits and Plasticity**, Salve Regina University.

Dragoi G, Buzsaki G (2003) "Representation" of space within hippocampal networks. Program No. 806.1. **2003 Abstract Viewer/Itinerary Planner.** Washington, DC: Society for Neuroscience, 2003. Online.

Dragoi G and Buzsaki G (2002) State- and pathway-dependent changes in the firing rate of hippocampal neurons in response to LTP. Program No. 577.3. **2002 Abstract Viewer/Itinerary Planner.** Washington, DC: Society for Neuroscience. Online.

Harris KD, Henze DA, Hirase H, Leinekugel X, **Dragoi G**, Czurko A, Buzsaki G (2002) Information coding by firing rate and spike timing in hippocampal pyramidal cells. Program No. 577.4. **2002 Abstract Viewer/Itinerary Planner.** Washington, DC: Society for Neuroscience. Online.

Dragoi G, Harris KD, Buzsaki G (2002) Stability of hippocampal place fields can be perturbed by LTP and epilepsy. **FENS Abstract** p260, Paris.

Dragoi G and Buzsaki G (2001) The influence of long term potentiation on the stability of hippocampal place fields. **Soc.Neurosci.Abstr.** 537.5.

Dragoi G, Hirase H and Buzsaki G (2000) Changes in spontaneous discharge rates of hippocampal neurons by LTP and LTD. **Soc.Neurosci.Abstr.** 69.14.

Dragoi G, Carpi D, Recce M, Csicsvari J, Buzsaki G (1999) Differential Regulation of Medial Septum Unit Activity by the Hippocampal Output during Sharp Waves and Theta in Freely-Moving Rat. **Soc.Neurosci.Abstr.** 561.12.

Csicsvari J, **Dragoi G**, Mamyia A, Hirase H, Czurko A, Buzsaki G (1999) Fast network oscillatory patterns in the CA1 region of the hippocampus in freely moving rats. ***Soc.Neurosci.Abstr*.** 561.13.

Carpi D, **Dragoi G**, Benuck M, Buzsaki G (1997) Neural Activity of Lateral Septum During Hippocampal Theta and Sharp Waves in the Behaving Rat. **Soc.Neurosci.Abstr.** 485.

Invited Talks

Internal representation of spatial information by hippocampal cellular assemblies (2012) Feinberg School of Medicine, Northwestern University, Chicago, IL

Internal representation of spatial environment by hippocampal cellular assemblies (2012) Psychology Department, Berkeley University, Berkeley, CA

Internal representation of spatial environment by hippocampal cellular assemblies (2012) Graduate School of Medicine, Kyoto University, Kyoto, Japan

Internal representation of sequential information by hippocampal cellular assemblies (2012) RIKEN Brain Science Institute, Wako, Japan

Preplay of future place cell sequences by hippocampal cellular assemblies (2012) The 12th Winter Workshop on Mechanism of Brain and Mind, Rusutsu, Japan

Preplay of future spatial sequences by hippocampal cellular assemblies. (2011) Neuroscience Department, Tufts University, Boston, MA

Preplay of future spatial sequences by hippocampal cellular assemblies. (2010) Institut d'Investigacions Biomèdiques and IDIBAPS-Hospital Clinic, Barcelona, Spain.

Preplay of future place cell sequences by hippocampal cellular assemblies. (2010) Volen Center for Complex Systems, Brandeis University, Waltham, MA.

Preplay of novel place sequences by hippocampal cellular assemblies. (2009) CMBN, Rutgers University, Newark, NJ.

Temporal preplay of novel place sequences by hippocampal cellular assemblies. (2009) Seminar series, Center for Molecular Neurobiology and University Medical Center Hamburg-Eppendorf, ZMNH, Hamburg, Germany.

Oscillatory binding of place sequences by hippocampal cell assemblies. (2007) Hippocampal and entorhinal plasticity, coding and computation workshop. COSYNE, Salt Lake City, UT.

Place representation within hippocampal networks is modified by LTP. (2003) Learning and Memory Meeting. Cold Spring Harbor Laboratories, Cold Spring Harbor, NY.

Teaching Experience

Spring 1997	Teaching Assistant, Cognitive Psychology (Undergraduate Course), Department of Psychology, Rutgers University, Newark, NJ
Fall 1997	Teaching Assistant, Molecular Biology (Undergraduate Course), Department of Biology, Rutgers University, Newark, NJ
Spring 1998	Teaching Assistant, Foundations of Neuroscience (Graduate Course), Department of Neuroscience, Rutgers University, Newark, NJ

Referee for the following Journals

European Journal of Neuroscience
Hippocampus
Journal of Neuroscience
Learning and Memory
Neuron
Trends in Neuroscience

Scientific Membership and Service

1996 - present	Society for Neuroscience
1999 - 2002	NY/NJ Hippocampus Club Coordinator. Rockefeller University, NY.

Selected Media Coverage

The "preplay" button. Preplay, navigate, replay – how the brain gets us from A to B. (December 2010) **Nature** podcast (http://www.nature.com/neurosci/neuropod/index-2010-12-23.html).

Preplay of future place cell sequences by hippocampal cellular assemblies. (Winter/Spring 2011, Vol. 5 No. 1) **Neuroscience News.** The Picower Institute for Learning and Memory at MIT.

Encoding unchartered territory. Ensembles of neurons in the brain's hippocampus inform about future as well as past experiences. (March 25 2011) **RIKEN Research: Biology.**

References

György Buzsáki, M.D., Ph.D.
Board of Governors Professor
Center for Molecular and Behavioral Neuroscience
Rutgers University
197 University Avenue
Newark, NJ 07102
Tel: (973) 353-1080 ext. 3638
Fax: (973) 353-1820
E-mail: buzsaki@axon.rutgers.edu

Susumu Tonegawa, Ph.D.
Picower Professor of Biology
Picower Institute for Learning and Memory
Departments of Brain and Cognitive Sciences, and Biology
Massachusetts Institute of Technology
Building 46 Room 5285
43 Vassar Street
Cambridge, MA 02139
Tel: (617) 253-6459
Email: tonegawa@mit.edu

Edvard I. Moser, Ph.D.
Kavli Institute for Systems Neuroscience
Olav Kyrres gate 9
Centre for Biology of Memory, NTNU
NO-7489 Trondheim
Norway
Tel: 47 47-73-59-82
Fax: 47 47-73-59-82
Email: edvard.moser@ntnu.no

STATEMENT OF RESEARCH INTERESTS

My long-standing scientific interest is in deciphering the neuronal mechanisms of information representation during spatial learning and episodic memory formation in hippocampal-neocortical networks. It is increasingly realized that novel information is not encoded and consolidated in isolation, but is rather integrated within a distributed cortical network of related pre-existing knowledge. Whereas the neuronal response to a novel experience can be determined 'online' during the external stimuli exposure, pre-existing network activity and its changes induced by novel experience can be assessed 'offline' during task-free default network states, such as resting and sleep. My goal is to understand at the neuronal ensemble level how network activity during resting and sleep interacts with activity induced by novel external stimuli across different brain states and regions to encode and consolidate new experiences and support animal learning. To attain this goal, I intend to set up a laboratory that will benefit from the use of a combination of techniques: high-density large-scale tetrode electrophysiological recordings in freely behaving mice and rats, optogenetic stimulation of specific classes of neurons, brain region restricted transgenic animals, injection of neural tracers and viral vectors, immunohistochemistry and microscopy, animal behavior analysis, and advanced data analysis methods. Accomplishing my goal will have significant implications for the understanding of brain function in both normal states and in neuropsychiatric diseases such as schizophrenia, autism, and Alzheimer's.

I. Summary of Past and Current Achievements

PhD research. The first aim of my doctoral research in the laboratory of Dr. Gyorgy Buzsaki at Rutgers University was to understand the interaction between the hippocampus and medial septum during network activity associated with encoding and memory consolidation. Using simultaneous recording of single units and local field potential from three brain areas in the rat (hippocampus CA1, medial, and lateral septum), I found that the hippocampus-medial septum interaction is state-dependent: excitatory during encoding of new experiences, when the medial septum imposes theta oscillation onto the hippocampus; and inhibitory during high-frequency ripple oscillations associated with hippocampal-neocortical transfer and memory consolidation, when the hippocampus inhibits the medial septum (Dragoi, Carpi, Recce, Csicsvari, and Buzsaki, J.Neurosci., 1999).

After the completion of this study, I became interested in the high-density tetrode recording technique that I applied together with electrical stimulation to simultaneously record and manipulate large ensembles of neurons across different hippocampal sub-regions in freely behaving rats. I found that after stimulation-induced long-term potentiation (LTP) of synaptic transmission within the hippocampal network, new internal representations of familiar spatial environments emerge in the hippocampus due to the re-organization of neurons into different cellular assemblies. This indicates a sufficient role for synaptic plasticity within the hippocampal network in forming a stable internal representation of a spatial environment (Dragoi, Harris, and Buzsaki, Neuron, 2003; reviewed by Nathe and Frank, Neuron, 2003 and Moser, Faculty of 1000 Biology, 2003). My interest in temporal coding of spatial information, organization of neurons in cellular assemblies, and pyramidal cell-interneuron interaction fueled several successful collaborations during my doctoral studies (Harris, Henze, Hirase, Leinekugel, Dragoi, Czurko, and Buzsaki, Nature, 2002; Harris, Csicsvari, Hirase, Dragoi, and Buzsaki, Nature, 2003; Marshall, Henze, Hirase, Leinekugel, Dragoi, and Buzsaki, J.Neurosci., 2002).

Postdoctoral research. Toward the end of my PhD training, I realized that in order to pursue my full set of research interests I needed to train in using more specific ways to manipulate neuronal networks in behaving animals. Impressed by the growing success of brain region-specific knock-out technology at the time, I joined the laboratory of Dr. Susumu Tonegawa at MIT for my postdoctoral research. In parallel with designing and conducting new experiments involving high-density large-scale tetrode recordings in transgenic mice, I continued to explore the principles by which spatial information is encoded by hippocampal cellular assemblies in the rat. I found that the overall spatial information encoded by neurons grouped in cellular assemblies exceeds the information encoded by groups of multiple independent neurons. I proposed that chaining of hippocampal place cells into coordinated sequential cell assemblies during theta oscillations underlies the linking of individual chunks of spatial information into larger representations (Dragoi and Buzsaki, Neuron, 2006, cover article; reviewed by Suzuki, Neuron, 2006 and Moser, Faculty of 1000 Biology, 2006). These findings raised questions of whether and how the organization of

neurons into cellular assemblies develops during encoding of novel experiences. I found that temporal firing sequences reflecting the new place cell order corresponding to a novel spatial experience pre-exist during the rest and sleep periods preceding the novel experience, even in mice that had no prior experience on linear tracks. I call these internally generated temporal sequences 'preplay'. These results indicate that internal neuronal dynamics during resting and sleep preconfigure the hippocampal cellular assemblies into temporal sequences that contribute to the encoding of a related novel experience occurring in the future (Dragoi and Tonegawa, Nature, 2011; reviewed by Moser and Moser, Nature, 2011; Wolfer, Faculty of 1000 Neuroscience, 2011; Allen and Stark, Faculty of 1000 Neuroscience, 2011).

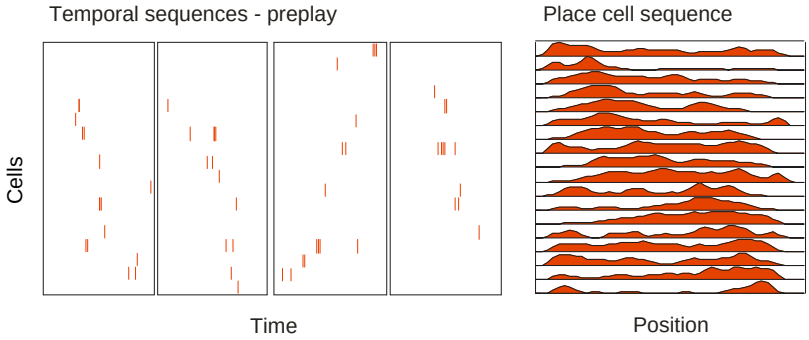

Preplay. Temporal sequences of firing recorded during sleep (left) correspond closely to novel place cell firing sequences observed when naïve mice subsequently explore a new environment (right).

This demonstration of temporal preplay of novel spatial sequences challenges a long-standing dogma in neuroscience stating that novel place cell sequences are formed in the hippocampus in response to a novel experience and are only subsequently replayed to enable memory consolidation. It also represents the first proof that neurons organize in temporal and place cell sequences in the mouse brain, and opens up possibilities for studies of temporal coding and cell assembly organization in the normal mouse, as well as in a variety of mouse models of neuropsychiatric disease.
To expand my previous findings on the effect of induction of LTP of the CA3-CA1 synaptic transmission on the neuronal ensemble organization in CA1, I investigated the effect of blocking CA3 NMDAR-dependent plasticity on the dynamics of learning-induced neuronal ensemble organization in the downstream CA1 area. I found that novel representations of first-time spatial experiences are formed in the CA1 area within the framework of the preconfigured hippocampal network, which is partially reorganized during the experience and stabilized primarily via CA3 NMDAR-dependent plasticity. Furthermore, the internal repertoire of the reorganized network rapidly assimilates a related novel experience independent of CA3 NMDAR, in what may represent a neuronal correlate of schema-based accelerated learning (Dragoi and Tonegawa, in preparation).

II. Future Research Plan

In my own laboratory, I will investigate the mechanisms by which coordinated neuronal ensemble activity during resting and sleep develops and further interacts with experience-induced activity to support the formation and consolidation of novel representations and guide animal behavior. Despite the fact that most of an animal's life and consequently most of the brain's energy is spent during network states associated with resting and sleep, the function of these states and their interplay with experience-induced brain activity in supporting animal cognition and behavior is not clearly understood. Previous electrophysiological studies in the hippocampus have assumed that neuronal activity during resting and sleep is devoted to the replay of recent experience to promote spatial navigation ability and memory consolidation. However, this tenet is challenged by my recent demonstration of temporal preplay of future spatial sequences in the hippocampus. While preplay is a fascinating phenomenon, additional work is needed to understand its full meaning in the context of other known network phenomena as well as its function in animal cognition and behavior. I will explore these topics using high-density tetrode electrophysiological recordings of single units and local field potentials from the CA1 area of the hippocampus and associated brain regions in freely behaving mice and rats. In addition, I will use a variety of silicon probes with known geometry of the recording sites (Neuronexus Technology) to localize neurons within the cellular layers and to compute the laminar profile of their synaptic inputs, combined with wireless recording technology (Triangle Biosystems) to allow for more natural, unconstrained animal behavior during recording. To explore the circuit mechanisms determining neuronal ensemble dynamics, I will experimentally manipulate network activity by stimulating or inhibiting specific neuronal classes

using optogenetic tools. I will use region-restricted transgenic mice to investigate the contribution of specific input pathways to the dynamics of neuronal ensemble activity in the hippocampus. My specific aims are as follows:

1. To examine how a complex novel spatial experience changes the structure and dynamics of network activity during resting and sleep. I will examine changes in network activity during resting and sleep states (both REM and slow-wave sleep) resulting from novel spatial experience by comparing the structure and dynamics of temporal sequence activity before (i.e., preplay) and after (i.e., replay) the novel experience. Previously, I have shown that temporal sequences that correlate with a simple novel spatial experience (i.e., a relatively short one-dimensional linear track) exist both before and after the particular experience. I now aim to investigate specific changes induced by a complex novel spatial experience, where complexity is created either by unpredictable geometry or by the introduction of bifurcation/decision points. My preliminary results indicate that the rat hippocampal network exhibits preplay of future place cell sequences under these circumstances. I will investigate whether the complex novel experience is: (i) selecting from a putative repertoire of pre-existing complex temporal sequences, (ii) linking together chunks of simpler pre-existing temporal sequences, (iii) increasing the specificity of pre-existing temporal sequences, and/or (iv) synchronizing pre-existing temporal sequences across associated brain regions.

2. To examine the factors, mechanisms, and neuronal circuits involved in the expression of preconfigured hippocampal network activity during resting and sleep. Towards this aim I will investigate: (i) whether the preconfigured hippocampal network results from stochastic ongoing internal cellular assembly dynamics, or instead, reflects current context-dependent external stimuli; (ii) whether and to what extent the preconfigured hippocampal network seen in adults is innate or experience-based; (iii) the effect that optogenetic interventions on different classes of excitatory or inhibitory neurons have on the dynamics of temporal sequence activity; and (iv) the effect of genetic dissection of specific neuronal circuits projecting to CA1 (e.g., from CA3) on the dynamics of temporal sequence activity. My preliminary results indicate that genetic blockade of NMDAR-dependent plasticity in the CA3 area in the mouse does not abolish the preplay and replay of novel place sequences, but rather affects experience-induced dynamics in the correlation between temporal and spatial sequences of place cells.

3. To examine whether and how network activity during resting and sleep influences the encoding of a novel experience. I will investigate: (i) whether and how network activity during resting and sleep prior to a new task influences the dynamics of encoding at both the single cell and neuronal ensemble level in naïve and experienced animals, and (ii) whether and how network activity during resting and sleep after initial exposure to a new task influences the dynamics of encoding in subsequent exposures to the same task or to related new ones. My preliminary results indicate that post-exposure resting and sleep improve single cell spatial tuning and cell assembly coordination in subsequent exposures to same task, and that this effect is transferred to the encoding of novel, related tasks.

4. To examine whether behavioral performance correlates with changes in network activity during resting and sleep and during task execution. I will investigate the network mechanisms underlying improved behavioral performance resulting from: (i) resting and sleep between trials, and (ii) prior experience with related tasks. Prior experience accelerates the acquisition of novel, related information through processes such as learning transfer and mental schema. I will use spatial behavioral tasks that require an intact hippocampus, such as radial mazes or flavor-place association. Following acquisition of the task, animals will be exposed to a related novel task. Rapid learning based on previous experience will be tested and neuronal activity during both first-time learning and related task learning will be assessed. I will investigate the existence of a correlation between a predictive/preplay signal at the neuronal level during resting and sleep and an increase in network and behavioral performance during the two learning conditions. Using optogenetic tools, I will transiently disrupt neuronal network activity at critical periods during the learning process to validate the proposed mechanisms. Recordings and interventions will be performed in the hippocampus and prefrontal cortex, which have been previously shown to be involved in schema-based learning.

TEACHING STATEMENT

As a teacher, my main goal is to encourage students to become independent thinkers, capable of approaching and solving problems on their own. I want to educate my students in the fundamentals of neurobiological systems and their function, enabling them to build from this foundation of knowledge even after they leave my classroom. I believe that student participation is crucial for learning, and my classroom will be an engaging place where there is both discussion and lecture, and where students always feel free to ask questions as well as contribute their own ideas. I also want to give students insight into the extraordinary possibilities of present day research in neuroscience and the excitement of scientific discovery.

Some of my general teaching principles can be formulated as follows:

1. No matter how experienced a teacher is, every new class and every new student pose a challenge. There is always room for improvement and learning when striving for excellence in teaching.
2. A teacher has to appeal to different learning styles, offer a variety of instructional experiences, and give every student the opportunity to participate fully and actively in the learning process.
3. Being a successful teacher depends on creating a learning environment that fosters the exploration of ideas. A teacher should establish relationships in which students feel respected as well as challenged. Students should be encouraged to push themselves beyond their comfort level and leave every class feeling that they have successfully overcome a new challenge.
4. Though student satisfaction is important for learning, teaching should not become a popularity contest. A teacher is responsible to the intellectual community in general, and should resist pressure to lower academic standards.

As a teacher, I also aim to promote the communication of science across society, something crucial to the future of science. A better understanding of science across society is critical if we are to deliver on the extraordinary possibilities that the future holds for neuroscience research, including their medical and therapeutic implications.

I will prepare thoroughly for my classes, but remain open to improvising rather than delivering rigid lectures. I will open each session with a brief reminder of the previous session's material and an outline of the day's topic, and typically conclude with a summary of key points. I like to combine textbook-level material with recent examples from the research literature showing how new knowledge enters the field and what areas are currently being investigated. It is critical to ensure that student comprehension of basic principles is not compromised while trying to incorporate in-depth discussion of current research.

Hands-on research in the laboratory is crucial for a thorough understanding of science. Labs are a great opportunity to get students excited about research in neuroscience, often inspiring them to explore more and become involved in research.

My previous teaching experience consists of formal training toward my degree in Psychology and Special Education during college and of several Teaching Assistantships for undergraduate and graduate level courses during my PhD program. As part of my duties as a TA, I conducted seminars and occasionally lectures, administered and graded tests, and provided consultation hours to students. During my postdoctoral years I mentored one visiting PhD student and one prospective PhD student.

My teaching interests range from systems to cognitive neuroscience, including state-of-the-art techniques to investigate brain function *in vivo*. My background in medicine, psychology, and neuroscience also allows me to teach more integrative courses, such as Neural Basis of Learning and Memory and Foundations of Neuroscience. I look forward to the opportunity to educate students in a field I feel passionate about.

LETTER

doi:10.1038/nature09633

Preplay of future place cell sequences by hippocampal cellular assemblies

George Dragoi[1] & Susumu Tonegawa[1]

During spatial exploration, hippocampal neurons show a sequential firing pattern in which individual neurons fire specifically at particular locations along the animal's trajectory (place cells[1,2]). According to the dominant model of hippocampal cell assembly activity, place cell firing order is established for the first time during exploration, to encode the spatial experience, and is subsequently replayed during rest[3–6] or slow-wave sleep[7–10] for consolidation of the encoded experience[11,12]. Here we report that temporal sequences of firing of place cells expressed during a novel spatial experience occurred on a significant number of occasions during the resting or sleeping period preceding the experience. This phenomenon, which is called preplay, occurred in disjunction with sequences of replay of a familiar experience. These results suggest that internal neuronal dynamics during resting or sleep organize hippocampal cellular assemblies[13–15] into temporal sequences that contribute to the encoding of a related novel experience occurring in the future.

We recorded neuronal firing sequences from the CA1 area of the mouse hippocampus (Supplementary Fig. 1) during periods of awake rest (Fam-Rest) alternating with periods of running (Fam-Run) on a familiar track (Fam session; Supplementary Fig. 2a) that preceded the exploration of a novel linear arm in contiguity with the familiar track (Contig-Run on L-shaped track; Fig. 1, Supplementary Fig. 2a and Methods). All the place cells active on the novel arm during Contig-Run, whether previously silent[16] (19% in both directions and 31% in at least one direction; Methods and Supplementary Tables 1–3) or active during Fam-Run (subpanels a in Fig. 1), fired during Fam-Rest at the ends of the familiar track (range, 0.17–11.7 Hz; Supplementary Fig. 3) as part of a number of 'spiking events'. The spiking events were defined as epochs composed of multiple individual spikes from at least four different place cells active on the novel arm or familiar track, separated by less than 50 ms and flanked by at least 50 ms of silence[3,4]. More significantly, the temporal sequence in which the cells active on the novel arm fired during Fam-Rest (subpanels b in Fig. 1) was significantly correlated with the spatial sequence in which they fired later as place cells on the novel arm during Contig-Run (subpanels c in Fig. 1), despite being uncorrelated with their spatial sequence as place cells on the familiar track during Fam-Run. This is illustrated as place cell sequences during Contig-Run (subpanels c in Fig. 1) and Fam-Run (subpanels a in Fig. 1) compared with the firing sequences of these cells within individual spiking events observed during Fam-Rest (subpanels b in Fig. 1). We refer to this process as 'preplay' of place cell sequences because the temporal sequence of firing during Fam-Rest had occurred before the actual exploration of the novel arm in the subsequent Contig-Run and was not a replay of the place cell sequences from the previous Fam-Run.

To quantify the significance of preplay and to compare it with replay, we created place cell sequence templates according to the spatial order of the peak firing of place cells[3,4,10] on the novel arm during Contig-Run (novel arm templates; subpanels c in Fig. 1 and Methods) and on the familiar track during Fam-Run (familiar track templates) for each run direction. The spikes of all the place cells used to construct the two types of template that were emitted during Fam-Rest were sorted by time, and spiking events were determined as explained above (subpanels b in Fig. 1). For each spiking event, we calculated a rank-order correlation between the novel arm templates and the temporal sequence of firing of the corresponding cells in the spiking events during Fam-Rest. The event correlation was considered significant if it exceeded the 97.5th percentile of a distribution of correlations resulting from randomly shuffling the order of place cells in the novel arm templates 200 times ($P < 0.025$). Forward[4] and reverse[3,4] preplay refers to the cases in which the sequence of place cells during Contig-Run and the firing order of the corresponding cells in Fam-Rest were in the same and opposite directions, respectively. In 91% of the preplay cases, the spiking events were correlated with the novel arm template in one direction only. The distribution of event correlation values obtained using the original novel arm templates was significantly shifted towards higher positive or negative values in comparison with the distribution of correlation values obtained using shuffled templates (Fig. 2a and Supplementary Fig. 4). Figure 2a also shows the distribution of significant preplay events (in red). Of all the spiking events detected as above and in which at least four novel arm place cells were active, 14.2% were significant preplay events for the place cell sequence on the novel arm ($P < 10^{-32}$, binomial probability test[4]) in the forward or reverse order (Fig. 2b).

The occurrence of significant preplay events was correlated with the occurrence of high-frequency ripple oscillations in CA1 (Fig. 2c). The majority of the significant preplay events (81.1%; Fig. 2d, total, blue) took place at the junction between the familiar and novel arms, and the remaining 18.9% took place at the free end of the familiar track (Fig. 2d, total, purple). The proportion of significant preplay events among the total events at each of the two track ends was higher at the junctional end (15.2%, $P < 10^{-26}$) than at the free end (8.5%, $P < 10^{-4}$) of the familiar track ($P < 0.035$, Z-test; Fig. 2d, normalized).

We found a relatively high correlation between the place field maps (Fig. 1A, B and Supplementary Fig. 5) of the familiar track before and after the novel experience (median $r = 0.66$; Fig. 2e, familiar track, blue); it was significantly higher than the correlations obtained when the cell identities were shuffled (median $r = 0.23$, $P < 10^{-4}$; Fig. 2e, familiar track, black). A similar correlation analysis showed a relatively high stability of the newly formed place fields on the novel arm from the beginning to the end of Contig-Run (median $r = 0.62$ (newly formed) versus median $r = 0.21$ (shuffled), $P < 10^{-3}$; Fig. 2e, novel arm, blue versus grey). These results suggest that preplay of the novel arm does not occur over an entirely new (that is, remapped) representation of the whole L-shaped track but rather benefits from the relative stability of the familiar track representation across sessions and perhaps facilitates the rapid, stable encoding of the novel arm experience.

Using the familiar track templates and spiking events during Fam-Rest, constructed as above, we determined that 16.2% ($P < 10^{-91}$; data not shown) were significant replay events[3–6,17] among the spiking events in which a minimum of four familiar track place cells were active. All significant preplay events occurring during Fam-Rest ($n = 75$) were

[1]The Picower Institute for Learning and Memory, RIKEN-MIT Center for Neural Circuit Genetics, Department of Biology and Department of Brain and Cognitive Sciences, Massachusetts Institute of Technology, Cambridge, Massachusetts 02139, USA.

©2011 Macmillan Publishers Limited. All rights reserved

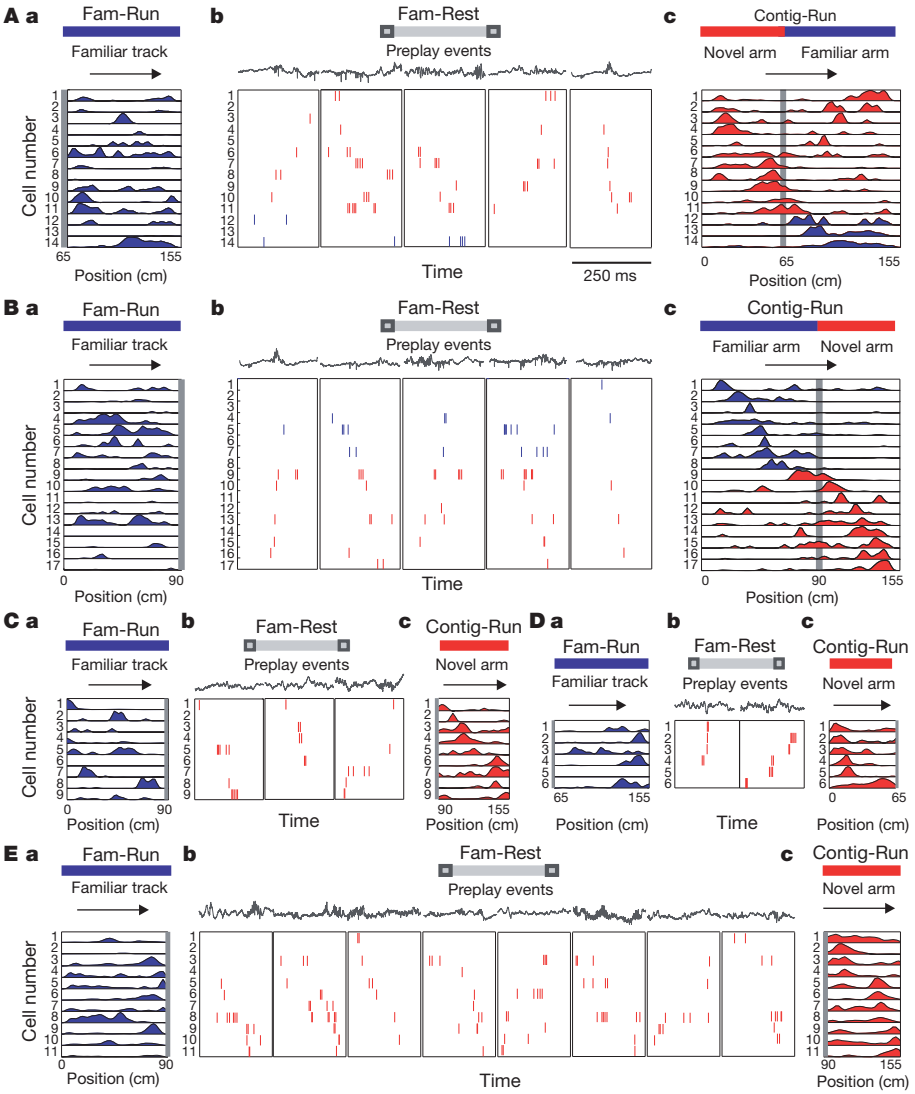

Figure 1 | Preplay of novel place cell sequences. Fam-Run and Fam-Rest respectively denote run and rest sessions on the familiar linear track before barrier removal; Contig-Run denotes run sessions on the L-shaped track after barrier removal. The L-shape track was linearized for display/analysis. **A**, **B**, mouse 1; **C**, **D**, mouse 2; **E**, mouse 3. **A**–**E**, **a**, Spatial activity on the familiar track during Fam-Run of the cells that had place fields in Contig-Run and preplayed during Fam-Rest (one cell per row); activity on the novel arm and familiar track are on the same scale. Horizontal arrows indicate run directions. Vertical grey bars indicate barrier locations during Fam-Run and Fam-Rest. **A**–**E**, **b**, Examples of representative spiking events in the forward or reverse direction during Fam-Rest in 250-ms time windows (350 ms for the second and fourth panels from left in **E**, **b**). Tick marks indicate individual spikes: red, preplay events for place cell sequences in the novel arm; blue (in **A**, **b** and **B**, **b**), additional spikes from the familiar track place cells participating in the spiking event (not shown in **C**–**E**, **b**). Numbers on the left denote cell numbers and correspond to the place cell numbers in **A**–**E**, **a**. Square boxes indicate the ends of the familiar track where preplay events occurred. Local field potentials recorded simultaneously with the spikes are shown above spiking events. **A**–**E**, **c**, Place cell sequences in the novel arm (**C**–**E**, **c**; red) or in both the novel arm (red) and the familiar arm (blue) (**A**, **c** and **B**, **c**) in Contig-Run.

tested for possible replay of the familiar track spatial sequence: these spiking events were more correlated with the novel arm template (Fig. 2f, red) than the familiar track template (Fig. 2f, blue). Seventy-two percent ($n = 54$) of the significant events previously considered to be preplay had no significant correlation with the familiar track template. An additional 16% ($n = 12$) of those events were better correlated with the novel arm templates (mean absolute $r = 0.92$) than with the familiar track template (mean absolute $r = 0.67$, $P < 10^{-3}$). Together, these findings reject the hypothesis that the preplay events simply represent a replay of the familiar track activity (see additional controls in Supplementary Information). Moreover, we found that the proportion of events exclusively composed of silent cells that perfectly matched the novel arm spatial templates was 0.67 (16 of 24 triplets), which is significantly greater ($P < 0.025$) than the proportion of by-chance perfect matches (0.33).

To illustrate the distribution and relative proportions of preplay and replay events among all significant spiking events during Fam-Rest, we calculated a 'template specificity index' (Fig. 2g and Methods) for each event. Pure preplay events (Fig. 2g, red) and pure replay events (Fig. 2g, blue) were segregated, and only a minority of events were significant for both preplay and replay (Fig. 2g, yellow). Consistent with this segregation of preplay and replay events, the novel arm and the 'corresponding familiar track' templates were not significantly correlated (Fig. 2h and Methods). The ratio between the number of pure replay events ($n = 171$) and the number of pure preplay events ($n = 54$) during Fam-Rest was about 3.1 (Fig. 2g, inset; see Supplementary Information for proportions of events). Preplay and replay events were distributed in time across Fam-Rest (Supplementary Fig. 6a–c) and their occurrences were generally uncorrelated (Supplementary Fig. 6d). The majority (79.9%) of the spiking events during Fam-Rest did not significantly correlate with either of the two templates (data not shown).

We used a Bayesian reconstruction algorithm[2,5,6,18,19] (Methods) to decode the animals' position from the spiking activity during Fam-Run (Fig. 3a) or Fam-Rest (Fig. 3b, c). For all original and shuffled[6]

©2011 Macmillan Publishers Limited. All rights reserved

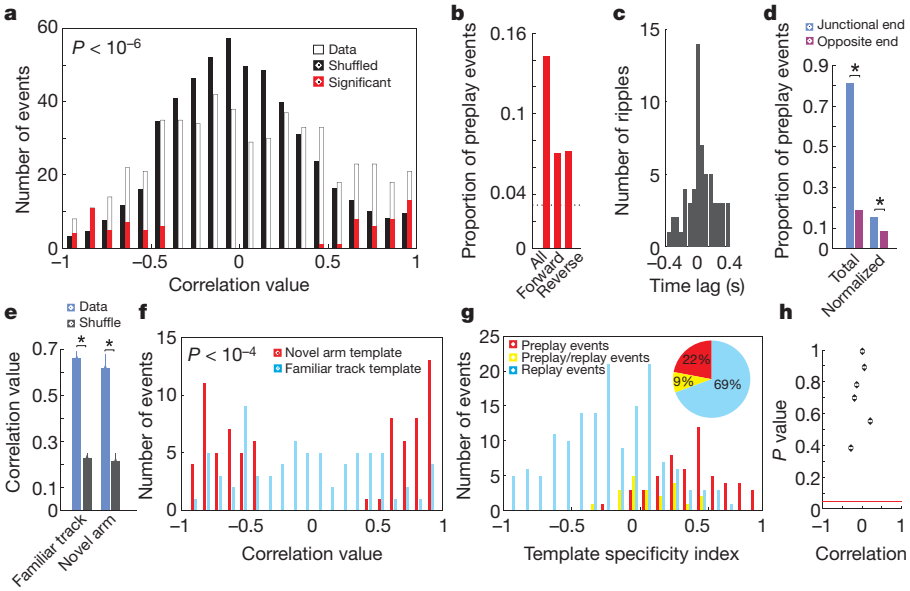

Figure 2 | Quantification of the preplay phenomenon and comparison with replay. **a**, Distribution of correlations between spiking events in Fam-Rest and spatial templates of the novel arm. Open bars indicate spiking events versus the original (unshuffled) templates; filled bars indicate spiking events versus 200 shuffled templates scaled down 200 times; red bars show the distribution of preplay (that is, significant) events. Similar distributions (not shown) of corresponding spiking events were obtained when spatial templates were constructed using all place cells active on the L-shaped track (Figs 1A, b, c and 1B, b, c; red and blue). **b**, Proportion of all, forward and reverse preplay events among the spiking events in Fam-Rest. The dotted line indicates the chance level (3.2%). **c**, Cross-correlation between preplay events and ripple epochs. **d**, Location of preplay events on the familiar track: total, proportions of preplay events at ends of the track; normalized, proportion of preplay events normalized by the number of spiking events at each end of track. Preplay events represented a trajectory running from the free end of the novel arm to the junctional end (40%) or begun near the familiar track (60%); the latter suggests that in some cases preplay events could be triggered by the activity of the familiar track place cells during Fam-Rest. **e**, Stability of place cell spatial tuning across the novel experience: familiar track, stability of the place fields active on the familiar track before (Fam-Run) versus after (Contig-Run) barrier removal; novel arm, stability of the place fields active on the novel arm at the beginning (first four laps of run) versus the end (last four laps) of the Contig-Run session. Data (blue), within-cell correlation of place cell spatial tuning for the corresponding track/arm; shuffle (black), cell identity shuffle (Supplementary Information). Error bars, s.e.m.; asterisks in **d** and **e** indicate significant differences. **f**, Distribution of preplay event correlations (red) versus distribution of these event correlations with the familiar track template (blue). Spiking events were detected using all place cells from the familiar track and novel arm templates (>1 Hz). Red bars are the same as in **a**. Correlation is strong with the novel arm template (preplay) and weak with the familiar arm template (replay). The *P* value corresponds to there being a significant difference between the two distributions. **g**, Disjunctive distribution of pure preplay (red), pure replay (blue) and preplay/replay (yellow) events during Fam-Rest over their template specificity index (Supplementary Information). Inset, proportions of pure preplay events (red), pure replay events (blue) and preplay/replay events (yellow) among all of the spiking events that were significantly correlated with at least familiar track templates or novel arm templates. **h**, Lack of correlation between the novel arm template and the corresponding familiar track template. Each of the six dots represents either a forward or a reverse run direction of one of the three mice analysed. Red horizontal line denotes a *P* value of 0.05. The correlation values were not significant in any of the cases (Supplementary Information).

probability distributions, a line was fitted to the data using a line-finding algorithm[6] to represent the decoded virtual trajectory (Methods and Supplementary Information). In 16.36% of cases representing trajectories, the reconstructed trajectory during spiking events in Fam-Rest was contained within the novel arm (Fig. 3c, top), a place the animal had not yet visited (that is, trajectory preplay). Moreover, in 79.8% of the trajectory preplay cases the shuffling procedures resulted in lines that were significantly less or not at all contained within the novel arm (that is, not preplay; Supplementary Information). The remaining trajectories decoded during Fam-Rest represented replay of the familiar track (64.15%; Fig. 3c, middle) or spanned the joint familiar track/novel arm space (19.49%; Fig. 3c, bottom). Means of absolute rank-order correlations between spiking activity and novel arm templates (Fig. 2a) restricted during epochs of trajectory preplay were significantly larger than those between spiking activity and familiar track templates calculated during the same epochs (0.75 versus 0.59, $P < 10^{-4}$). Overall, these results support the existence of the preplay phenomenon.

To investigate the possibility that preplay of novel arm place cell sequences during Fam-Rest depends on the prior run experience on the familiar track, mice with no prior experience on any linear track were placed in a high-walled sleep box and recorded while resting/sleeping. The animals were then transferred to a novel isolated linear track that was in the same room but could not be seen from inside the box, and the recording continued during *de novo* formation of place cells (Supplementary Fig. 2b, *de novo* session). We found that in a relatively large proportion (16.1%) of spiking events identified during sleep/rest in the sleep box, the neuronal firing sequences were significantly correlated with the place cell sequences observed during the first run session on the novel track (Fig. 4A, B and Methods); this was the case for all four individual mice (Supplementary Fig. 7). Preplay events were associated with the ripple occurrence (Fig. 4C). The place cells established on the novel track in the *de novo* session were more dynamic (median $r = 0.42$; Fig. 4D, blue) than in Contig-Run (median $r = 0.62$, $P < 0.016$; Fig. 2e, right, blue).

We have demonstrated that a significant number of temporal firing sequences of CA1 cells during resting periods of a familiar track exploration that preceded a novel track exploration in the same general environment were correlated with the place cell sequences of the novel track rather than the familiar track. This phenomenon, preplay, is temporally opposite to the process of replay[3–10,19,20], when activity during rest or sleep periods recapitulates place cell sequences that have already occurred during previous explorations. Preplay differs fundamentally from replay because it occurs before exploration of novel tracks.

Although our recordings were carried out in CA1, we believe that what we observed could be a reflection of the output of the recurrent cellular assemblies from upstream regions (CA3 or entorhinal cortex).

©2011 Macmillan Publishers Limited. All rights reserved

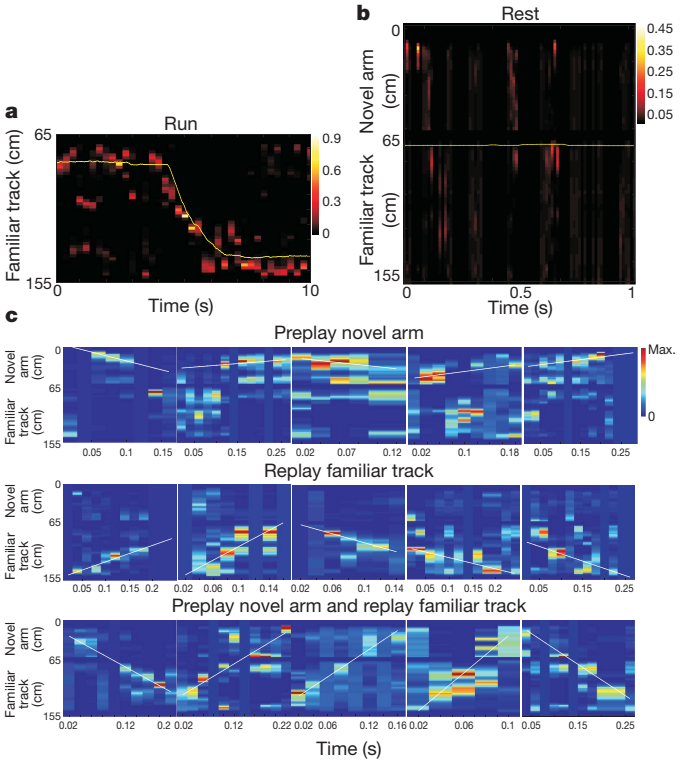

Figure 3 | Bayesian reconstruction of the animal's trajectory in the familiar track (replay) and novel arm (preplay). **a**, Position reconstruction of a one-lap run on the familiar track from the ensemble place cell activity during Fam-Run. The heat map displays the reconstructed position of the animal using ensemble place cell activity during the run (250-ms bins; animal velocity, >5 cm s^{-1}). The yellow line indicates the actual trajectory of the animal during Fam-Run. **b**, Example of virtual trajectory reconstruction (familiar track and novel arm) from the ensemble place cell activity during Fam-Rest at the ends of the familiar track (20-ms bins; animal velocity, <5 cm s^{-1}) before barrier removal and novel arm exploration. The yellow line reflects the spatial location of the animal in time: the animal was immobile at the junction end of the familiar track. The time-compressed ($\sim$5 m s^{-1}) trajectory reconstruction often 'jumps' over the barrier (top of the figure) into the novel arm area. At around 0.5 s, a preplay of the novel arm initiated from the distal (free) end of the novel arm 'propagates' towards the location of the animal. **c**, Examples of preplay of the novel arm (top), replay of the familiar track (middle) and preplay of the novel arm together with replay of the familiar track (bottom) during Fam-Rest. All conditions are the same as in **b**. The white line shows the linear fit maximizing the likelihood along the virtual trajectory. Colour bars indicate probability of trajectory reconstruction.

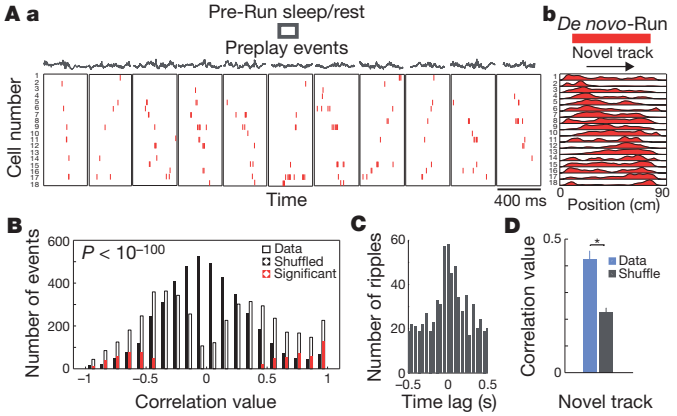

Figure 4 | Preplay of novel place cell sequences before any linear track experience. **A**, Sleep/rest session in the sleep box (Pre-Run sleep/rest) before the first run session on a linear track (*De novo*-Run). Display format is the same as in Fig. 1. **A**, **a**, Representative spiking events in the forward or reverse order during Pre-Run sleep/rest in 400-ms time windows. **A**, **b**, Place cell sequences on the novel track (red) during the *De novo*-Run session. Each row represents one cell in which the activity was normalized to the maximum firing rate. One run direction in one animal is shown. The median number of place cells active on the novel track participating in preplay events is six. **B**, Distribution of spiking events in Pre-Run sleep/rest as a function of the rank-order correlation with the place cell sequence template of the novel track. Display format is the same as in Fig. 2a. **C**, Cross-correlation between preplay events and ripple epochs during Pre-Run sleep/rest. **D**, Stability of place cell spatial tuning across the novel track experience. Display format is the same as in Fig. 2e (novel arm). Error bars, s.e.m.; asterisk indicates significant difference.

During running on a familiar track, some of the cells in the postulated upstream cellular assemblies fire sequentially at spatial locations while others, although connected anatomically to these cells, remain silent. The lack of expression of preplay sequences during Fam-Run may reflect their state-dependent suppression or subthreshold activation during these exploratory behaviours. Owing to increased net excitation during rest periods predominantly during ripples[21], some of these silent cells together with some of the familiar track cells are activated above threshold and fire in a certain sequence. Their sequence of activation may be determined in part by their functional connectivity within the hippocampal formation network. Some of these sequences may in turn be activated on a novel track as place cell sequences (Supplementary Fig. 8). The activation of the novel place cell sequences during running may strengthen their pre-existing assembly organization manifested during preplay.

It could be argued that during Contig-Run the animals simply considered the novel arm to be an extension of the familiar arm and, thus, what we considered to be preplay events were replays of the previous runs on the familiar track. If this was the case, preplay events would not be expected to be found when the experience of the familiar track run is eliminated. This idea was refuted by the demonstration of frequent preplay events in the sleep box before the mice were transferred onto a novel linear track (*de novo* condition). Under this condition, the place cell sequences were more dynamic and a higher proportion of all spiking events correlated with the place cell sequences in these runs than in the later runs on novel linear tracks. These results suggest a shift in the relative contribution of internal[22,23] and external drives in the formation of place cell sequences on encounter with a novel track. In the early phase, internal drives originating in the dynamic cellular assembly activities, which probably reflect numerous past experiences distinct from the current one and expressed as preplay, may have a greater role, whereas in the late phase, external drives that come from the specific set of stimuli of the current experience may dominate. Thus, place cell sequences on novel tracks seem to be products of a dynamic interplay between the internal and external drives.

Several previous studies did not reveal preplay[7,8,10,20]. Although it is difficult to pinpoint the apparent discrepancies between these studies and the present one, we suggest that the use of insufficiently sensitive methods (pairwise correlations) by some studies[7,8,20] and small sample sizes by others[10] might have precluded detection of preplay in previous work (see Supplementary Information for details). Data from the *de novo* condition (Fig. 4), in which we observed an even higher proportion of preplay events, have not been reported previously.

Our data showed that novel preplay events coexist in disjunction with familiar replay events during the rest periods on the familiar track. This and the finding that these preplay and replay events together make up fewer than one-quarter of all detected spiking events suggest that they are part of a dynamic repertoire of temporal sequences in the hippocampus that are past-experience dependent (replay) or future-experience expectant[24] (preplay). Post-experience replay of place cell sequences during resting[3–6] or slow-wave sleep[8–10] has been proposed to have an important role in memory consolidation[11,12]. The temporal preplay of new place cell sequences during resting or sleep is consistent with a predictive function for the hippocampal formation[25] and may contribute to accelerating learning[26]

©2011 Macmillan Publishers Limited. All rights reserved

when a new experience is introduced in multiple steps of increasing novelty.

METHODS SUMMARY

We recorded place cells from the CA1 area of the hippocampus with six independently movable tetrodes in four mice during sleep/rest sessions in the sleep box before any experience on linear tracks and during the first run session on a novel track. Following familiarization with the linear track, animals were subsequently allowed to explore a continuous (L-shaped) track in which the now familiar track and a new novel arm were made contiguous. To quantify the significance of the preplay and replay processes, spiking events in which at least four cells were active were detected during sleep/rest (speed, $<1\ \mathrm{cm\ s^{-1}}$) periods in the sleep box or awake rest (speed, $<2\ \mathrm{cm\ s^{-1}}$) periods at the ends of the familiar track and novel arm, predominantly during ripple epochs.

We calculated statistical significance at the $P<0.025$ level for each event by comparing the rank-order correlation between the event sequence and the place cell sequence (template) with the distribution of correlation values from 200 templates obtained by shuffling the original order of the place cells. Proportions of significant events were calculated as the ratio between the number of significant events and the total number of spiking events. We calculated the overall significance of preplay or replay processes by comparing the distribution of correlation values of all events with the distribution of correlation values of shuffled templates (Kolmogorov–Smirnov test). The significance of the proportion of significant events out of the total number of spiking events was determined as the binomial probability of observing the number of significant events (as successes) from the total number of spiking events (as independent trials), with a probability of success of 0.025 in any given trial. We reconstructed the position of the animal from the spiking activity emitted during resting periods using Bayesian decoding procedures[6].

Full Methods and any associated references are available in the online version of the paper at www.nature.com/nature.

Received 4 December 2009; accepted 29 October 2010.
Published online 22 December 2010.

1. O'Keefe, J. & Nadel, L. *The Hippocampus as a Cognitive Map* (Oxford Univ. Press, 1978).
2. Wilson, M. A. & McNaughton, B. L. Dynamics of the hippocampal ensemble code for space. *Science* **261,** 1055–1058 (1993).
3. Foster, D. J. & Wilson, M. A. Reverse replay of behavioural sequences in hippocampal place cells during the awake state. *Nature* **440,** 680–683 (2006).
4. Diba, K. & Buzsaki, G. Forward and reverse hippocampal place-cell sequences during ripples. *Nature Neurosci.* **10,** 1241–1242 (2007).
5. Karlsson, M. P. & Frank, L. M. Awake replay of remote experiences in the hippocampus. *Nature Neurosci.* **12,** 913–918 (2009).
6. Davidson, T. J., Kloosterman, F. & Wilson, M. A. Hippocampal replay of extended experience. *Neuron* **63,** 497–507 (2009).
7. Wilson, M. A. & McNaughton, B. L. Reactivation of hippocampal ensemble memories during sleep. *Science* **265,** 676–679 (1994).
8. Skaggs, W. E. & McNaughton, B. L. Replay of neuronal firing sequences in rat hippocampus during sleep following spatial experience. *Science* **271,** 1870–1873 (1996).
9. Nádasdy, Z., Hirase, H., Czurko, A., Csicsvari, J. & Buzsaki, G. Replay and time compression of recurring spike sequences in the hippocampus. *J. Neurosci.* **19,** 9497–9507 (1999).
10. Lee, A. K. & Wilson, M. A. Memory of sequential experience in the hippocampus during slow wave sleep. *Neuron* **36,** 1183–1194 (2002).
11. Buzsáki, G. Two-stage model of memory trace formation: a role for "noisy" brain states. *Neuroscience* **31,** 551–570 (1989).
12. Nakashiba, T., Buhl, D. L., McHugh, T. J. & Tonegawa, S. Hippocampal CA3 output is crucial for ripple-associated reactivation and consolidation of memory. *Neuron* **62,** 781–787 (2009).
13. Hebb, D. O. *The Organization of Behavior: A Neuropsychological Theory* (Wiley, 1949).
14. Harris, K. D., Csicsvari, J., Hirase, H., Dragoi, G. & Buzsaki, G. Organization of cell assemblies in the hippocampus. *Nature* **424,** 552–556 (2003).
15. Dragoi, G. & Buzsaki, G. Temporal encoding of place sequences by hippocampal cell assemblies. *Neuron* **50,** 145–157 (2006).
16. Thompson, L. T. & Best, P. J. Place cells and silent cells in the hippocampus of freely-behaving rats. *J. Neurosci.* **9,** 2382–2390 (1989).
17. O'Neill, J., Senior, T. & Csicsvari, J. Place-selective firing of CA1 pyramidal cells during sharp wave/ripple network patterns in exploratory behavior. *Neuron* **49,** 143–155 (2006).
18. Zhang, K., Ginzburg, I., McNaughton, B. L. & Sejnowski, T. J. Interpreting neuronal population activity by reconstruction: unified framework with application to hippocampal place cells. *J. Neurophysiol.* **79,** 1017–1044 (1998).
19. Johnson, A. & Redish, A. D. Neural ensembles in CA3 transiently encode paths forward of the animal at a decision point. *J. Neurosci.* **27,** 12176–12189 (2007).
20. Kudrimoti, H. S., Barnes, C. A. & McNaughton, B. L. Reactivation of hippocampal cell assemblies: effects of behavioral state, experience, and EEG dynamics. *J. Neurosci.* **19,** 4090–4101 (1999).
21. Csicsvari, J., Hirase, H., Czurko, A., Mamiya, A. & Buzsaki, G. Oscillatory coupling of hippocampal pyramidal cells and interneurons in the behaving rat. *J. Neurosci.* **19,** 274–287 (1999).
22. Dragoi, G., Harris, K. D. & Buzsaki, G. Place representation within hippocampal networks is modified by long-term potentiation. *Neuron* **39,** 843–853 (2003).
23. Pastalkova, E., Itskov, V., Amarasingham, A. & Buzsaki, G. Internally generated cell assembly sequences in the rat hippocampus. *Science* **321,** 1322–1327 (2008).
24. Black, J. E. & Greenough, W. T. *Advances in Developmental Psychology* (Lawrence Erlbaum, 1986).
25. Hassabis, D., Kumaran, D., Vann, S. D. & Maguire, E. A. Patients with hippocampal amnesia cannot imagine new experiences. *Proc. Natl Acad. Sci. USA* **104,** 1726–1731 (2007).
26. Tse, D. *et al.* Schemas and memory consolidation. *Science* **316,** 76–82 (2007).

Supplementary Information is linked to the online version of the paper at www.nature.com/nature.

Acknowledgements We thank M. A. Wilson for assistance with data acquisition, discussions and comments on an earlier version of the manuscript; J. O'Keefe, A. Siapas, F. Kloosterman, D. L. Buhl for comments on earlier versions of the manuscript; and F. Kloosterman for providing assistance with the line detection for the Bayesian decoding. This work was supported by NIH grants R01-MH078821 and P50-MH58880 to S.T., who was an HHMI Investigator in an earlier part of this study.

Author Contributions S.T. and G.D. conceived the project jointly. G.D. designed and performed the experiments and the analyses. G.D. and S.T. wrote the paper.

Author Information Reprints and permissions information is available at www.nature.com/reprints. The authors declare no competing financial interests. Readers are welcome to comment on the online version of this article at www.nature.com/nature. Correspondence and requests for materials should be addressed to G.D. (gdragoi@mit.edu) or S.T. (tonegawa@mit.edu).

©2011 Macmillan Publishers Limited. All rights reserved

METHODS

Surgery and experimental design. Electrophysiological recordings were performed on four C57BL/6 mice (strain NR1-floxed[27]) with ages between 18 and 22 weeks. All animals were implanted under Avertin anaesthesia with six independently movable tetrodes aiming for the CA1 area of the right hippocampus (1.5–2 mm posterior to bregma and 1–2 mm lateral to the midline; Supplementary Fig. 1). The reference electrode was implanted posterior to lambda over the cerebellum. During the following week of recovery, the electrodes were advanced daily while animals rested in a small, walled sleeping box ($12 \times 20\,cm^2$, 35 cm high). The animal position was monitored by means of two infrared diodes attached to the headstage.

The experimental apparatus consisted of a $90 \times 65\,cm^2$ rectangular, walled, linear track maze. All tracks were 4 cm wide at the bottom and 8–9 cm wide at the top, and all linear track walls were 10 cm high. Experimental sessions were conducted while the animals explored for chocolate sprinkle rewards placed always at the ends of the corresponding linear tracks (one sprinkle at each end of the track on each lap). Neuronal activity was recorded in naive animals (four mice) during the sleep/rest session in the sleep box immediately preceding the first experience on linear tracks, and continued (Fig. 4) during the first run session on a novel track. After familiarization with the linear track, the animals went through a recording session of 15–60 min (Fam session), and the recordings continued for the next 34–42 min (Contig session) while the animals explored an L-shaped track for the first time. In this track, the familiar arm and the novel arm were made contiguous by removing the barrier that had separated them (Fig. 1). For the purpose of analysing the recording data, the Fam session was further divided into Fam-Run, in which the animals ran through the track (velocity of animal's movement was higher than $5\,cm\,s^{-1}$), and Fam-Rest, where the animals took awake rests at the ends of the track (velocity of animal's movement was less than $2\,cm\,s^{-1}$). During resting periods, the animals consumed the chocolate sprinkle and groomed, but mostly they were still until they self-initiated the next lap of run on the linear track. After completion of the experiments, the brains of all mice were perfused, fixed, sectioned and stained using nuclear fast red (Supplementary Fig. 1) or cresyl violet for electrode track reconstruction.

Recordings and single-unit analysis. A total of 87 neurons were recorded from the CA1 area of the hippocampus in four mice during the Fam and Contig sessions (Supplementary Tables 1–3). A total of 69 CA1 neurons were recorded from the four mice in the *de novo* condition (26, 20, 10 and 13 cells, respectively). Single cells were identified and isolated using the manual clustering method Xclust[2] and the application of cluster quality measurements[28]. Pyramidal cells were distinguished from interneurons on the basis of spike width, average rate and autocorrelations[22].

Place fields were computed as the ratio between the number of spikes and the time spent in 2-cm bins along the track, smoothed with a Gaussian kernel with a standard deviation of 2 cm. Bins where the animal spent a total of less than 0.1 s and periods during which the animal's velocity was below $5\,cm\,s^{-1}$ were excluded. Place field length and peak rate were calculated after separating the direction of movement and linearizing the trajectory of the animal. Linearized place fields were defined as areas with a localized increase in firing rate above 1 Hz for at least five contiguous bins (10 cm). The place field peak rate and location were given by the rate and location of the bin with the highest ratio between spike counts and time spent. Place field borders were defined as the points where the firing rate became less than 10% of the peak firing rate or 1 Hz (whichever was bigger) for at least 2 cm.

Local field potential analysis. Ripple oscillations were detected during sleep/rest periods in the sleep box and during rest periods at the ends of the tracks. The electroencephalography signal was filtered (120–200 Hz) and ripple-band amplitude was computed using the Hilbert transform. Ripple epochs with maximal amplitude more than 5 s.d. above the mean, beginning and ending at 1 s.d. were detected. The time of ripple occurrence (Figs 2c and 4C) was the time of its maximal amplitude. The proportion of ripples with which cells with place fields on the novel arm of the L-shaped track fired in the preceding session (Supplementary Fig. 3) was calculated for each qualifying cell as the ratio between the number of ripples during which the cell fired at least one spike and the total number of ripples during the corresponding exploratory session.

Preplay and replay analyses. To analyse the preplay and replay processes, spiking events were detected during Pre-Run sleep/rest periods in the sleep box (*de novo* condition; velocity, $<1\,cm\,s^{-1}$) or during awake rest periods at the ends of the running tracks (Contig condition; velocity, $<2\,cm\,s^{-1}$). A spiking event was defined as a transient increase in the firing activity of a population of at least four different place cells within a temporal window preceded and followed by at least 50 ms of silence. Overall, similar results were obtained using 50-, 60-, 75- and 100-ms time windows. The spikes of all the place cells active on the novel track that were emitted during the Pre-Run sleep/rest in the box for the *de novo* condition as well as the spikes of all the place cells active on the familiar track or the novel arm that were emitted during Fam-Rest session at the two ends of the familiar track for Contig condition were respectively sorted by time and further used for the detection of the spiking events.

All four animals exhibited a significant number of spiking events in the Pre-Run session of the *de novo* condition. Three of the four animals (mice 1–3) exhibited a significant number of spiking events in the Contig condition, the remaining animal (mouse 4) having a below-threshold number of simultaneously active CA1 place cells. The time of the spiking event used to compute the cross-correlation with ripple epoch occurrence (Figs 2c and 4C) was the average time of all spikes comprising the spiking event. The place cell sequences (templates) were calculated for each direction of the animal's movement and for each run session (*De novo*-Run, Fam-Run and Contig-Run) by ordering the spatial location of the place field peaks that were above 1 Hz. For place cells with multiple place fields above 1 Hz on a particular arm or track in the Contig condition (six of 52 place cells active on the novel arm in the two directions, or 12%: two for each direction in mouse 1, one in mouse 2 and one in mouse 3), only the place field corresponding to the peak firing rate of the place cell on that arm or track was considered for the construction of the template of that particular arm or track, to be consistent with all the previous studies that used spatial templates to demonstrate replay during sleep or awake rest[3,4,10]. Place cells with fields on both the novel arm in the Contig-Run session and the familiar track in the Fam-Run session participated in the construction of both the novel arm and familiar track templates.

Statistical significance was calculated for each event by comparing the rank-order correlation between the sequence of cells' firing during the event (that is, event sequence) and the place cell sequence (template), on the one hand, and the distribution of correlation values between the event sequence and 200 surrogate templates obtained by shuffling the order of place cells, on the other[4] (Fig. 2a). The significance level was set at 0.025 to control for multiple comparisons (two directions of run). The proportions of significant events (preplay novel track, preplay novel arm (Fig. 2b), replay novel arm and replay familiar track) were each calculated as the ratio between the number of significant events and the total number of spiking events in which at least four corresponding place cells were active[4]. Corresponding familiar track templates (Fig. 2h) were constructed by ordering the location of peak firing on the familiar track during Fam-Run (no minimum threshold of firing) of all place cells that subsequently fired on the novel arm. Cells comprising the corresponding familiar track templates are the same as those comprising the novel arm templates. We note that these corresponding familiar track templates are different from the ones used in Figs 1 and 2a–g, which were constructed by ordering the peak firing of all place cells active on the familiar track >1 Hz.

The overall significance of the preplay (Fig. 2a) or replay process was calculated by comparing the distribution of correlation values of all events relative to the original template with the distribution of correlation values relative to the shuffled surrogate templates, using the Kolmogorov–Smirnov test[3]. Quantification of the replay versus preplay events during the Fam-Run session (Fig. 2f, g) was performed as described above using different spatial templates for the familiar track and the novel arm. All spiking events were correlated with both the novel arm and the familiar track templates. Events significantly correlated only with familiar track or with novel arm templates were considered pure replay and pure preplay, respectively. The template specificity index was calculated for each event as the difference between the absolute value of the event's correlation with the novel arm template (preplay, high positive index) and the event's correlation with the familiar track template (replay, high negative index). For the purpose of displaying the template specificity index, events correlated with the novel arm but not with the familiar track templates were considered preplay and events correlated with the familiar track but not with the novel arm templates were considered replay (Fig. 2g). Additionally, events correlated with both the familiar track and the novel arm templates formed a third group, preplay/replay events, displayed in yellow in the inset of Fig. 2g.

Correlations between pairs of familiar track and novel arm templates (Fig. 2h) were performed using modified familiar track templates that were constructed using the location of peak firing (>0 Hz) of only those cells that had place fields on the novel arm (peak rate, >1 Hz). The lack of significant correlation in this case demonstrates that the novel arm place cell sequence is not simply a transposition of a familiar track place cell sequence on the novel arm.

We also identified neurons that did not fire during Fam-Run, that activated during Fam-Rest events and that corresponded to trajectories on the novel arm during Contig-Run (silent cells). We calculated the correlation between the order in which they fired during Fam-Rest events and their spatial sequence as new place cells on the novel arm during Contig-Run, as previously explained. Owing to the low absolute number of silent neurons, only triplets of cells were available for further analysis ($n = 24$). The proportion of events perfectly matching the spatial template was compared with the proportion of by-chance perfect matching (0.33).

©2011 Macmillan Publishers Limited. All rights reserved

Stability of place cell maps. Stabilities of place cell firing on the familiar track before and after barrier removal as well as on the novel track (*de novo* condition) and the novel arm (Contig condition) in the beginning versus the end of the run session were assessed by calculating, for each place cell and each direction, a correlation between the spatial firing in the corresponding paired situations (before versus after barrier removal for the familiar track or the first four laps versus the last four laps of the *De novo*-Run or Contig-Run session for the novel track or arm, respectively). The place cell activity was not partitioned in place fields; rather, the whole activity on the particular track or arm was considered separately for each cell and direction (average correlations are shown in Figs 2e and 4D, blue bars). In addition, we calculated the same type of correlation after shuffling the identity of the cell in one member of the correlation (once for each different cell; average correlations are in Figs 2e and 4D, black bars). Shuffle results (Figs 2e and 4D, black bars) were computed as correlation between spatial tuning of cells on the familiar track during Fam-Run and spatial tuning of all other simultaneously recorded cells on the familiar arm during Contig-Run (familiar track group; Fig. 2e, left), or correlation between spatial tuning of cells on the novel arm (or novel track) during the beginning of Contig-Run (or *De novo*-Run) and spatial tuning of all the other simultaneously recorded cells on the novel arm (or novel track) during the end of Contig-Run (novel arm group; Fig. 2e, right) or *De novo*-Run (Fig. 4D). Original and shuffled correlations were compared using the rank-sum test. The average number of laps (traversal of the novel track in both directions) per session was 20.5 in *De novo*-Run (21, 16, 27 and 18 in the four mice) and 16.3 in Contig-Run (13, 14 and 22 in the three mice).

Bayesian reconstruction of actual and virtual trajectories. For each cell, we calculated a linearized spatial tuning curve on the familiar track during the Fam-Run session and a linearized spatial tuning curve on the novel arm during the Contig-Run session. The tuning curves were constructed in 2-cm bins from spikes emitted in both run directions at velocities higher than 5 cm s^{-1}, and were smoothed with a Gaussian kernel with a standard deviation of 2 cm. We constructed a joint spatial tuning curve for each cell by juxtaposing the spatial tuning curve on the familiar track during the Fam-Run session and the spatial tuning curve on the novel arm during the Contig-Run session. We also detected for each cell all the spiking activity emitted at velocities below 5 cm s^{-1} during the Fam-Rest session, where replay and preplay events where shown to occur using the rank-order correlation method. We used a Bayesian reconstruction algorithm[6,18] to decode the virtual position of the animal from the spiking activity during Fam-Rest (Fig. 3b) in non-overlapping, 20-ms bins using the joint spatial tuning curves. We then extracted epochs of reconstructed trajectory matching the time of the spiking events as detected using multiunit activity of place cells from the familiar track and novel arm (rank-order correlation method; see 'Preplay and replay analyses', above).

We used two shuffling procedures to measure the quality of the Bayesian decoding. In the first shuffling procedure, for each event, the original time-bin columns of the probability distribution function (PDF) were replaced with an equal number of time-bin columns randomly extracted from a pool containing the time-bin columns of all PDFs of all detected events[6]. The shuffling procedure was repeated 500 times. In the second shuffling procedure, the identity of the place cells was randomly shuffled 100 times and new PDFs were calculated for all events. For all original and shuffled PDFs, a line was fitted to the data using a previously described line-finding algorithm[6]. Lines fitted to the original and shuffled data were compared using slope, spatial extent, location on the track and probability score. We defined replay and preplay as the epochs of Fam-Rest in which the reconstructed trajectory was located on the familiar track or the novel arm, respectively. The trajectory was defined across a set of position estimates during the corresponding epoch (Fig. 3c). Only epochs that lasted at least 60 ms (three bins) and which contained reconstructed trajectories spanning at least 10 cm were considered for further analysis. Trajectories for which 75% or more of their length was located on the familiar track were considered to represent replay of an animal's trajectory on the familiar track (Fig. 3c, middle), and trajectories for which 75% or more of their length was located in the novel arm were considered to represent preplay of the animal's future trajectory on the novel arm (Fig. 3c, top). The remaining events were considered preplay–replay (Fig. 3c, bottom).

An epoch was considered significant if the new line was less than 75% contained in the familiar track for replay or novel arm for preplay in at least 95% of the shuffled cases. For each epoch that was significant for replay or preplay using the reconstruction method, we retrieved the value of the rank-order correlation between the neuronal firing sequences and the familiar track and novel arm spatial templates as calculated using the rank-order correlation method. We compared the absolute correlation values between the epoch's firing sequences and familiar track templates with the absolute correlation values between the same epoch's firing sequences and novel arm templates. We also reconstructed the trajectory of the animal on the familiar track from the spiking activity during the Fam-Run session at velocities above 5 cm s^{-1} in 250-ms bins using the spatial tuning curves on the familiar track[6,18] (Fig. 3a) to validate the decoding procedure.

27. Tsien, J. Z., Huerta, P. T. & Tonegawa, S. The essential role of hippocampal CA1 NMDA receptor-dependent synaptic plasticity in spatial memory. *Cell* **87,** 1327–1338 (1996).
28. Schmitzer-Torbert, N., Jackson, J., Henze, D., Harris, K. & Redish, A. D. Quantitative measures of cluster quality for use in extracellular recordings. *Neuroscience* **131,** 1–11 (2005).

©2011 **Macmillan Publishers Limited. All rights reserved**

Neuron 50, 145–157, April 6, 2006 ©2006 Elsevier Inc. DOI 10.1016/j.neuron.2006.02.023

Temporal Encoding of Place Sequences by Hippocampal Cell Assemblies

George Dragoi[1,2,*] and György Buzsáki[1,*]
[1] Center for Molecular and Behavioral Neuroscience
Rutgers, The State University of New Jersey
Newark, New Jersey 07102
[2] Picower Institute for Learning and Memory
Massachusetts Institute of Technology
Cambridge, Massachusetts 02139

Summary

Both episodic memory and spatial navigation require temporal encoding of the relationships between events or locations. In a linear maze, ordered spatial distances between sequential locations were represented by the temporal relations of hippocampal place cell pairs within cycles of theta oscillation in a compressed manner. Such correlations could arise due to spike "phase precession" of independent neurons driven by common theta pacemaker or as a result of temporal coordination among specific hippocampal cell assemblies. We found that temporal correlation between place cell pairs was stronger than predicted by a pacemaker drive of independent neurons, indicating a critical role for synaptic interactions and precise timing within and across cell assemblies in place sequence representation. CA1 and CA3 ensembles, identifying spatial locations, were active preferentially on opposite phases of theta cycles. These observations suggest that interleaving CA3 neuronal sequences bind CA1 assemblies representing overlapping past, present, and future locations into single episodes.

Introduction

A challenging goal in neuroscience is to understand how a particular neuronal mechanism that evolved for a given function at an earlier stage of evolution can be employed for another function in subsequently evolved brains. In humans, the hippocampus and associated structures are believed to support episodic and semantic memories (Scoville and Milner, 1957; Tulving, 1972; Squire, 1992; Eichenbaum et al., 1999). In contrast, work on rodents suggests that these same structures play a critical role in map-based spatial navigation (O'Keefe and Nadel, 1978; Hafting et al., 2005) and/or dead reckoning navigation/"path integration" (McNaughton et al., 1996; Redish and Touretzky, 1997). Neuronal mechanisms of path integration and episodic memory are related because both processes require a coordinated integration of sequential information in a spatial-temporal context.

Sequential activation of hippocampal place cells on a track is believed to require a temporal context, as indicated by the systematic relationship between spike timing and the phase of the ongoing theta oscillation in the rat (O'Keefe and Recce, 1993). As the rat enters the receptive field of the neuron, the spikes occur on the peak of the theta cycle recorded at the CA1 pyramidal layer and may precess a full period as the rat passes through the entire receptive field of the cell. One explanation of the "phase precession" phenomenon is the interaction between two inputs to place cells ("pacemaker" model). One input represents environmental information, whereas the exact timing is paced by a rhythmic theta oscillation to all neurons, presumably from the septal pacemaker (O'Keefe and Recce, 1993; Skaggs et al., 1996; Mehta et al., 2002; Harris et al., 2002). A consequence of the pacemaker model is a predictable temporal relationship between different place cells within the theta cycle, even if place cells do not interact with each other (Skaggs et al., 1996). An implication of this hypothesis is that the best prediction of the rat's position is reflected by the phase-place correlation of the recorded multiple "independent" cells (Huxter et al., 2003). Because the pacemaker model does not require synaptic interactions among place cells, the variability of the space-spike phase relationship across subsequent trials is considered to be "noise." Therefore, the "ideal" phase for each trial would be the average phase value of all trials. Alternatively, sequential segments of the track are represented by unique sets of cell assemblies, which are bound together by synaptic interactions into an episode (Tsodyks et al., 1996; Jensen and Lisman, 1996). This organization implies temporally coordinated activity within and between anatomically distributed groups of sequential cell assemblies (Hebb's "phase sequence") (Hebb, 1949). According to the latter (assembly) model, phase precession of spikes within the theta cycle would result from the intrinsic oscillatory dynamics of the hippocampal formation in the framework of an attractor dynamical systems model (Tsodyks et al., 1996; Jensen and Lisman, 1996; Wallenstein and Hasselmo, 1997; Samsonovich and McNaughton, 1997; Wills et al., 2005). In the assembly model, spike phase variability of the place cells are temporally correlated because timing of neuronal action potentials depends on the activity of the synaptically connected cell assemblies in which individual cells are embedded. To address these competing hypotheses, we recorded from hippocampal CA1 and CA3 neuronal ensembles as the animals explored a rectangular elevated track for food reward (Dragoi et al., 2003), and we examined the temporal correlations between cell pairs in various aspects of the task. The findings support an internally coordinated assembly model and show that the most active assembly, representing the current location/item and anchored to the trough of the local theta cycle, is bound with the surrounding assemblies, representing past and future locations/items.

Results

Representation of Spatial Distances by Temporal Correlation

We recorded from hippocampal CA1 and CA3 neurons (n = 256 in four rats) during navigation on a rectangular elevated track for food reward (Dragoi et al., 2003).

*Correspondence: gdragoi@mit.edu (G.D.); buzsaki@axon.rutgers.edu (G.B.)

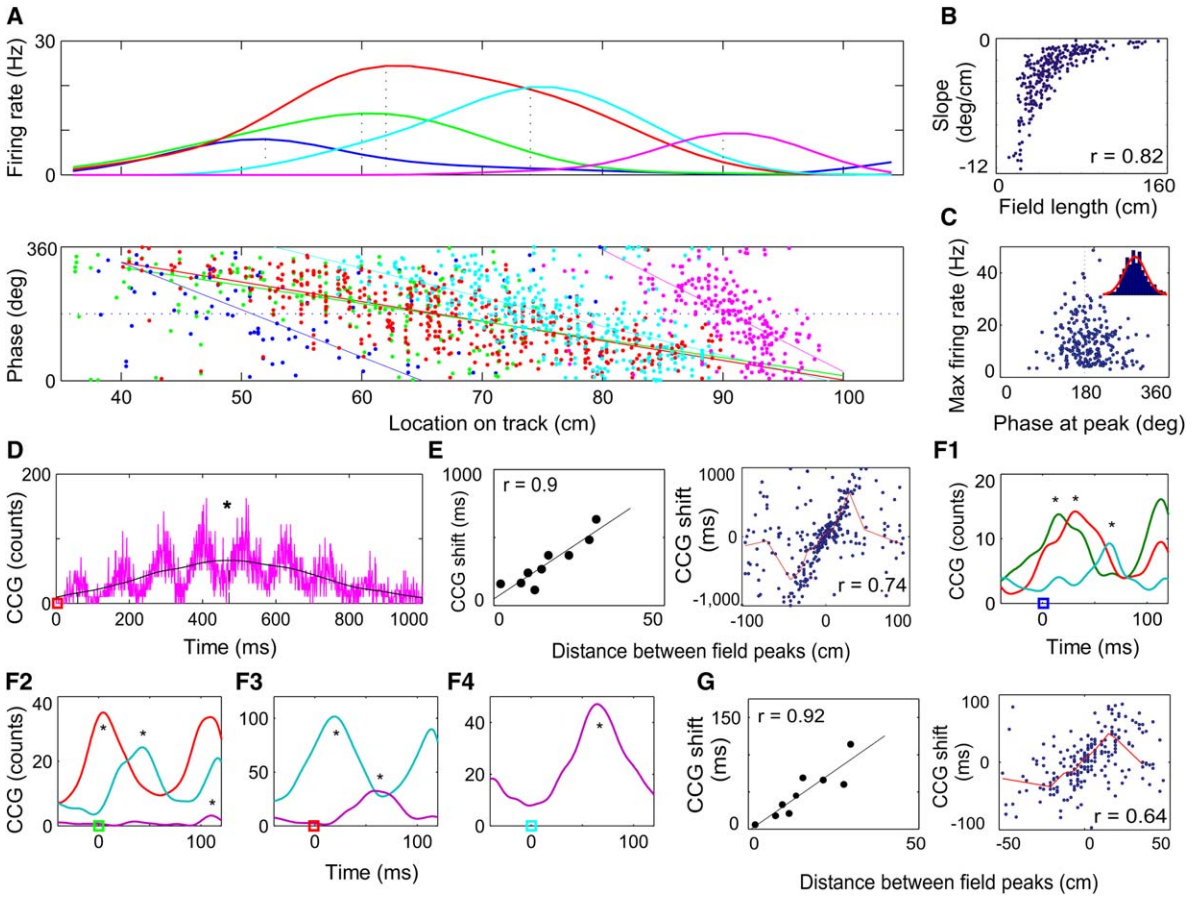

Figure 1. Representation of Place Sequences by Temporal Correlation

(A) Encoding of spatial location in five sequential place cells (color coded) by rate (top) and phase precession (bottom). Lines, position-phase regression slopes.

(B) Significant position-phase linear regression slopes as a function of place field length (n = 270 fields).

(C) Relationship between median phase at field peak and firing rate. Inset: normal distribution of median phase at place field peak (mean is at 180°).

(D) Cross-correlogram (CCG) between two cells (orange cell at time zero versus magenta cell). Note theta frequency modulation over nine cycles in 1 s. Star, peak of the smoothed (line) cross-correlogram at 470 ms.

(E) Time differences, determined by the peaks of the smoothed CCG of the nine cell pair combinations (left) and all pairs (right), as a function of distance between field peaks, determined by the peak firing rates of the individual neurons ("coding by real-time scale"). Red line, running median.

(F) Cross-correlograms (CCG) between blue (reference) cell versus green, orange, and cyan (partner) neurons at a short (theta) scale (F1) and between other pairs ([F2–F4], color squares, reference neuron). Stars, peaks of cross-correlograms.

(G) Time differences, determined by the peaks of the short time scale CCG of the nine cell-pair combinations (left) and all pairs (right), as a function of distance between field peaks ("coding by theta time scale").

Figure 1 illustrates a typical sequential activation of place cells with partially overlapping place fields (Jensen and Lisman, 1996). As shown earlier, the spatial position of the animal correlated with both the firing rates (O'Keefe and Nadel, 1978) of hippocampal pyramidal neurons (Figure 1A, top) as well as the phase of spikes within the theta cycle (O'Keefe and Recce, 1993; Huxter et al., 2003) (Figure 1A, bottom). Thus, the spike phase information provided an estimate of the distance traveled from the beginning of the place field for a given neuron. This distance information was cell specific rather than expressed in an absolute metric, since the slope of the spike phase shift depended on the size of the place field (Figure 1B; see also Huxter et al., 2003). Therefore, the distances between sequentially visited places cannot be accurately calculated solely from the phase precession of individual place cells.

The current position of the animal is defined by the maximum firing activity of a population of place cells (Wilson and McNaughton, 1993). Peak firing rates of hippocampal pyramidal neurons were anchored to the trough of the locally recorded theta cycle (Figures 1A and 1C), as if the trough functioned as an attractor for the assembly representing the current position (Wallenstein and Hasselmo, 1997; Tsodyks, 1999). Spikes moved toward and away from the trough while the rat traveled toward or away from the place field center, respectively, resulting in an opposite phase relationship of the spikes, on average, for the rising (beginning-to-peak) and falling (peak-to-end) parts of the place field (Figure 1C; see below).

The distance between adjacent place field peaks of two neurons could be estimated from the temporal relationship of the corresponding neuronal spikes at two

different time scales. At the longer or "real-time scale," the time difference between the peaks of the smoothed cross-correlograms (CCG) corresponded to the time it took the rat to traverse the distance between place field peaks (Figures 1D and 1E). At the shorter or "theta time scale," the same distances were represented by the temporal relations of spikes at the tens of millisecond time scale (Figures 1F and 1G). Below, we refer to this distance versus theta-scale time-lag correlation as "sequence compression" and to its correlation coefficient as "sequence compression index."

Assembly Coding of Place Sequence Information

Sequence compression was suggested to be the direct consequence of the linear phase precession of individual neurons, relative to a global theta timing signal (Skaggs et al., 1996). It was also hypothesized that the phase of the spikes within the theta cycle but not their firing rate is the critical variable for place representation (Huxter et al., 2003). Because the pacemaker model does not assume direct interactions among the place cells, the most accurate prediction of the rat's position at any given place would be reflected by the phase-position correlation of the recorded multiple cells (Jensen and Lisman, 2000). Furthermore, the correlation between place field distances and the temporal differences of place cell spikes at the theta time scale would result exclusively from the theta phase precession. Alternatively, in the assembly model of place representation, the temporal differences between neuron pairs and the distances between corresponding place fields could reflect the strength of synaptic interactions between cell assemblies representing the two sequential positions (Muller et al., 1996). The two models predict identical phase precession slopes of individual place cells. However, the temporal correlation among assembly members and the encoding of spatial relations (distances) between their place fields should be better in the assembly model than in the pacemaker model because the former model assumes synaptic interactions among the neurons. To distinguish between these alternative mechanisms, we examined the transformation between real-time scale and theta-scale representations, the relationship between "dependent" and "independent" cell pairs, and spike time coordination during the rising and falling parts of the place fields.

To display the dynamics of ensemble representation of the corresponding spatial distances as the animal passed through sequential places, we plotted the sequence compression for the whole population of pairs (as in Figure 1G) over several theta cycles within a 1 s period. In Figure 2A, zero time-lag corresponds to the occurrence of spikes of the reference neurons averaged over multiple trials. The blue dots correspond to the averaged time-space occurrence of spikes of the paired neurons (Dragoi et al., 2003). This representation is analogous to simultaneously recording from every neuron in the hippocampus, each representing a single place field, and displaying the spatial-temporal evolution of the correlated ensemble spiking as the rat traverses the corresponding place field of a reference neuron. In Figure 2A, up to nine "clouds" can be recognized, spaced by 110–120 ms intervals, relating to the duration of theta oscillation. Spatial distances were repeatedly represented by the discharges of the partner neurons, beginning ~500 ms before the animal reached the center of the place and lasted for another 500 ms until the rat exited the field. The neuronal sequences were direction specific because distance versus time-lag plots of the same cell pairs poorly correlated on the opposite journey on the track (compare blue and black lines in Figure 2A). The accuracy of predicting the field center gradually increased in subsequent theta cycles as the animal approached it, as indicated by the strongest distance versus time correlation at the central cloud (Figure 2A). The spatial extent of the central cloud was ~40 cm, corresponding to the mean size of a place field in the dorsal hippocampus (Samsonovich and McNaughton, 1997). Because the average walking velocity of the rats on the track was 34 ± 0.21 cm/s, corresponding to ~5 cm per theta cycle, shifting parts of the same field were repeatedly and intermittently represented by the same groups of cells in six to nine subsequent theta cycles (Figure 2A). Because of the large size of the place fields, several place cells were active together in each theta cycle, but the group composition varied from cycle to cycle. The whole extent of the field was represented only once in the central cycle, surrounded by place cells of past and future positions. The similar sequence compression within the past and future clouds, as reflected by their similar axis orientation, is an indication of a relatively fixed temporal relationship among the active neurons. The real-time and theta-scale representations correlated at all distances (Figure 2B). The ratios between real-time and theta time scale representation of distances ("compression") increased with the length of the represented distance (Figure 2C), suggesting that the temporal coordination of neuronal discharges at the theta-scale improved as the animal approached the predicted place.

We addressed the stability of sequence compression by comparing runs in the first and last quarters of the sessions. Although each recording session was preceded by hours of activity in a different environment (i.e., home cage), sequence compression was present in the first quarter of laps and was not different from that of the last quarter (Figure 2D; $p = 0.3$, Z test for two correlation coefficients). This result suggests that once formed, the sequence compression emerges instantaneously in the proper spatial context.

Within sessions, individual place cells exhibited variable firing rates across different laps (Mehta et al., 1997; Fenton and Muller, 1998) (Figure 3A). We exploited this variability to contrast the predictions of the common pacemaker (independent phase-precession) versus coordinated assembly models. In principle, across-lap variability may occur independently within groups of neurons that separately encode nearby spatial positions and are most active on different laps (Samsonovich and McNaughton, 1997). Alternatively, spike activity may be temporally coordinated among sequentially active cell assemblies that bind adjacent locations into larger places on the linear track and whose discharges therefore covary within laps. To distinguish between these possibilities, cell pairs were separated on the basis of their lap-by-lap covariation of firing rates. Pairs with significant within-lap covariation of firing rates at the minute scale (corresponding to trial lengths) were

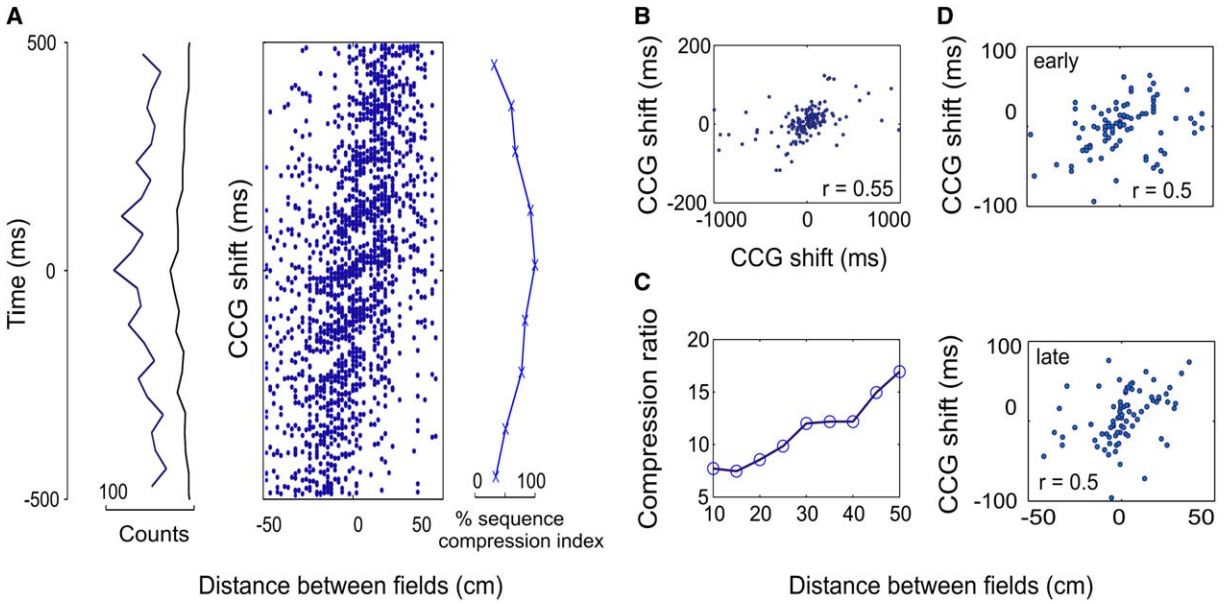

Figure 2. Repeated, Asymmetric, and Compressed Representation of Spatial Sequences by Populations of Place Cells

(A) Prospective (negative values) and retrospective (positive values) repeated encoding of spatial distances (box). Oscillatory (repetitive) asymmetric distribution of short time scale CCG peaks (left histograms), at ~9 Hz (blue line), and representation of distances by the same pairs (black line) recorded during runs in the opposite direction, demonstrating increased asymmetry of the internal representation. Dynamics of sequence compression indices across several cycles (right curve). Values on the x axis represent percentage of the sequence compression index at the central cloud (100%).

(B) Correlation between "real" (x axis) and theta time scale (y axis) CCG peaks of the same place cell pairs ("compression ratio").

(C) Magnitude of compression ratio is proportional with the encoded distance. Each data point was computed as the average compression ratio (y axis) of a subgroup of pairs that have their place field peaks separated by no more than the value displayed on the x axis. For each pair, compression ratio was calculated as the ratio between the temporal bias on the large time scale CCG and the temporal bias on the theta scale CCG.

(D) Sequence compression is present in the first quarter of the session (early) and is similar to the one in the end quarter of the session (late).

termed "dependent," whereas pairs with nonsignificant correlation were termed "independent" pairs. A pair was classified as dependent if its correlation coefficient, calculated over the whole session, was equal to or larger than the maximum of 500 times shuffled data of the same pair (mean r = 0.47 versus mean of the maximum shuffled correlation coefficient for each pair r = 0.33; $p = 10^{-11}$, paired t test) and independent when its correlation coefficient was smaller (Figure 3A). Eighty-one percent of the dependent pairs and 74% of the independent pairs were recorded from different electrodes. The sequence compression index (as calculated in Figure 1G and the central cloud in Figure 2A) in the dependent group (r = 0.82) was significantly larger than in the independent group (r = 0.51; Figures 3B and 3C, top; p = 0.0004; Z test for two correlation coefficients; Figure 3C, bottom; $p = 10^{-20}$, t test). Confining the analysis to dependent pairs recorded from separate electrodes did not affect the correlation values significantly (compare red and black lines in Figure 3C, top).

Although spatial proximity is a potential factor that favors binding of past, present, and future locations, it was not the primary cause of the observed increased correlation for the dependent group. Most of the dependent (90%) and independent (80%) pairs had their peaks separated by no more than 25 cm. For this critical, strongly overlapping range, the distance between place field peaks was similar among the dependent and independent groups (p = 0.073, Kolmogorov-Smirnov test). If spatial proximity were the single cause of sequence compression, one would expect no difference between the dependent and independent pairs with comparable distances. However, when the analysis was confined to these subgroups, the sequence compression index remained significantly higher in the dependent (r = 0.81) versus independent group (r = 0.55) (Figure 3C, top, compare blue and red lines, p = 0.004; Z test for two correlation coefficients).

To examine how well *individual* place cells from the dependent and independent groups predicted position by their firing rate or spike phase, we calculated the in-field peak rate and the correlation coefficient between position and phase of spikes for each neuron (we refer to this as "phase-position correlation"). The peak firing rates and the phase-position correlations were indistinguishable between the two groups (Figure 3D; p = 0.35 and p = 0.1, respectively, ranksum tests). Further control analyses excluded the contribution of four additional individual place cell features as the cause of the significantly larger sequence compression index in the dependent versus independent group. First, the fraction of spikes in burst (<6 ms interspike intervals) was comparable in the two groups (0.21 ± 0.01 versus 0.22 ± 0.01, p = 0.55, ranksum test). No difference was observed in the comparison of the place field lengths (Figure 3D; 50.3 ± 2.4 versus 54.9 ± 2.4 cm, p = 0.44, ranksum test) or the spatial distribution of place field peaks on the track (standard deviation: 71.1 versus 65.3 cm, p = 0.95, Kolmogorov-Smirnov test). In addition, the sequence compression index did not depend on the similarity in

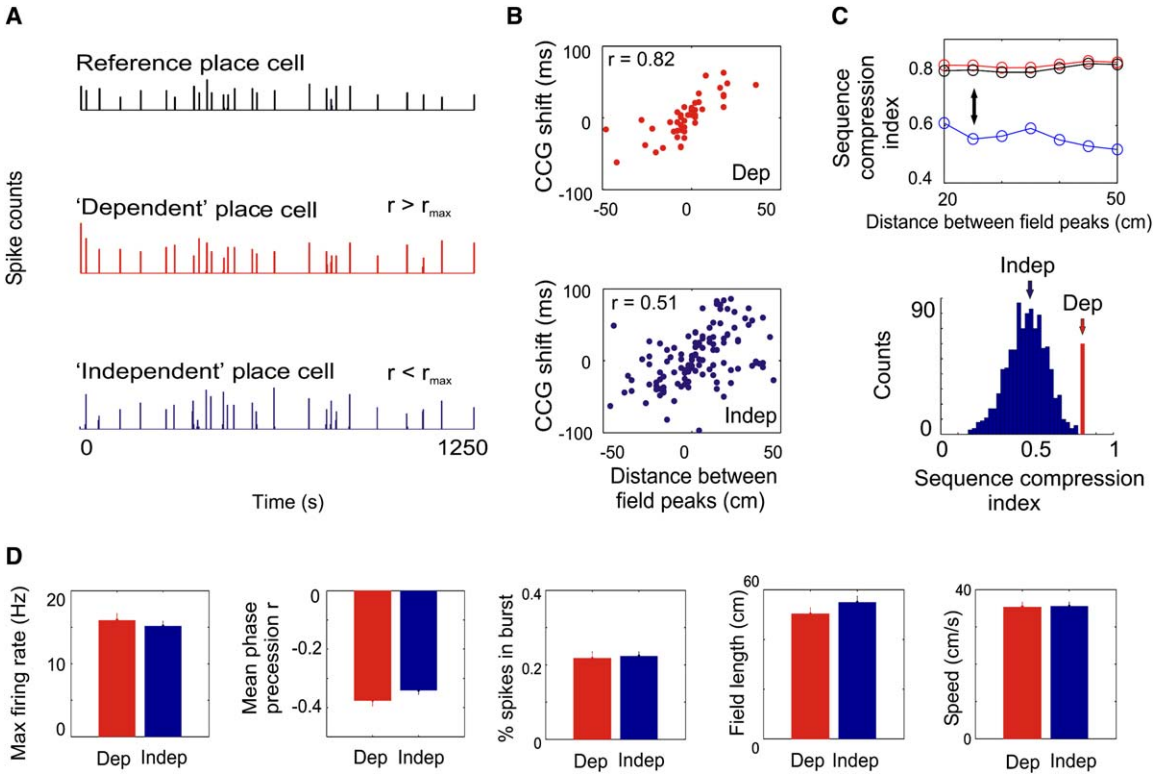

Figure 3. Place Sequences Are Best Represented by Temporal Coordination between Cell Assemblies

(A) Firing rates (counts per 2 s bins) of three place cells in a single session. The reference and "dependent" neuron (red) had a significant correlation of firing rates between laps (r), whereas the "independent" neuron (blue) did not (i.e., $r < r_{max}$). r_{max} = maximum value of the distribution of correlation coefficients between the reference and target cells after 1000 times random shuffling (see Experimental Procedures).

(B) Sequence compression (as in Figure 1G) for "dependent" (dep, red) and "independent" (indep, blue) pair of neurons.

(C) Tests of significance of temporal correlation among dependent (red) versus independent (blue) place cell pairs. (Top) Z test for two correlation coefficients applied to subgroups of data with similar distances between field peaks from the dependent (red) and independent (blue) groups. Arrow marks 25 cm distance between field peaks. In black are values for the dependent group after the elimination of cell pairs recorded by the same electrode. (Bottom) t test. Blue: the distribution of sequence compression indices for the independent pairs calculated repeatedly on a number of data points equal to the number of dependent pairs selected randomly (1000 iterations) from the larger population of independent pairs. Red: correlation value for the dependent pairs. The height of the red bar is magnified 60× for comparison.

(D) Individual cells of the "dependent" (red) and "independent" (blue) groups have similar in-field peak firing rates, phase-position correlation, percent of spikes in burst mode, place field length, and instantaneous speed of the animal while emitting spikes.

Bars are means and error bars are SEM.

slopes of phase precession, as the difference in slopes of dependent (median 2.68°/cm) and independent pair groups (median 2.01°/cm) were similar ($p = 0.59$, ranksum test). Finally, the instantaneous speed of the animal at which spikes were emitted by the included cells was also comparable for the two groups (Figure 3D; 35.25 ± 1.3 versus 35.57 ± 1 cm/s, $p = 0.78$, ranksum test), indicating that activity restricted to a particular area of the track or locations where the animal might have spent more time cannot account for the observed difference between the dependent and independent groups. Altogether, these results support the hypothesis that increased spatial-temporal correlation between dependent cell pairs is not caused by differences in individual place field features or by the animal's different motor behavior but rather by the enhanced temporal coordination among sequentially activated cells.

Firing rates of place cells increase in the rising part and decrease in the falling part of the field. It has been suggested that the linear nature of phase precession of place cell spikes through the entire theta cycle in multiple cells serves to disambiguate the relative position of the animal, in accordance with the common theta drive model (O'Keefe and Recce, 1993; Jensen and Lisman, 2000; Huxter et al., 2003). To compare and contrast the behavior of multiple independent single place cells with the hypothesized coordinated ensemble activity, we calculated the sequence compression index separately from spikes fired by pairs of cells in the rising or falling part of their fields. The sequence compression index was significantly higher during the rising ($r = 0.63$) than in the falling ($r = 0.3$) part (Figure 4A; $p = 0.0007$, Z test for two correlation coefficients). Accordingly, the theta-scale cross-correlograms between spikes fired by neuron pairs during the rising part of the place fields had significantly sharper peaks than those calculated from spikes fired in the falling part (Figure 4B; kurtosis excess for all pairs = −0.42 ± 0.05 and −0.77 ± 0.03, respectively; $p = 10^{-7}$, ranksum test). These findings suggest different degrees of temporal coordination in the two parts of the place field (roughly corresponding to the theta half-cycles, Figure 1C). Since the field theta

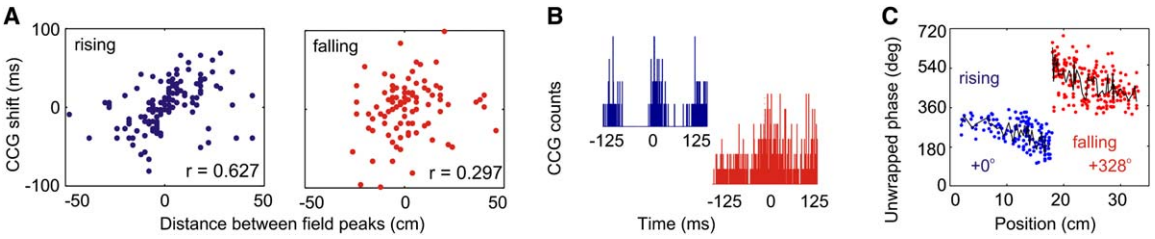

Figure 4. The Accuracy of Spatial Sequence Representation Is Different in the Rising and Falling Parts of the Place Field

(A) Sequence compression index for spikes emitted in the rising (blue) and falling (red) parts of the place field.

(B) Cross-correlograms (CCG) for a representative place cell pair in the rising (blue) versus falling (red) parts of the field. Note stronger modulation of the CCG in the rising part of the place field.

(C) Phase-position correlation plot for the rising (blue) and falling (red) parts of an example place field. Phase was "unwrapped" (O'Keefe and Recce, 1993) separately for each part of the field (values indicated under the data points) until the best position-unwrapped phase correlation was obtained. Black lines, running means for each part of the field.

oscillation remains the same while the rat crosses the entire field, these observations imply forces of coordination other than a common theta drive acting in the two parts of the field, consistent with the assembly/attractor model. On the other hand, several studies have shown that even in individual place cells, spike phase coupling is more reliable while the animal approaches the center of the place field compared to after it passed the field center (Skaggs et al., 1996; Mehta et al., 2002; Yamaguchi et al., 2002). Indeed, several parameters of single-cell activity were also different in the two parts. The phase-position correlation was significantly larger in the rising (−0.35 ± 0.009) than in the falling (−0.30 ± 0.008) part of the fields ($p = 10^{-4}$; ranksum test; an example is shown in Figure 4C). Consistent with this, phase variance was smaller in the rising versus falling part of the field (8571 ± 199 versus 9850 ± 182 deg^2, $p = 3 \times 10^{-6}$, paired t test; Figure 5A), while ordering and binning the data by position estimated a 24% (30.6° ± 3.5°, $p = 10^{-12}$, paired t test) increase in theta phase range (see Experimental Procedures) in the falling part of individual place fields. In addition, the fraction of spikes in bursts was significantly higher in the rising than in the falling part of the fields (0.23 ± 0.009 versus 0.17 ± 0.009; $p = 10^{-4}$, paired t test; Figure 5A). Neither the position variance (95.9 ± 15.7 versus 87.8 ± 11.6 cm^2, see Experimental Procedures) nor the position-phase slope (−4.81 ± 0.24 versus −4.48 ± 0.28°/cm) were different in the rising versus falling part of the fields ($p = 0.67$ and $p = 0.94$, respectively, paired t test; Figure 5A). According to the pacemaker model, the increased phase variability of independent single cells in the falling part of the place field accounts for the decreased sequence compression index. In contrast, the assembly model predicts that both the increased variability in single cells and the decreased sequence compression index reflect a decrease in spike coordination among the assembly members.

To examine whether the significant differences between the two parts of the field arise from a pacemaker mechanism only, we introduced temporal or phase jitter (see Experimental Procedures) to the spike times recorded during the rising part of the place fields to increase their variability (Figure 5B). Adding a 10 ms or 30° jitter to the spikes emitted in the rising part was sufficient to equalize the phase-position correlation (−0.29 ± 0.002, $p = 0.3$, t test), phase variance (9847 ± 35 deg^2, $p = 0.98$, t test), position-phase slope (−4.97 ± 0.04°/cm, $p = 0.65$, t test), and burst fraction (0.17 ± 0.004, $p = 0.54$, t test) with the values calculated from the original (nonjittered) spikes in the falling part of the fields (Figure 5B). Nevertheless, the sequence compression index calculated from the spikes after shuffling in the rising part remained significantly larger compared to the falling part of the place field (0.51 versus 0.30; $p = 10^{-200}$, t test; Figure 5B). Abolishing the difference in spike time coordination between the two parts of the field required a time jitter of at least 35 ms (78% above the observed variability) added to the spikes emitted in the rising part of the field ($r = 0.296$ versus $r = 0.297$; Figure 5B, left arrow; $p > 0.6$, t test). Importantly, the latter time jitter exceeded the physiologically estimated 10–30 ms long "lifetime" of the cell assemblies (Harris et al., 2003). Altogether, these observations indicate that temporal coordination of neurons and distance representation at theta time scale cannot be simply explained by a pacemaker drive of multiple independent phase-precessing cells but rather relies on precise timing among cell assemblies. To test this idea more directly, the cross-correlograms of the 10 ms jittered spikes from the rising part of the fields were compared with the cross-correlograms constructed from the original spike trains of cell pairs in the falling part of the fields. The jittered spikes maintained a significantly better temporal coordination (kurtosis excess = −0.69 ± 0.002, $p = 5 \times 10^{-7}$, ranksum test) than the spikes emitted in the falling part of the fields, despite similar phase-precession profiles. This suggests the existence of a transiently increased temporal correlation among and across assembly members that is more resistant to small perturbations in individual spike trains than their phase relationship to a global theta signal, representing a more robust way of preserving sequences.

Cooperation of CA3 and CA1 Assemblies

Recent studies have emphasized the distinct functional roles of CA3 and CA1 neurons (Leutgeb et al., 2004; Lee et al., 2004a, 2004b). Our findings add further support for the functional differences between these regions and explore their interactions within theta cycle. CA3 place fields were more often bidirectional than CA1 neurons, as measured by the median distance between the place

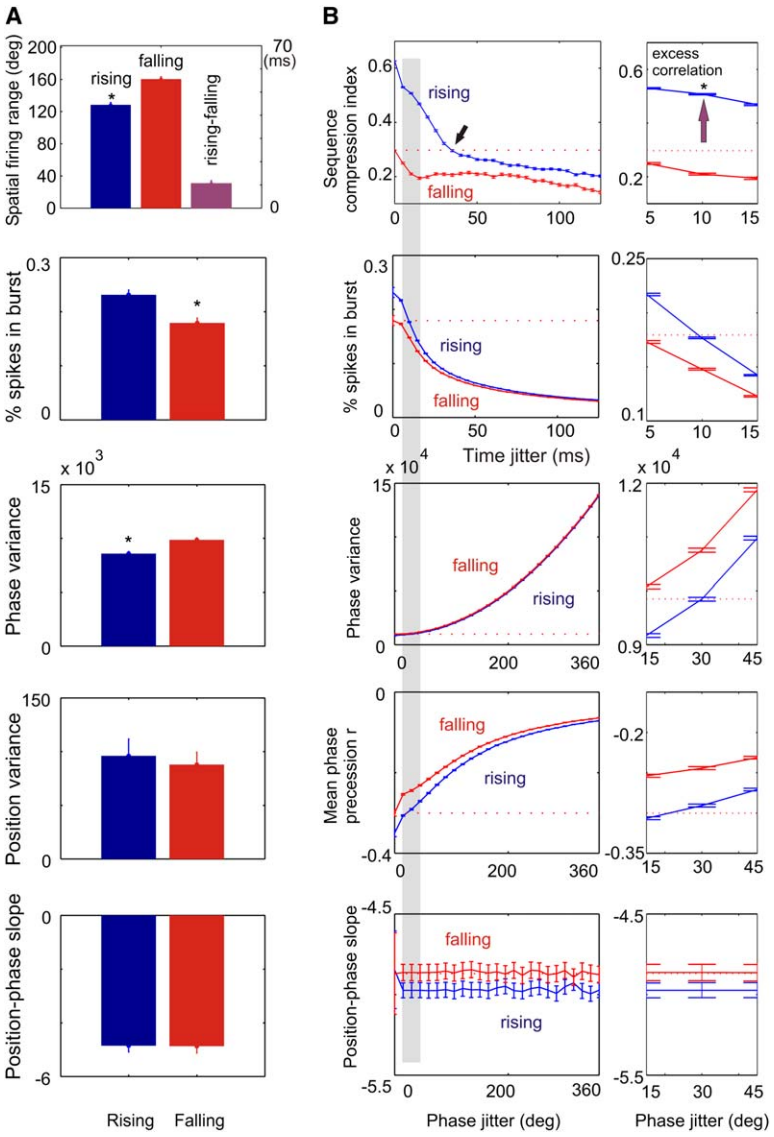

Figure 5. Comparison of Individual Cell and Cell-Pair Features in the Rising and Falling Parts of the Place Field without (Original) and with Spike Time/Phase Jitter

(A) Original spike trains. Blue, rising part; red, falling part of the place field. From top to bottom, averages of phase ranges, burst fraction, phase variance, spike position variance, and place-phase slope. Purple: mean of the paired falling minus rising part differences in phase ranges. Scale on the right y axis is in milliseconds (for 8 Hz theta). Bars are means and error bars are SEM.

(B) Changes in individual cell and cell-pair features as a function of jittered spike times/phases (x axis: 5 ms or 30° steps). Blue, rising part; red, falling part of the place field. (Left) From top to bottom (mean ± SEM): sequence compression index, burst fraction, phase variance, position-phase correlation, and slope of phase-place plot. Red dotted line: nonjittered value for the falling part of the field. Arrow: adding 35 ms jitter to spikes in the rising part of the fields reduced the sequence compression index to that of the nonjittered spikes emitted in the falling part of the field. Gray rectangle, critical time/phase window within which jittered activity in the rising part of the fields becomes similar to the original spike trains in the falling part of the fields. (Right panels) Higher-resolution view of the critical time window. Arrow, "excess" sequence compression index.

field peaks while the rat was running in clockwise and counterclockwise directions (Figure 6A; 37 ± 3.7 cm for CA1, 16 ± 4.8 cm for CA3 neurons; $p = 0.015$, ranksum test). Moreover, the firing rates of place cells in the two directions of movement were significantly more correlated for the CA3 ($r = 0.58$) than the CA1 ($r = 0.35$) place cells ($p = 0.02$; Z test for two correlation coefficients). The phase-position correlation was significantly smaller for the falling part of the field in CA1 pyramidal cells, compared to the rising part ($r = -0.32$ versus $r = -0.37$; $p = 10^{-4}$, ranksum test) and comparable to the correlation coefficients of CA3 neurons in both parts of the field (Figure 6B; $r = -0.28$ versus $r = -0.31$; $p = 0.54$, ranksum test). This pattern of results was not altered when, for each cell, spike phases were referenced to the locally recorded theta signal (in the CA3 or CA1 pyramidal layer) rather than CA1 pyramidal layer (CA1 theta versus local theta: $p > 0.44$, paired t tests). Whereas the firing rates of CA1 pyramidal cells were comparable in the two parts of the field, CA3 neurons were more active in the rising than falling half of the place field (CA3 skewness = −0.14 ± 0.04 versus −0.04 ± 0.03 in CA1; $p = 0.003$, ranksum test; Figure 6C). The increased negative skewness (see also Lee et al., 2004a) and reduced directionality of CA3 versus CA1 neurons suggest that direction of movement and sequential order are specified in a different manner within the two populations of pyramidal cells.

Differences between the two parts of the place field presented above are further supported by the theta scale temporal relationship of CA1 and CA3 pyramidal cells. The two principal cell populations preferentially fired on opposite phases of the theta oscillation in both the rising and falling parts of the place field (Figure 6D). This result suggests that CA3 assemblies predicted the current location of the animal about one-half theta cycle earlier than the CA1 representation and implies that different processes take place across different phases of the theta oscillation (Hasselmo et al., 2002). Despite these differences, spatial distances were represented within and across hippocampal regions by the theta scale temporal lags between CA3-CA3 (15% of all pairs),

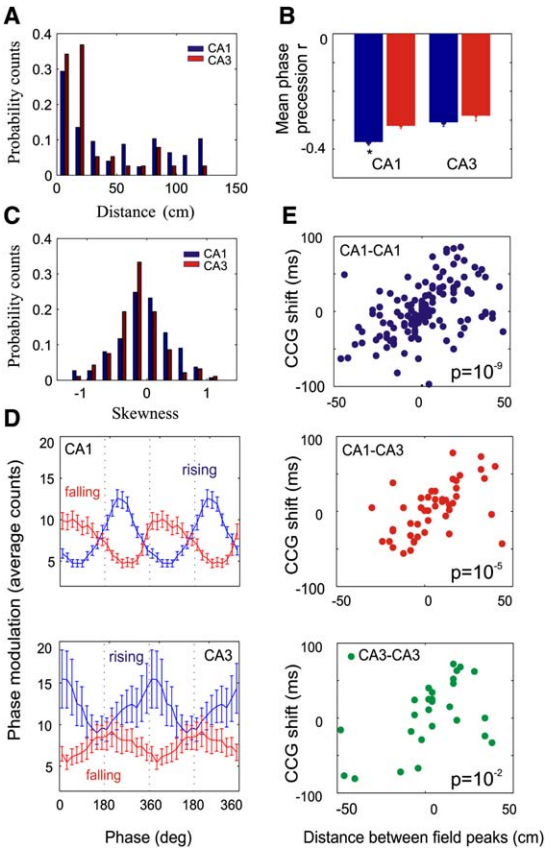

Figure 6. Different Computations in the CA1 and CA3 Regions

(A) Directionality measure, defined as distance between place field peaks of the same cell while the rat is running in clockwise versus counterclockwise directions (normalized). Note reduced directionality of CA3 fields (red) compared to CA1 (blue).

(B) Phase-position correlations for the rising (blue) and falling (red) parts of the place fields for CA1 and CA3 cells (mean ± SEM.). *, significant difference between the two parts ($p = 10^{-4}$, ranksum test).

(C) Increased negative skewness of CA3 (red) versus CA1 (blue) place fields (normalized).

(D) Phase of unit discharge of place cell spikes for the rising (blue) and falling (red) parts of the field for CA1 (left) and CA3 (right) place cells (reference: CA1 pyramidal layer theta). Note nearly opposite phase preference of CA1 and CA3 place cells in both parts of the field. Error bars are SEM.

(E) Sequence compression index for neuron pairs within and across hippocampal subfields.

CA3-CA1 (23%), and CA1-CA1 place cell pairs, as indicated by the significant sequence compression indices in each comparison (Figure 6E).

The peaks of the unit autocorrelograms allowed us to compare the frequency of the oscillating action potential trains across regions and with the field theta rhythm (O'Keefe and Recce, 1993). The frequency of place cell oscillation of both CA1 and CA3 place cells (9.77 ± 0.12 Hz and 10.51 ± 0.28 Hz) was significantly faster than the mean theta frequency in the CA1 pyramidal layer (O'Keefe and Recce, 1993) (7.93 ± 0.15 Hz; $p = 5 \times 10^{-6}$ and $p = 10^{-6}$, respectively, ranksum test). The frequency of spike oscillations of both CA1 and CA3 neurons were comparable in the rising and falling parts of the place field (CA1 cells [n = 123]: 9.78 ± 0.15 Hz and 9.76 ± 0.23 Hz, respectively; CA3 [n = 44 cells]: 10.52 ± 0.34 Hz and 10.06 ± 0.43 Hz, respectively). Nevertheless, analysis of variance revealed a significant group effect (CA3 faster than CA1, p = 0.004), and a post hoc comparison indicated that this difference was due to the higher-frequency oscillatory activity of CA3 neurons in the first half of place fields (p = 0.016, ranksum test).

Discussion

Our findings suggest that sequential but phase-shifted activation of CA3 and CA1 cell assemblies in the hippocampus can maintain past information, identify a current item, predict future ones, and bind them into a sequence. We hypothesize that the sequences are stored in the autoassociative CA3 recurrent and CA3-CA1 collateral systems (Muller et al., 1996; Jensen and Lisman, 1996; Tsodyks, 1999) and are updated by entorhinal cortex-mediated environmental signals (Zugaro et al., 2005; Hafting et al., 2005) according to the following scenario (Figure 7). During each theta cycle, the CA3-CA1 synaptic space is searched, recalling several temporally linked cell assemblies, each representing spatial fields that the rat just passed and would traverse during the next second or so. Therefore, this compression mechanism provides a spatial-temporal context for the current item represented by the most active assembly. The internal sequence readout in the CA3 autoassociator (Kanerva, 1988; Treves and Rolls, 1992) is triggered by the environmental input of the previous locations by way of the entorhinal cortex (Frank et al., 2000; Hafting et al., 2005). The readout is forward in time, reflecting the sequence order during learning. The receptive fields of the cell assemblies are ~40 cm in size and shifted by 4–5 cm, corresponding to the distance moved by the rat in a single theta cycle (Samsonovich and McNaughton, 1997). The predicted and perceived locations are replayed in tandem by the CA3 and CA1 assemblies. The asymmetric nature of spike timing-dependent plasticity (Levy and Steward, 1979; Markram et al., 1997; Magee and Johnston, 1997; Bi and Poo, 1999) favors temporally forward associations in sequentially active assemblies (Mehta et al., 1997). A consequence of the oscillatory temporal organization of cell assemblies is the theta phase precession of spikes of single place cells. We suggest that the overlapping past, present, and future locations are combined into single episodes by sequential CA3 and CA1 assemblies in successive theta cycles. Several computational models and empirical observations are compatible with the above scenario (Hebb, 1949; Levy and Steward, 1979; Lisman and Idiart, 1995; Muller et al., 1996; Jensen and Lisman, 1996; Mehta et al., 1997; Wallenstein and Hasselmo, 1997; Samsonovich and McNaughton, 1997; Tsodyks, 1999; Nakazawa et al., 2002; Brun et al., 2002; Hasselmo et al., 2002; Zugaro et al., 2005).

Temporal Coordination of Position Sequences

The distances between place field centers could be deduced from both the peak firing rates of neuron pairs on the track and their temporal differences at theta time scale. During successive theta cycles, multiple neurons, representing overlapping place fields, shifted together and sustained a temporal order relationship with each

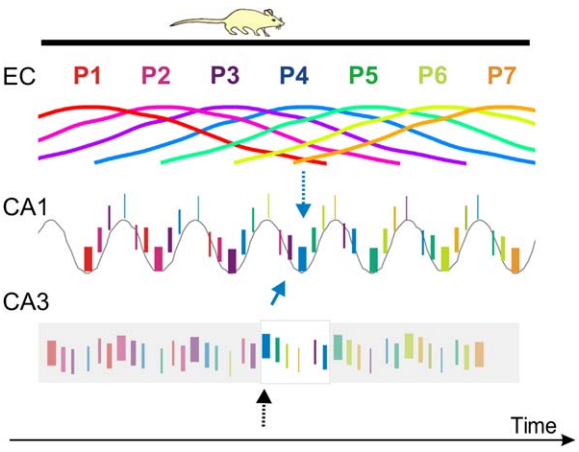

Figure 7. Illustration of the Spatial-Temporal Context and the Interactions among CA3 and CA1 Cell Assemblies

Each position (P1 to P7) is defined by the most active cell assembly firing at the trough of the theta cycle (e.g., P4 by the blue assembly). The width of the bars indicates firing rates of the hypothesized assemblies while the theta time scale temporal differences between assemblies reflect distances of their spatial representations. Because each assembly contributes to multiple place representations, multiple assemblies are coactivated in each theta cycle. As a result, the current position/item, represented by the maximally active assembly at the cycle trough, is embedded in the temporal context of past and future representations. Assembly sequences within theta cycles could reflect strengthening of connections not only between adjacent places/items (e.g., P4-P5) but also between nonadjacent (e.g., P3-P5; P4-P6) items. This mechanism may allow distances to be translated into time and time into synaptic weights. The CA3 and CA1 representations correspond to the predicted (blue solid arrow) and updated positions (blue dotted arrow) by the entorhinal cortex (EC), respectively. One position is indicated by the boxed area. In the CA3 recurrent system, the temporal differences among assembly members are assumed to be reflecting synaptic strengths between assembly members. Black dotted arrow: hypothesized initiation of sequence recall.

other so that the cell that fired on the earliest phase represented a place field whose center the rat visited first. This sequence compression was suggested to be the consequence of spike phase precession of individual neurons, relative to a global theta timing signal (Skaggs et al., 1996). In the simplest case, pyramidal neurons are paced by the interference of two harmonic oscillators with a small period offset, such as the medial septal "pacemaker" input and the entorhinal input (O'Keefe and Recce, 1993). However, without additional mechanisms, the phase interference model cannot explain the phase-shifted sequences of CA3 and CA1 neurons described here or the field size-determined differential slopes of individual place cells. A refined version of the dual-oscillator model operates at a single-cell level. In this case, a transient dendritic depolarization from spatial inputs produces a voltage-dependent oscillation at a frequency slightly faster than the somatic pacemaker theta input (Kamondi et al., 1998; Mehta et al., 2002; Harris et al., 2002). Because neurons with stronger spatial inputs oscillate faster, they have steeper phase precession slopes and smaller place fields. If place cells are sequentially activated on the track, a direct consequence of the single-cell model of spike phase precession is the theta time scale temporal correlation between neuron pairs with overlapping place fields. However, because the pacemaker interference models do not assume direct interactions among the place cells, the "ideal" phase precession slope for a single place neuron in any given trial would be that of the average slope across all trials. According to this model, the correlation between distances of place fields and the time/phase differences of place neurons at the theta time scale should arise from externally regulated timing mechanisms (Jensen and Lisman, 2000).

Our findings showed a significantly better temporal coordination among place cells than predicted by the phase interference pacemaker models. This is not surprising, because hippocampal neurons are embedded in an interactive synaptic environment, and the timing of their action potentials is biased not only by theta oscillation pacing but also by all their synaptically connected and spiking peers (Harris et al., 2003). The great majority of intrahippocampal synapses is established by the collateral system of CA3 neurons (Amaral and Witter, 1989; Li et al., 1994), and it has been hypothesized that distances between place fields are encoded in the synaptic strengths between CA3-CA3 and CA3-CA1 neuron pairs (Muller et al., 1996). The excess temporal correlations, therefore, may be explained by the experience-dependent modification of synaptic strengths during the initial exploration of the maze.

Our alternative hypothesis for the theta time scale correlation among neurons is that sequential positions on the track are represented by unique sets of cell assemblies, and phase precession of spikes is a result of temporally coordinated activity within and between anatomically distributed groups of sequentially activated cell assemblies. A key mechanism in this process is the ability of the CA3 collateral system to support theta oscillation (Konopacki et al., 1988; Fisahn et al., 1998; Kocsis et al., 1999). While the rat is traversing the track, unique combinations of pyramidal cells are active in successive theta cycles. The most active group at the trough of the theta cycle (in the CA1 pyramidal layer) defines the current location, flanked by spikes of other neurons on the descending and ascending phases of theta, representing past and future locations, respectively. We hypothesize that as the rat moves forward, neurons on the ascending phase are attracted to the trough to represent a new location because the oscillating assembly representing the current position exerts an excitation on the trailing groups of neurons and advances their phase (Williams et al., 1990). The synaptic strengths among member neurons of an assembly, representing the same location and discharging within the same gamma cycle (Lisman and Idiart, 1995; Harris et al., 2003), determines the place field size and, consequently, the slope of the spike phase precession of the participating member neurons. Synaptic strengths across assemblies, representing different locations and discharging in different gamma cycles, can determine both their time/phase differences within the theta cycle and the distances between the respective place fields. In addition, the oscillating assemblies may also be responsible for the temporal coordination of medial septal neurons by way of the hippocampo-septally projecting inhibitory interneurons (Dragoi et al., 1999; Wang, 2002; Gulyas et al.,

2003). The self-organized assembly model is supported by the empirical observation that the learned neuronal sequences of place fields are spontaneously replayed during immobility and sleep-related sharp wave bursts (Wilson and McNaughton, 1994; Nadasdy et al., 1999; Lee and Wilson, 2002) without extrahippocampal influences at a time scale slightly faster than during a given theta cycle. The sharp wave-related activity may represent a mechanism for stabilization of assembly sequences (Buzsaki, 1989; Samsonovich and Ascoli, 2005). The observation that artificial plastic alteration of intrahippocampal connectivity can modify previously learned neuronal sequences of place fields (Dragoi et al., 2003) provides further support for the assembly model. However, the internally coordinated assembly model alone cannot account for the phase-shifted activity of CA3 and CA1 cell assemblies.

Complementary Representation of Place Sequences in CA1 and CA3 Regions

In the behaving animal, the concurrently active CA3 place cells are an important source of the intrahippocampal theta and gamma rhythms (Kocsis et al., 1999; Csicsvari et al., 2003). The excitatory CA3 recurrent collaterals activate and coordinate interneurons in both the CA3 and CA1 regions, building up temporally covarying inhibition and gamma power nested within the theta cycles (Csicsvari et al., 2003). Maximum inhibition and gamma frequency power occur simultaneously in the two regions, but coupled to the opposite phases of the respective local theta cycles. As a result, CA1 neurons can discharge maximally when their perisomatic inhibition is weakest, likely activated by the direct entorhinal input (Brun et al., 2002). The CA3 input can assist in this process by at least two different ways. First, the CA3 generated feedforward inhibition can facilitate rebound discharges of CA1 place cells (Cobb et al., 1995). Second, CA3 afferents can convert the dominant feedforward inhibition of the entorhinal input to excitation. In vitro experiments showed that electrical stimulation of the entorhinal input typically evokes hyperpolarization in CA1 pyramidal cells. However, when the entorhinal input is activated 40–60 ms (i.e., half of the theta cycle) after stimulating the CA3 afferents, the hyperpolarization was converted into depolarization and discharge of the cell, due to a transient activation of NMDA receptors and decreased release of GABA from the inhibitory terminals (Ang et al., 2005).

The systems implication of the above findings is that the most active CA3 assembly in a given theta cycle represents the predicted location of the rat's head in the next half of the theta cycle. If the layer 3 entorhinal input, mediating the environmental effects (Hafting et al., 2005), "matches" the internal prediction, the CA1 pyramidal cells will respond. However, if the prediction is not confirmed, the entorhinal input remains ineffective. By temporally interleaving the entorhinal cortex-mediated input with the CA3-generated assembly sequences, the discharging CA1 pyramidal cells can provide an update of position information in each theta cycle (Zugaro et al., 2005). Viewed from this perspective, the CA3 and CA1 systems operate as a functional unit during theta oscillation.

Theta Cycle Compression of Sequences and Episodic Memory

An interesting and challenging question in hippocampal research is how a given physiological mechanism that evolved in a small-brain animal (e.g., navigation in physical space) can be employed for more complex tasks in humans (e.g., memory storage and retrieval). A route passed by the rat in a simple maze can be tracked by calculating the distances between cues, using self-generated signals and time by a mechanism referred to as dead reckoning or path integration navigation (McNaughton et al., 1996). There are many parallels between path integration and episodic memory (Buzsaki, 2005). First, return to the home base by path integration is possible after a single exploration. Similarly, episodic learning usually requires a single trial. Second, both path integration and episodic memory are self-referenced and both require a spatio-temporal context (Tulving, 1972; Squire, 1992). Third, both processes rely on sequential information, primarily on the temporal relationship between successive items. Fourth, in episodic learning, stronger associations are formed between stimuli that occur near each other in time, compared to those that are separated by a greater interval, although temporal links are established in both cases. Finally, in learning, forward serial associations are stronger than backward associations (Tulving, 1969; Kahana, 1996; Fortin et al., 2004; Howard et al., 2005). The neuronal firing patterns observed physiologically in the rat hippocampus could account for these behavioral observations in humans. The temporal relationship between neuron pairs was dramatically different in the opposite directions of locomotion (McNaughton et al., 1983). The position sequences in the maze were compressed into single theta cycles, i.e., within the time window of spike timing-dependent plasticity. The temporally compressed representation of distances can facilitate the association of not only immediately adjacent positions but also integrates nonadjacent ones (higher-order relations) because what matters for the strengthening of synapses is the temporal interval between the spikes in the pre- and postsynaptic neurons (Levy and Steward, 1979). Testing of free recall of the learned episodes in rats is difficult because the animals are exposed to the same environment in repeated trials. Nevertheless, the time compression of spikes into single theta cycles and the phase shifts of cells assemblies in the CA3 and CA1 regions indicate that hippocampal neurons do not simply represent the sensory environment, but generate sequence information required for both path integration and episodic memory.

Experimental Procedures

Four male Sprague-Dawley rats were implanted with eight independently movable tetrodes in the dorsal hippocampus. Surgery, recording, behavioral training, and unit separation were as described earlier (Dragoi et al., 2003). A total of 391 place fields in both directions were analyzed in this study, 298 fields from 193 CA1 place cells and 93 from 63 CA3 cells.

Theta Phase Analyses

The theta phase of unit firing was determined by a Hilbert transform (Harris et al., 2003), after filtering the EEG in the theta range (6–10 Hz). The phase preference of unit discharge for rising/falling parts

of the field of place cells was calculated using a unique reference theta EEG signal recorded from the CA1 pyramidal layer as confirmed histologically and physiologically by the presence of many active pyramidal cells and large-amplitude ripples at rest. Phase histograms were constructed for each cell using 20° bins, and the significant histograms ($p < 0.005$, Rayleigh test) were averaged, and mean and standard errors were calculated for each bin. Phase-position correlations and slopes were calculated using circular statistics (O'Keefe and Recce, 1993; Huxter et al., 2003) on at least 100 data points (50 for half-fields). For each place cell and for the whole session, the position of the spikes was plotted against their phase, separately for the rising and falling part of the field after maximizing the corresponding phase-position correlation considering the circular nature of the phase (see Figure 4C). From the beginning to peak and peak to end of the place field, a phase range was calculated for each nonoverlapping subgroup of four consecutive data points (bin size = four points). The median of the distribution of phase ranges, calculated for the rising versus falling part of the field for each cell, was used further for comparison. The spatial size of each bin was similar for the inbound and outbound portions of the field (0.31 ± 0.02 cm inbound and 0.34 ± 0.02 cm outbound; $p = 0.3$, paired t test). Phase variance and position versus phase slopes (slope of the least-squares linear regression line) were calculated after maximizing the corresponding phase-position correlation, considering the circular nature of phase. Spike position variance was calculated as the variance of the distribution of on-track spatial positions (distance in centimeters from the beginning of the track) corresponding to the emitted spikes. For computing the average theta frequency, theta oscillation epochs were detected (Dragoi et al., 2003), power spectrum was calculated for the entire session, and the local frequency maximum in the theta range (6–10 Hz) was detected.

Cross-Correlation and Sequence Compression Analyses

"Real-time" scale cross-correlograms (CCGs) between cell pairs were calculated in 3 s windows with 3 ms bin size. The single peak on the CCG was detected after low-pass filtering below 1.5 Hz. The theta time scale CCGs were calculated in 350 ms or 1 s (Figure 2A) windows, with 1 ms bin size. Fast CCG peaks were detected in 50 ms windows after filtering below 40 Hz. CCGs with <1 count/ms or with no significant peak (< mean + 1.5 SD for CA1-CA1 and CA3-CA1 pairs; +1 SD for CA3-CA3 pairs; +0.5 SD for rising/falling parts of the field and for first/last quarters of sessions) were discarded. Autocorrelograms (ACGs) were calculated as described above for the CCGs in 1 s windows. The time lag between the two largest peaks (low pass 40 Hz) was calculated and converted into frequency to compute place cell oscillation frequency. Distances between any two locations were calculated as the difference between the positions of the peaks of the two place fields, defined by the maximum firing rates. Both the spatial distance versus CCG time-lag correlations (sequence compression indices) and the position-phase correlation coefficients were calculated using Spearman's rank correlation. Sessions were divided into quarters by laps. The average number of laps in each direction was 32.5.

Dependent/Independent Pairs Analyses

For the detection of "dependent" pairs, spike times of each cell were binned at 2 s such that the entire rate activity on a lap was compressed in one bin (or occasionally two adjacent bins). After excluding the common zero-value bins, for all cell pairs, a correlation coefficient was calculated between the binned activities of the pair members. This measure reflected the degree of coactivation of neuron pairs on multiple trials and was thus independent from the fine temporal analysis of the CCG. The correlation coefficient was subsequently compared with a distribution of correlation values obtained by time shuffling the nonzero bins of one member of the pair 500 times. The criterion of "dependent pair" was met for each individual pair when the data-based correlation coefficient was larger or equal than the maximum of the distribution of shuffled values for that pair. The use of a qualitative criterion for pair separation leading to noncontinuous variables was imposed by the fact that sequence compression index reflects a group value while dependence/independence (coordination index) is calculated for each pair of neurons. Computing a one-to-one correlation between sequence compression and dependence as a continuous variable was thus not possible. Using the criterion of absolute value of the lap-by-lap correlation coefficient to arbitrarily create several groups of cell pairs indicated the possibility of a nonlinear relationship between correlation coefficients and sequence compression index. Because the number of dependent pairs was smaller than that of independent pairs, the value of the sequence compression index for the dependent pairs (one value for the whole group of pairs) was compared (t test) with a population (distribution) of indices created using an equal number of data points with the dependent group selected randomly (1000 iterations) from the larger population of independent pairs (Figure 3C, bottom). Skewness was calculated as the ratio between the third central moment and the cube of the standard deviation. Kurtosis was calculated as the ratio between the fourth central moment and the fourth power of the standard deviation. Kurtosis excess is generally a measure of "peakedness" of a distribution. In our case, the closest to zero "cycle" of the oscillatory theta scale CCG (see Figure 1F) was treated as a distribution whose kurtosis excess value measured how sharp/precise the CCG/temporal coordination was. The length of place field was generally defined as the distance (in centimeters) between the two borders of the place field (places where the rate was more than 10% of the peak firing rate). Burst events were defined as spikes emitted within 6 ms interspike intervals. Instantaneous velocity of the animal was determined separately for each place cell, by dividing the length of its field by the time it took the animal to traverse it.

Time/Phase Jitter Analyses

The time (phase) jitter of spikes was performed by adding to the original spike time epochs (phases)—for each spike time (phase) individually—of a value extracted from a random normal population of time intervals (phase values) with mean zero and standard deviation equal with the value of the time (phase) jitter. The procedure was repeated 500 times for each value of the jitter: 5–125 ms in 5 ms increments (time), or 15° to 360° in 15° increments (phase).

Acknowledgments

We thank S. Tonegawa for his support and discussions; and M.A. Wilson for discussions. We also thank N. Kopell and J.E. Lisman for comments on an earlier version of the manuscript; and D. Nguyen for technical advice. Supported by grants from the NIH. The authors declare that they have no competing financial interest.

Received: November 3, 2005
Revised: January 3, 2006
Accepted: February 16, 2006
Published: April 5, 2006

References

Amaral, D.G., and Witter, M.P. (1989). The three-dimensional organization of the hippocampal formation: a review of anatomical data. Neuroscience *31*, 571–591.

Ang, C.W., Carlson, G.C., and Coulter, D.A. (2005). Hippocampal CA1 circuitry dynamically gates direct cortical inputs preferentially at theta frequencies. J. Neurosci. *25*, 9567–9580.

Bi, G., and Poo, M. (1999). Distributed synaptic modification in neural networks induced by patterned stimulation. Nature *401*, 792–796.

Brun, V.H., Otnass, M.K., Molden, S., Steffenach, H.A., Witter, M.P., Moser, M.B., and Moser, E.I. (2002). Place cells and place recognition maintained by direct entorhinal-hippocampal circuitry. Science *296*, 2243–2246.

Buzsaki, G. (1989). Two-stage model of memory trace formation: a role for "noisy" brain states. Neuroscience *31*, 551–570.

Buzsaki, G. (2005). Theta rhythm of navigation: link between path integration and landmark navigation, episodic and semantic memory. Hippocampus *15*, 827–840.

Cobb, S.R., Buhl, E.H., Halasy, K., Paulsen, O., and Somogyi, P. (1995). Synchronization of neuronal activity in hippocampus by individual GABAergic interneurons. Nature *378*, 75–78.

Csicsvari, J., Jamieson, B., Wise, K.D., and Buzsaki, G. (2003). Mechanisms of gamma oscillations in the hippocampus of the behaving rat. Neuron *37*, 311–322.

Dragoi, G., Carpi, D., Recce, M., Csicsvari, J., and Buzsaki, G. (1999). Interactions between hippocampus and medial septum during sharp waves and theta oscillation in the behaving rat. J. Neurosci. *19*, 6191–6199.

Dragoi, G., Harris, K.D., and Buzsaki, G. (2003). Place representation within hippocampal networks is modified by long-term potentiation. Neuron *39*, 843–853.

Eichenbaum, H., Dudchenko, P., Wood, E., Shapiro, M., and Tanila, H. (1999). The hippocampus, memory, and place cells: is it spatial memory or a memory space? Neuron *23*, 209–226.

Fenton, A.A., and Muller, R.U. (1998). Place cell discharge is extremely variable during individual passes of the rat through the firing field. Proc. Natl. Acad. Sci. USA *95*, 3182–3187.

Fisahn, A., Pike, F.G., Buhl, E.H., and Paulsen, O. (1998). Cholinergic induction of network oscillations at 40 Hz in the hippocampus in vitro. Nature *394*, 186–189.

Fortin, N.J., Wright, S.P., and Eichenbaum, H. (2004). Recollection-like memory retrieval in rats is dependent on the hippocampus. Nature *431*, 188–191.

Frank, L.M., Brown, E.N., and Wilson, M. (2000). Trajectory encoding in the hippocampus and entorhinal cortex. Neuron *27*, 169–178.

Gulyas, A.I., Hajos, N., Katona, I., and Freund, T.F. (2003). Interneurons are the local targets of hippocampal inhibitory cells which project to the medial septum. Eur. J. Neurosci. *17*, 1861–1872.

Hafting, T., Fyhn, M., Molden, S., Moser, M.B., and Moser, E.I. (2005). Microstructure of a spatial map in the entorhinal cortex. Nature *436*, 801–806.

Harris, K.D., Henze, D.A., Hirase, H., Leinekugel, X., Dragoi, G., Czurko, A., and Buzsaki, G. (2002). Spike train dynamics predicts theta-related phase precession in hippocampal pyramidal cells. Nature *417*, 738–741.

Harris, K.D., Csicsvari, J., Hirase, H., Dragoi, G., and Buzsaki, G. (2003). Organization of cell assemblies in the hippocampus. Nature *424*, 552–556.

Hasselmo, M.E., Bodelon, C., and Wyble, B.P. (2002). A proposed function for hippocampal theta rhythm: separate phases of encoding and retrieval enhance reversal of prior learning. Neural Comput. *14*, 793–817.

Hebb, D.O. (1949). The Organization of Behavior: A Neuropsychological Theory (New York: Wiley).

Howard, M.W., Fotedar, M.S., Datey, A.V., and Hasselmo, M.E. (2005). The temporal context model in spatial navigation and relational learning: toward a common explanation of medial temporal lobe function across domains. Psychol. Rev. *112*, 75–116.

Huxter, J., Burgess, N., and O'Keefe, J. (2003). Independent rate and temporal coding in hippocampal pyramidal cells. Nature *425*, 828–832.

Jensen, O., and Lisman, J.E. (2000). Position reconstruction from an ensemble of hippocampal place cells: contribution of theta phase coding. J. Neurophysiol. *83*, 2602–2609.

Jensen, O., and Lisman, J.E. (1996). Hippocampal CA3 region predicts memory sequences: accounting for the phase precession of place cells. Learn. Mem. *3*, 279–287.

Kahana, M.J. (1996). Associative retrieval processes in free recall. Mem. Cognit. *24*, 103–109.

Kamondi, A., Acsady, L., Wang, X.J., and Buzsaki, G. (1998). Theta oscillations in somata and dendrites of hippocampal pyramidal cells in vivo: activity-dependent phase-precession of action potentials. Hippocampus *8*, 244–261.

Kanerva, P. (1988). Sparse Distributed Memory (Cambridge, MA: MIT Press).

Kocsis, B., Bragin, A., and Buzsaki, G. (1999). Interdependence of multiple theta generators in the hippocampus: a partial coherence analysis. J. Neurosci. *19*, 6200–6212.

Konopacki, J., Bland, B.H., and Roth, S.H. (1988). Carbachol-induced EEG 'theta' in hippocampal formation slices: evidence for a third generator of theta in CA3c area. Brain Res. *451*, 33–42.

Lee, A.K., and Wilson, M.A. (2002). Memory of sequential experience in the hippocampus during slow wave sleep. Neuron *36*, 1183–1194.

Lee, I., Rao, G., and Knierim, J.J. (2004a). A double dissociation between hippocampal subfields: differential time course of CA3 and CA1 place cells for processing changed environments. Neuron *42*, 803–815.

Lee, I., Yoganarasimha, D., Rao, G., and Knierim, J.J. (2004b). Comparison of population coherence of place cells in hippocampal subfields CA1 and CA3. Nature *430*, 456–459.

Leutgeb, S., Leutgeb, J.K., Treves, A., Moser, M.B., and Moser, E.I. (2004). Distinct ensemble codes in hippocampal areas CA3 and CA1. Science *305*, 1295–1298.

Levy, W.B., and Steward, O. (1979). Synapses as associative memory elements in the hippocampal formation. Brain Res. *175*, 233–245.

Li, X.G., Somogyi, P., Ylinen, A., and Buzsaki, G. (1994). The hippocampal CA3 network: an in vivo intracellular labeling study. J. Comp. Neurol. *339*, 181–208.

Lisman, J.E., and Idiart, M.A. (1995). Storage of 7 +/− 2 short-term memories in oscillatory subcycles. Science *267*, 1512–1515.

Magee, J.C., and Johnston, D. (1997). A synaptically controlled, associative signal for Hebbian plasticity in hippocampal neurons. Science *275*, 209–213.

Markram, H., Lubke, J., Frotscher, M., and Sakmann, B. (1997). Regulation of synaptic efficacy by coincidence of postsynaptic APs and EPSPs. Science *275*, 213–215.

McNaughton, B.L., Barnes, C.A., and O'Keefe, J. (1983). The contributions of position, direction, and velocity to single unit activity in the hippocampus of freely-moving rats. Exp. Brain Res. *52*, 41–49.

McNaughton, B.L., Barnes, C.A., Gerrard, J.L., Gothard, K., Jung, M.W., Knierim, J.J., Kudrimoti, H., Qin, Y., Skaggs, W.E., Suster, M., and Weaver, K.L. (1996). Deciphering the hippocampal polyglot: the hippocampus as a path integration system. J. Exp. Biol. *199*, 173–185.

Mehta, M.R., Barnes, C.A., and McNaughton, B.L. (1997). Experience-dependent, asymmetric expansion of hippocampal place fields. Proc. Natl. Acad. Sci. USA *94*, 8918–8921.

Mehta, M.R., Lee, A.K., and Wilson, M.A. (2002). Role of experience and oscillations in transforming a rate code into a temporal code. Nature *417*, 741–746.

Muller, R.U., Stead, M., and Pach, J. (1996). The hippocampus as a cognitive graph. J. Gen. Physiol. *107*, 663–694.

Nadasdy, Z., Hirase, H., Czurko, A., Csicsvari, J., and Buzsaki, G. (1999). Replay and time compression of recurring spike sequences in the hippocampus. J. Neurosci. *19*, 9497–9507.

Nakazawa, K., Quirk, M.C., Chitwood, R.A., Watanabe, M., Yeckel, M.F., Sun, L.D., Kato, A., Carr, C.A., Johnston, D., Wilson, M.A., and Tonegawa, S. (2002). Requirement for hippocampal CA3 NMDA receptors in associative memory recall. Science *297*, 211–218.

O'Keefe, J., and Nadel, L. (1978). The Hippocampus as a Cognitive Map (Oxford: Oxford University Press).

O'Keefe, J., and Recce, M.L. (1993). Phase relationship between hippocampal place units and the EEG theta rhythm. Hippocampus *3*, 317–330.

Redish, A.D., and Touretzky, D.S. (1997). Cognitive maps beyond the hippocampus. Hippocampus *7*, 15–35.

Samsonovich, A., and McNaughton, B.L. (1997). Path integration and cognitive mapping in a continuous attractor neural network model. J. Neurosci. *17*, 5900–5920.

Samsonovich, A.V., and Ascoli, G.A. (2005). A simple neural network model of the hippocampus suggesting its pathfinding role in episodic memory retrieval. Learn. Mem. *12*, 193–208.

Scoville, W.B., and Milner, B. (1957). Loss of recent memory after bilateral hippocampal lesions. J. Neurol. Neurosurg. Psychiatry *20*, 11–21.

Skaggs, W.E., McNaughton, B.L., Wilson, M.A., and Barnes, C.A. (1996). Theta phase precession in hippocampal neuronal populations and the compression of temporal sequences. Hippocampus *6*, 149–172.

Squire, L.R. (1992). Memory and the hippocampus: a synthesis from findings with rats, monkeys, and humans. Psychol. Rev. *99*, 195–231.

Treves, A., and Rolls, E.T. (1992). Computational constraints suggest the need for two distinct input systems to the hippocampal CA3 network. Hippocampus *2*, 189–199.

Tsodyks, M. (1999). Attractor neural network models of spatial maps in hippocampus. Hippocampus *9*, 481–489.

Tsodyks, M.V., Skaggs, W.E., Sejnowski, T.J., and McNaughton, B.L. (1996). Population dynamics and theta rhythm phase precession of hippocampal place cell firing: a spiking neuron model. Hippocampus *6*, 271–280.

Tulving, E. (1969). Retrograde amnesia in free recall. Science *164*, 88–90.

Tulving, E. (1972). Episodic and semantic memory. In Organization of Memory, D.W. Tulving, ed. (New York: Academic), pp. 382–403.

Wallenstein, G.V., and Hasselmo, M.E. (1997). GABAergic modulation of hippocampal population activity: sequence learning, place field development, and the phase precession effect. J. Neurophysiol. *78*, 393–408.

Wang, X.J. (2002). Pacemaker neurons for the theta rhythm and their synchronization in the septohippocampal reciprocal loop. J. Neurophysiol. *87*, 889–900.

Williams, T.L., Sigvardt, K.A., Kopell, N., Ermentrout, G.B., and Remler, M.P. (1990). Forcing of coupled nonlinear oscillators: studies of intersegmental coordination in the lamprey locomotor central pattern generator. J. Neurophysiol. *64*, 862–871.

Wills, T.J., Lever, C., Cacucci, F., Burgess, N., and O'Keefe, J. (2005). Attractor dynamics in the hippocampal representation of the local environment. Science *308*, 873–876.

Wilson, M.A., and McNaughton, B.L. (1993). Dynamics of the hippocampal ensemble code for space. Science *261*, 1055–1058.

Wilson, M.A., and McNaughton, B.L. (1994). Reactivation of hippocampal ensemble memories during sleep. Science *265*, 676–679.

Yamaguchi, Y., Aota, Y., McNaughton, B.L., and Lipa, P. (2002). Bimodality of theta phase precession in hippocampal place cells in freely running rats. J. Neurophysiol. *87*, 2629–2642.

Zugaro, M.B., Monconduit, L., and Buzsaki, G. (2005). Spike phase precession persists after transient intrahippocampal perturbation. Nat. Neurosci. *8*, 67–71.

Neuron, Vol. 39, 843–853, August 28, 2003, Copyright ©2003 by Cell Press

Place Representation within Hippocampal Networks Is Modified by Long-Term Potentiation

George Dragoi,[1] Kenneth D. Harris, and György Buzsáki*
Center for Molecular and Behavioral Neuroscience
Rutgers
The State University of New Jersey
Newark, New Jersey 07102

Summary

In the brain, information is encoded by the firing patterns of neuronal ensembles and the strength of synaptic connections between individual neurons. We report here that representation of the environment by "place" cells is altered by changing synaptic weights within hippocampal networks. Long-term potentiation (LTP) of intrinsic hippocampal pathways abolished existing place fields, created new place fields, and rearranged the temporal relationship within the affected population. The effect of LTP on neuron discharge was rate and context dependent. The LTP-induced "remapping" occurred without affecting the global firing rate of the network. The findings support the view that learned place representation can be accomplished by LTP-like synaptic plasticity within intrahippocampal networks.

Introduction

Information in the brain is believed to be encoded and stored by the strength of synaptic weights within networks of connected neurons (Fregnac et al., 1988; Bliss and Collingridge, 1993; Martin et al., 2000; Kandel and Squire, 2000). A classic example of the representation of the environment is place-related activity of hippocampal pyramidal neurons (O'Keefe and Nadel, 1978). It has been hypothesized that the physical map of the environment is represented by the synaptic connectivity within the hippocampal neuronal populations (Wilson and McNaughton, 1993; Muller et al., 1996). Indeed, the firing patterns of pyramidal cells remain stable in a familiar environment for extended periods and new map representations emerge over time in a novel environment (Thompson and Best, 1990; Wilson and McNaughton, 1993; Lever et al., 2002). A leading candidate mechanism responsible for such stability and respective change of neuronal firing patterns is use-dependent synaptic plasticity. A laboratory model of synaptic plasticity is long-term potentiation (LTP) (Bliss and Lomo, 1973; Malenka and Nicoll, 1999; Kandel and Squire, 2000). There is controversy regarding the effects of LTP on neuronal firing as well as on solving spatial memory tasks. LTP of synaptic inputs has been associated with increased population spike and increased probability of action potential discharge to test stimulation (Taube and Schwartzkroin, 1988; Chavez-Noriega et al., 1990). Furthermore, the spontaneous firing of unidentified dentate neurons was increased after perforant path LTP (Deadwyler et al., 1976). In later experiments, however, LTP did not induce an overall increase in firing rate in anesthetized animals, even when only neurons discharged by the pre-LTP test pulse stimulation were considered (Martin and Shapiro, 2000; Kimura and Pavlides, 2000).

Numerous experiments demonstrate that various manipulations that affect electrically induced LTP also have an impact on the execution of spatial memory tasks (Morris et al., 1986; Silva et al., 1992; Kentros et al., 1998; Moser et al., 1998; Nakazawa et al., 2002). However, whether and how LTP exerts an impact on the firing patterns and place-related features of neuronal assemblies is not known. We hypothesized that if spatial representation is embedded in the weights of synaptic connectivity within hippocampal networks, then alterations of these connections by artificial stimulation should lead to the disappearance of established place fields and appearance of novel place fields even in a familiar environment.

Results

Because tetanic stimulation of hippocampal pathways induces long-term enhancement of evoked activity (Bliss and Lomo, 1973), we first examined whether induction of LTP affects the global excitability of the hippocampal network as measured by the firing rates of hippocampal neurons. High-frequency stimulation of the ventral hippocampal commissure (VHC) resulted in a long-lasting change of the slope of the evoked field responses measured in CA3 and CA1 pyramidal layers (Figure 1A). The evoked responses were periodically tested before and after the LTP train in the home cage with 10–20 pulses at 0.1 Hz and averaged. These test periods were exluded from the sleep periods over which firing rates were calculated. Responses at the various recording sites were affected differentially (Figure 1B). In some rats, enhancement at some sites was accompanied by a decrease at other sites. LTP, measured at the most effective site, varied from 12% to 107% (median, 37%, measured at 60–90 min after LTP induction; $p < 0.05$; Figure 1A, bottom; $n = 7$ rats) and in most cases lasted over 6 hr ($p < 0.05$). In contrast to the potentiated evoked potentials, the spontaneous firing rate of the total neuronal population, measured during the last sleep epoch before (30 min) and the first sleep epoch after (30 min) LTP induction ($n = 229$ CA1 pyramidal cells, $n = 171$ CA3 pyramidal cells, $n = 64$ CA1-3 interneurons, $n = 7$ rats), remained unchanged for all cell types (Figure 1C; $p > 0.05$, sign test), confirming previous observations in anesthetized animals (Martin and Shapiro, 2000; Kimura and Pavlides, 2000) and in rats exposed to a novel environment (Hirase et al., 2001). The incidence of sharp wave-associated ripples measured during the same slow-wave sleep periods (Figure 1D) was also not significantly different before and after LTP ($p > 0.5$; sign test).

*Correspondence: buzsaki@axon.rutgers.edu
[1]Present address: Picower Center for Learning and Memory, 77 Massachusetts Avenue, MIT, Cambridge, Massachusetts 02139.

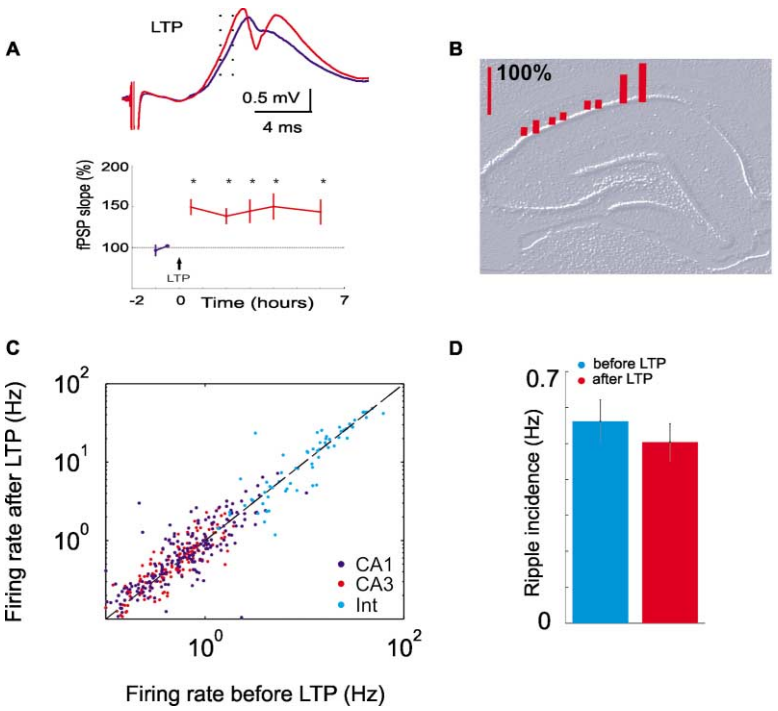

Figure 1. LTP Does Not Change the Global Spontaneous Excitability of the Hippocampal Network

(A) Example of average evoked potentials (n = 10) in CA1 pyramidal layer in response to VHC stimulation before (blue) and 90 min after (red) induction of LTP. Field postsynaptic potential (fPSP) slopes were calculated between the dotted lines. Note potentiation of EPSP slope and population spike after LTP. Below, LTP-induced slope changes at various intervals after the tetanus (n = 18 sessions in 7 rats). Averages were taken at the beginning of sleep episodes in the home cage. *$p < 0.05$, rank-sum test.

(B) Location dependence of LTP magnitude. Bar sizes reflect relative change in EPSP slopes in a single rat.

(C) Correlations between firing rate before and after LTP during sleep in the home cage. Each point corresponds to the mean firing rate of a single neuron. CA1, CA1 pyramidal cells; CA3, CA3 pyramidal cells; Int, interneurons in CA1 and CA3. Note that the grand mean firing rate of all populations is not affected by LTP.

(D) The incidence of sharp wave/ripple episodes during sleep was not affected by LTP. Ripples were detected in sleep sessions before and after (<1 hr) LTP induction.

Although LTP did not affect the global firing rate, it exerted a profound effect on the behavior-related firing patterns of place cells. The animals were tested on an elevated platform while searching for food. Place-correlated firing of parallel-recorded, multiple single neurons was determined in four test sessions. The position of the rat, local EEG, and the spiking pattern and stability of unit activity were continuously monitored throughout the experiment (Figure 2). Between the test sessions, the rats were placed back in their home cage and allowed to sleep. Evoked responses were tested at the beginning of sleep periods (10–20 pulses at 0.1 Hz; low-frequency stimulation, LFS) following the first and third test sessions. These control sessions served to assess the effects of handling, environment change (McNaughton et al., 1996), and brain stimulation on place cell activity. Between the second and third sessions, LTP was induced in the home cage (see Experimental Procedures). Since place cell activity depends on the direction of movement on linear track apparatus (McNaughton et al., 1983), clockwise and counterclockwise runs were examined separately. The effect of LTP on three representative CA1 place cells, recorded from the same tetrode, is illustrated in Figure 3. The neuron, shown in Figure 3A, had a similar place field during both directions of movement before LTP. Following the LTP-inducing trains, the neuron acquired a new place field during counterclockwise laps but remained unchanged during clockwise runs both in terms of place-related firing and "in-field" firing rate. Thus, disregarding the direction of movement, the neuron possessed two place fields after LTP, perhaps reflecting two different sets of functional inputs (Figure 3F). The second neuron was not affected by LTP and showed stable place field-related discharge in all sessions (Figure 3B). The third neuron had a well-developed place field only in the counterclockwise direction prior to LTP. After LTP, new place fields were present in both directions (Figure 3C). Importantly, 5.5 hr after LTP induction, when the slope of the evoked field response returned to pre-LTP level in this rat (Figure 3D), the neuron reinstated its direction-specific place field at the original position on the track (Figure 3E). This observation suggests that cell firing was controlled by the strongest synaptic input from a set of multiple existing synaptic pathways. Upon weakening of the potentiated set of input, control was resumed by the original set.

To allow for the simultaneous comparison of multiple neurons, the smoothed firing rates were plotted as a function of rat's position on the "linearized" track (see Experimental Procedures). In the example shown in Figure 4, the LTP-inducing train resulted in a larger potentiation of the evoked response at site A, including the emergence of a population spike, than at site B. Under tetrode A, cell #1 was "silent" before LTP. Following LTP, it acquired a robust place field when the animal ran counterclockwise (Figure 4B) but not clockwise (Figure 4A). Cell #4 lost its place field in clockwise direction after LTP (Figure 4A), but retained it while running counterclockwise (Figure 4B). Cell #3 shifted its place field for both directions of movement. Cell #2 reduced its in-field firing rate (clockwise, Figure 4A), whereas LTP had no significant effect on the remaining two place cells. The five neurons recorded with tetrode B (Figures 4C and 4D) showed only nonsignificant changes, comparable in magnitude to those observed after LFS or when a single session was split into two subsessions. These observations indicate that some neurons localized in the volume monitored by a single tetrode can be selectively affected by LTP, leaving their peers unaffected. The

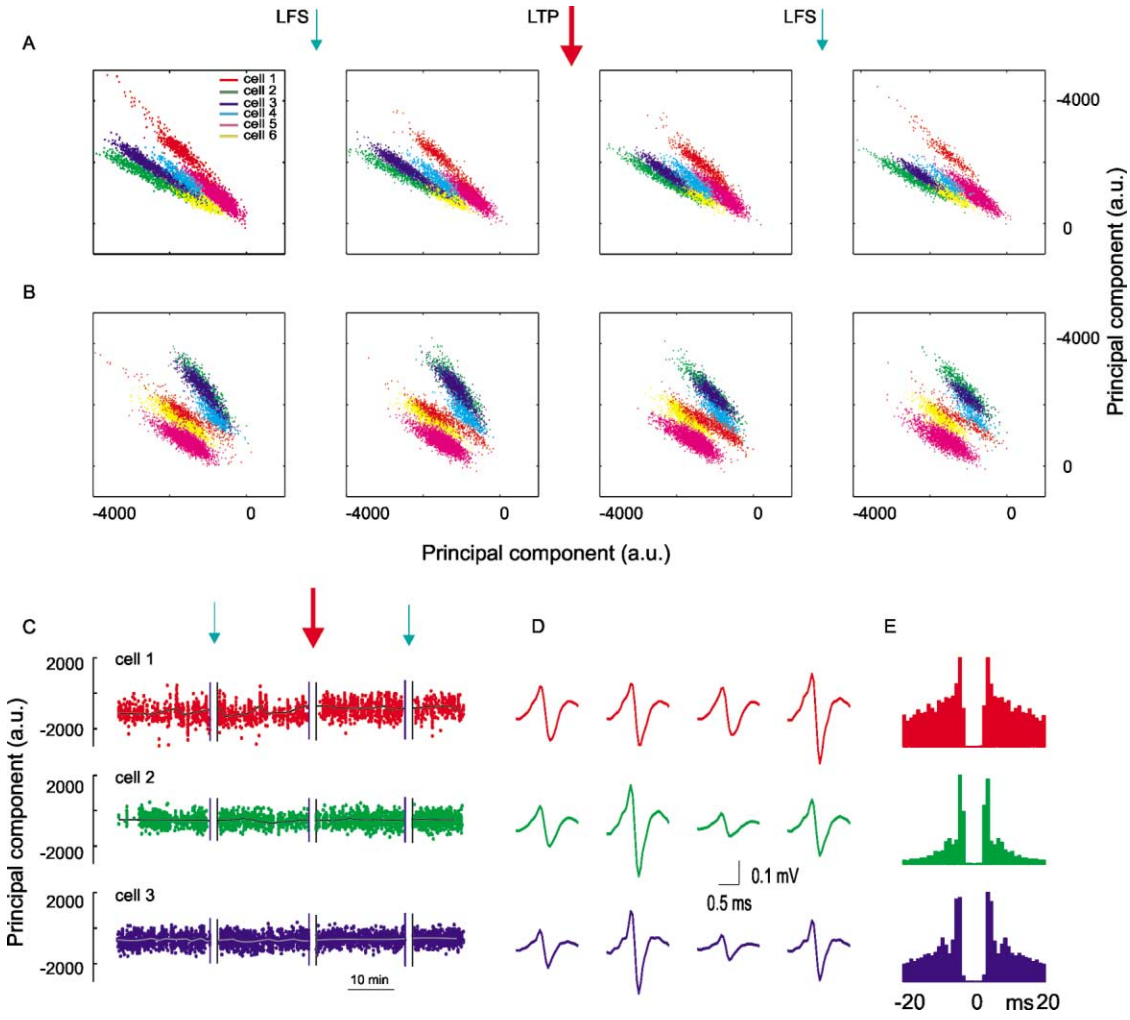

Figure 2. Stability of the Recorded Units in the Course of the Experiment

(A and B) Clusters of six CA1 pyramidal cells from a single tetrode (color-coded). Clustering was done using waveforms from all four tetrode sites. Only two projections (A and B) are shown separately for the four run sessions. *x* and *y* coordinates show the first principal components (arbitrary units; a.u.). Arrows: LFS, low-frequency stimulation; LTP, tetanic stimulation.

(C) First principal component for 3 place units (also shown in A and B and Figure 3) as a function of time. Black lines are medians of the smoothed distribution of the principal component in time. Vertical lines separate the four exploration sessions.

(D) Waveform of the three units (800 Hz–5 kHz) at each site of the tetrode.

(E) Autocorrelograms of the three units for the total duration of recording (exploration and sleep). Note peaks at 3–5 ms (complex spike bursts) and clear refractory periods.

findings also indicate that the LTP-induced effects on individual neurons cannot be accounted for by electrode drift or unit clustering errors.

To assess the effect of LTP at the population level, the difference between place field maps of CA1 and CA3 pyramidal cells before and after LTP was compared with the difference between maps computed during the first and second run sessions (LFS control). For each cell and each type of stimulation, the two place maps (one before and one after LFS or LTP) were pixel-by-pixel subtracted and the absolute values of all the pixel differences were added (see Experimental Procedures). For the place cell population, the place map differences produced by LFS were compared with those produced by LTP. LTP produced a significant change (firing rate and/or place shift) in place representation compared to the control LFS (Figure 5A; $n = 146$ CA1 and CA3 pyramidal cells; $p < 0.001$, sign test). To distinguish between shifts in place field position and in-field firing rate changes, place maps were first normalized by dividing the rate map by the sum of firing rate calculated in each pixel of the place map and the same differences were calculated and compared. Changes reflected in both nonnormalized and normalized place field maps were further interpreted as changes in place field location, whereas changes in only nonnormalized maps were considered to be rate changes within the same field. At the population level, LTP produced a significant shift in place representation compared to control LFS ($p < 0.05$, sign test). Using an arbitrary criterion (LTP-induced change at least twice as large as LFS-induced change, red dots in Figure 5A), 52 CA1 and CA3 place cells (35%

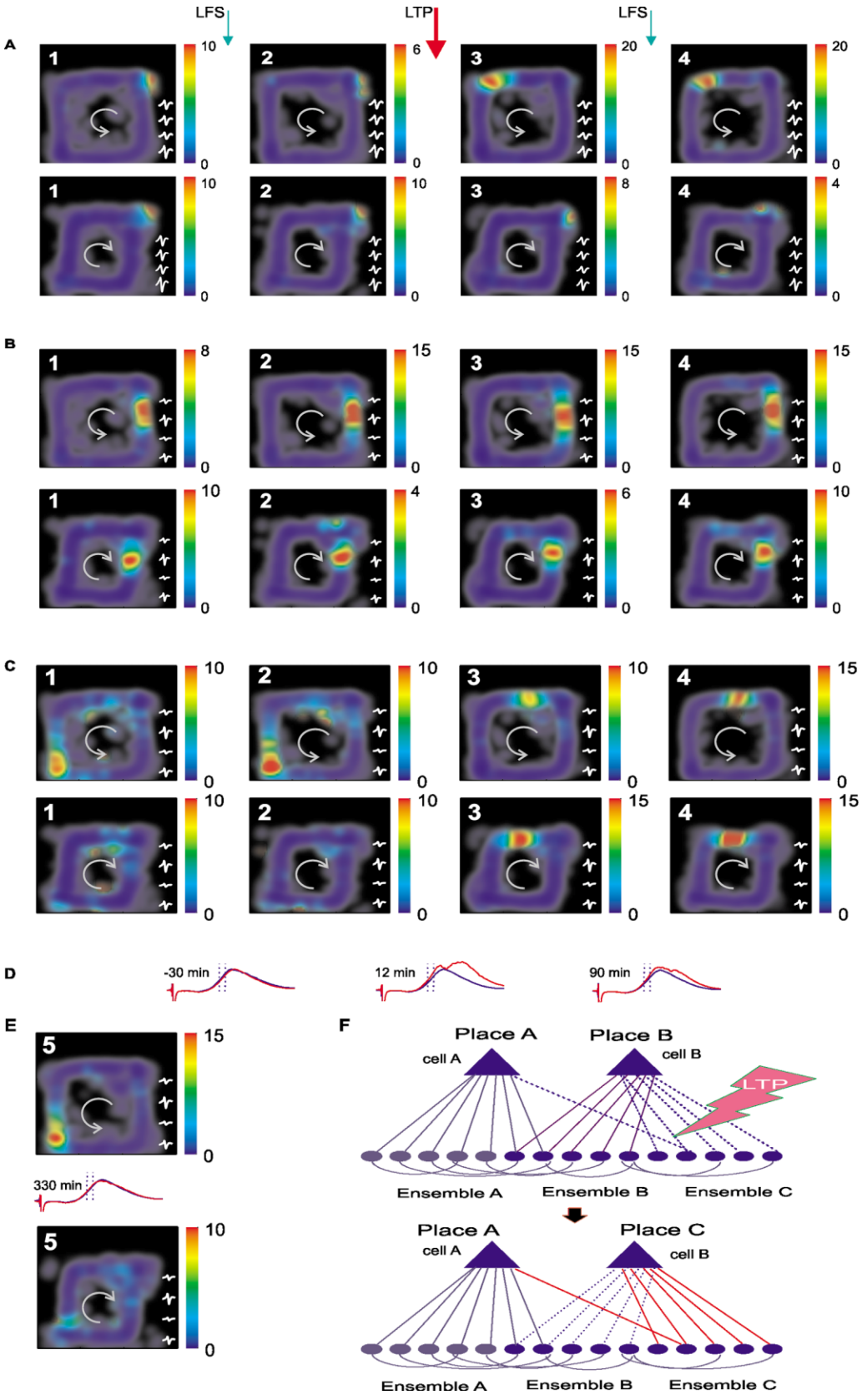

Figure 3. LTP-Induced Effects on Place Correlates of Neighboring Neurons

(A–C) Clusters of the three units are shown in Figure 2.

(A) Example place cell with unidirectional change of place field after LTP. Each map represents 10–20 min of counterclockwise or clockwise

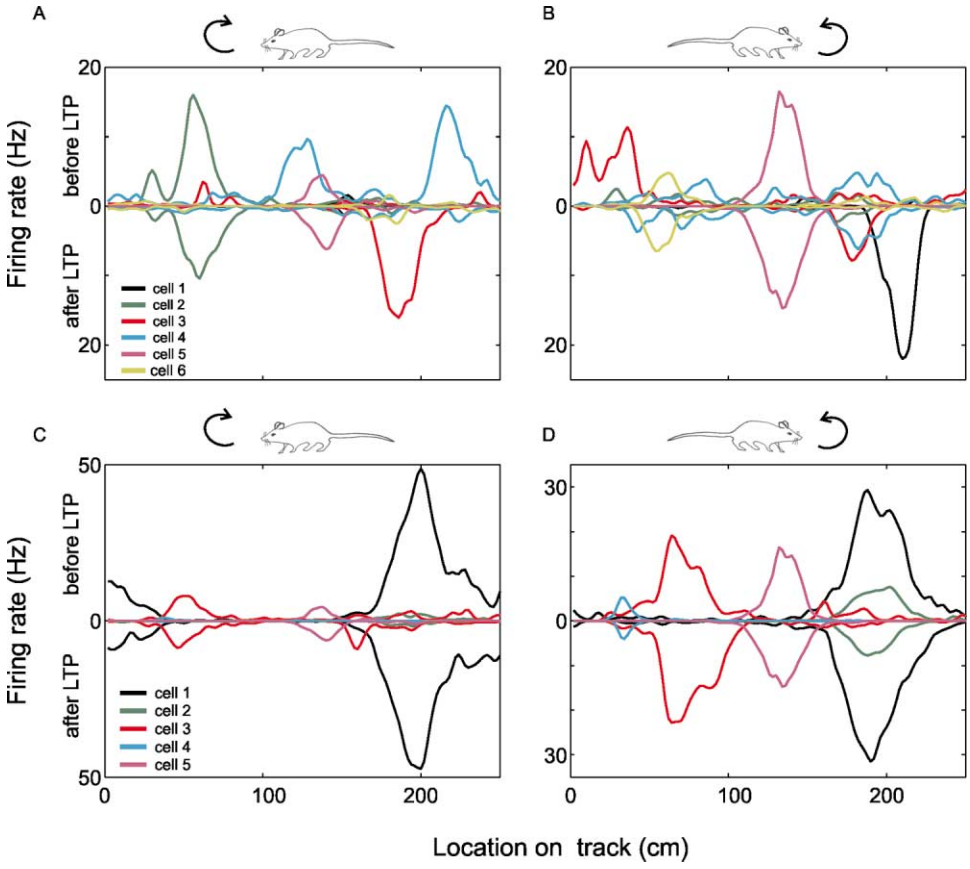

Figure 4. LTP-Induced Effects on the Place Correlates of Pyramidal Neurons

Units recorded simultaneously from two tetrodes are shown.

(A and B) The paths on the rectangular tracks were linearized. 0–250 cm represents a full turn. Smoothed firing rates before and after LTP (run sessions 2 and 3) as a function of the rat's position are shown separately for both directions; (A) is clockwise, (B) is counterclockwise. Novel place fields emerged for cell #1 and cell #3 (for counterclockwise and both directions, respectively). Cell #4 lost its double place field in clockwise direction. Cell #2 reduced its in-field firing rate, whereas no effect was observed on cells #5 and #6.

(C and D) The place fields of the five neurons simultaneously recorded by another tetrode were retained after LTP when the animal moved clockwise (C) or counterclockwise (D).

of the pyramidal cell population) were affected by LTP for at least one direction of movement. Approximately half of the affected cells shifted their place fields as well (39.4 $\pm$ 7.78 cm change after LTP versus 13.1 $\pm$ 4.97 cm after LFS; Figure 5A, inset). The majority of the affected cells showed unidirectional place field changes (changes expressed during either clockwise or counterclockwise movement), with only a minority displaying changes while moving in both directions (Figure 5A, inset). This latter finding suggests that in different contexts (e.g., direction of movement) the same cell is under the control of different sets of synaptic inputs that can be affected selectively.

To gain insight into the nature of the effect LTP exerted on the population representation of the environment, we examined the LTP effect on the distances (travelled by the rat) between initially overlapping place fields for pairs of neurons (fields with $<$30 cm distance, see be-

runs (gray arrows). Between run sessions the rat was placed back to the home cage. Arrows, LFS, low-frequency stimulation; LTP, tetanic stimulation. Color code: frequency of unit discharge (Hz). Note the difference in the colorbar scales across sessions. Blue, places visited but no spike present. Insets: average waveforms of the unit on each wire of the tetrode. Compare place fields before (1 and 2) and after (3 and 4) LTP. Note emergence of a new place field during counterclockwise runs and preservation of the pre-LTP field during clockwise runs. Note also the presence of some activity in the new place field prior to LTP (upper left corner, session 2).

(B) Example cell with no significant change in place representation after LTP. Same arrangement as in (A).

(C) Another example neuron with place field change in both directions after LTP.

(D) Average evoked potentials recorded before sessions 2, 3, and 4, superimposed on baseline recording (blue trace). Time is relative to the induction of LTP.

(E) Recovery of the original place field of cell 3 after 5.5 hr after LTP and the associated evoked field response.

(F) Schematic of hypothesized synaptic changes after LTP. Synaptic weight increases between input ensembles, representing distinct places, and target neurons are suggested to be responsible for the altered place representation. Competition of these inputs determines the place field characteristics of the pyramidal cells.

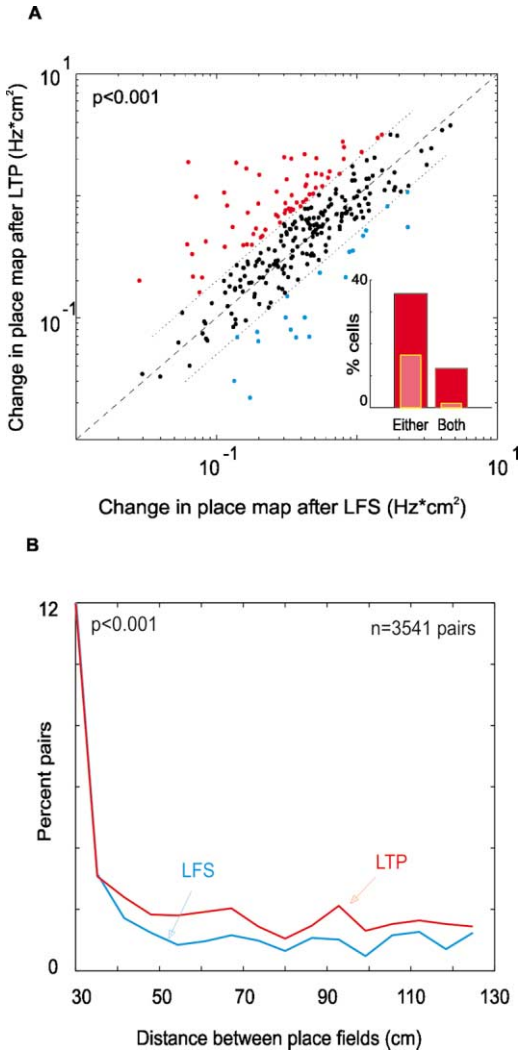

Figure 5. LTP Alters Place Field Properties

(A) Changes in place fields are significantly larger after LTP than after control LFS. Each dot corresponds to a place cell for one direction of movement. Red (blue) dots, cells for which LTP (LFS) produced a change in place map twice bigger than LFS (LTP) as marked by the corresponding dotted line. Inset: percentage of place cells that changed at least twice as much after LTP than after LFS. Red columns, in-field rate change or location change; pink columns, location change alone. Either, change in either clockwise or counterclockwise direction; Both, changes in both directions of movement. (B) LTP alters spatial relationship between neuron pairs. Histograms of distances between place field centers of pairs of neurons after stimulation. All neuron pairs included had <30 cm overlap during the respective baseline session. LTP induced shifts in a significantly larger proportion of pairs than did LFS.

low). Twenty percent of the neurons had more than one place field. For comparing distances between place fields of neuron pairs, only the field with the strongest firing rate was considered. Thirty percent of the overlapping pairs were dissociated after LTP and new pairs were formed. Spatial dissociation occurred in a significantly larger percentage of neuron pairs after LTP compared to LFS (Figure 5B; $p < 0.001$, Z-test for the equality of two proportions). This finding indicates that LTP affected not only the activity of individual cells, but also their functional connections within the network.

The change in spatial interaction by LTP occurred without a significant change in the global firing rate of the neuronal population during exploration (Figures 6A and 6B). The preservation of the grand mean rate was due to a balanced increase and decrease in firing rates of the LTP-affected neurons (Figures 6A and 6B). Moreover, the firing pattern of pyramidal cells (incidence of burst events, ratio of the number of spikes in burst versus tonic firing, number of spikes in a burst event) did not change after LTP ($p > 0.05$, paired t test). Comparison of the place field shape (mean ± SE skewness: before, 0.005 ± 0.047; after, 0.049 ± 0.049, Figure 6D) and size (mean ± SE integrated place field size: before, 156.24 ± 12.04 Hz·cm; after, 151.65 ± 12.65 Hz·cm, Figure 6E; place field width: before, 34.2 ± 1.7 cm; after, 30.5 ± 1.4 cm, Figure 6F) for all place cells active both before and after the tetanic stimulation revealed they were not significantly affected by LTP (for all comparisons, $p > 0.05$, paired t test and Kolmogorov-Smirnov test). Neither the time spent in each pixel of the track nor the power of theta during exploration (Figure 6C) was significantly different before and after LTP ($p > 0.5$, sign test). Thus, LTP induced remapping without affecting the properties of place coding.

The differential impact of LTP on single cells was assessed by comparing the magnitude of the location-specific evoked field response (Figure 1B) and the magnitude of place field changes. The site-dependent variability in the amount of potentiation within the same experimental session (Figure 1B) suggested that sites displaying larger potentiation received a stronger convergent input from the bulk of axons affected by the tetanic stimulation or were more susceptible to plastic changes. Stronger LTP is expected to exert a larger effect on place cell activity than weak LTP, as suggested by the representative example in Figure 4. At the population level, neurons recorded from sites with larger enhancement of the locally recorded evoked responses were significantly more strongly affected than those from sites with smaller changes of the field response (Figure 7A; $r = 0.41$; $p < 0.001$). Thus, in response to the same tetanus, place cells located at sites with stronger LTP displayed larger changes in their place fields than neurons recorded from less potentiated, control areas. This observation also supports the interpretation that an LTP-related process, rather than some undetected behavioral changes, was responsible for biasing place cell activity.

If the strength of synaptic inputs onto a cell is reflected by the in-field firing rate of the neuron, then strong synapses (and high firing rate cells) are expected to be more resistant to LTP than weak synapses (low firing cells). In line with this hypothesis, we found a significant negative correlation between maximal in-field discharge rate before LTP and the magnitude of place field shift (Figure 7B; $r = -0.54$, $p < 0.001$; rank correlation). To demonstrate that this relationship is not simply due to the larger discharge variability of slow firing neurons, we used the bootstrap resampling method to compare correlation coefficients obtained between sessions 2 and 3 (LTP change) and sessions 1 and 2 (LFS control variability) for the same population of place cells. The consistently larger correlation coefficients associated with LTP (Figure 7B, inset, $p < 0.001$, Kolmogorov-Smirnov test) indicate that LTP induced a differentially larger

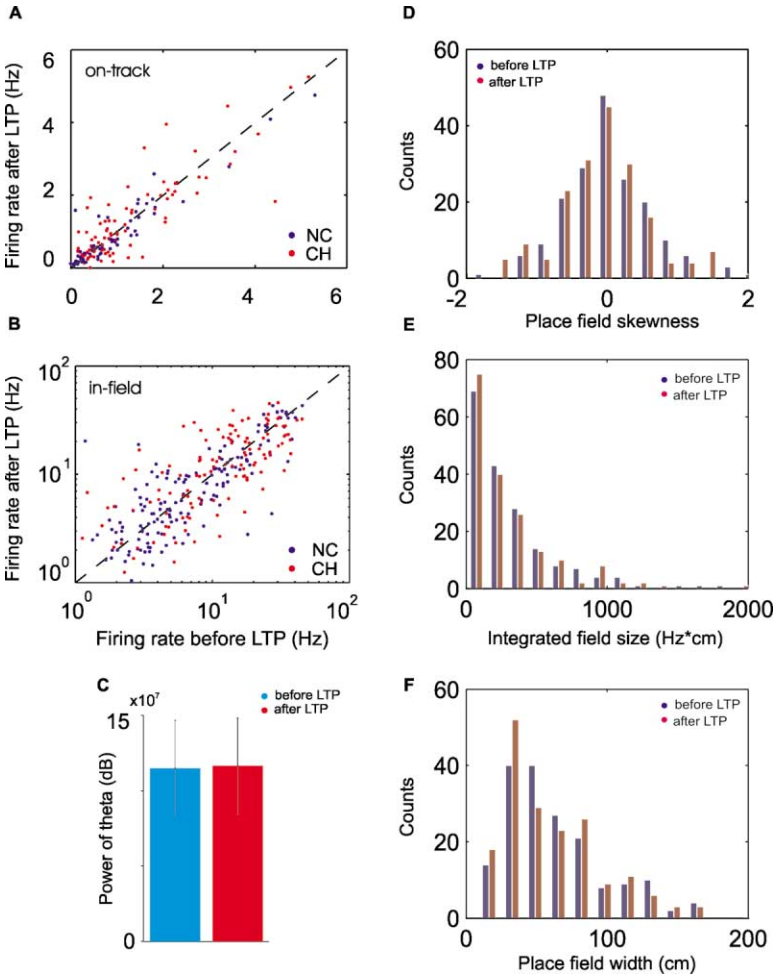

Figure 6. Preservation of the Place-Coding Properties after LTP

(A and B) Firing rate correlations before (session 2) and after (session 3) LTP during exploration for mean firing rates during the whole session on the track (A) and in-field peak firing rates (B) and for all place cells. Each dot corresponds to the mean firing rate of a single neuron. Blue dots code for neurons with no change (NC) and red dots for neurons that changed (CH) their in-field firing rate and/or location after LTP. Note that the grand mean firing rate of all populations is not affected by LTP. Note also cases when previously inactive neurons become active after LTP and vice versa.

(C) Power of theta during exploration was not changed after LTP.

(D–F) Similar distribution of place field skewness (D), integrated place field size (E), and place field width (F) before (blue bars) and after (red bars) LTP for all place cells that had a field both before and after LTP (each cell is represented for each direction of movement, i.e., twice).

change in slow firing place cells, compared to fast firing place cells, than expected on the basis of random variability. This finding indicates a competition between physiologically induced plastic changes and tetanic stimulation-induced synaptic plasticity.

To address the effect of LTP on the temporal aspects of network activity, we examined crosscorrelations between neuron pairs. Multiple place neurons, representing overlapping parts of the environment, are sequentially activated in space and time as the animal traverses the environment (Wilson and McNaughton, 1993). This spatial representation is "compressed" into individual theta cycles in the time domain by coordinated phase-precession (Skaggs et al., 1996). While firing rate and spike timing of individual cells within the theta cycle code for spatial location (O'Keefe and Nadel, 1978; Skaggs et al., 1996), the theta cycle-related temporal correlation between neuron pairs reliably predicted the distances between field centers of the neurons (Figure 8C). LTP induced a rearrangement of the hippocampal "map" but did not affect the mechanism of the theta cycle compression of place fields (Figures 8C and 8D). When the place representation of a newly generated place cell overlapped with the place field of another neuron, this newly created spatial relationship was faithfully reflected by the short-time scale (theta cycle) correlation of the neuron pair (Figures 8A and 8B). Conversely, when neurons with spatially overlapping fields were dissociated by LTP, their theta-cycle correlations were also lost. Figures 8C and 8D show the relationship between direction-corrected distance between place fields and respective temporal correlation for multiple pairs of neurons (see Experimental Procedures). The highest density of points corresponds to theta cycles (three clouds of points on the *y* axis) and reflects ~30 cm spatial coverage (*x* axis). LTP destroyed the temporal relationship of 40% of the preexisting neuronal pairs and created a similar number of new pairs (Figures 8C and 8D, insets). Nevertheless, the overall structure of place versus theta cycle-related correlation was not altered by LTP (Figure 8D).

Discussion

It has been assumed that spatial and other types of memories are encoded in the synaptic weights of hippocampal networks (O'Keefe and Nadel, 1978; Wood et al., 1999) and that modification of synapses alter memory traces and spatial representations (Kentros et al., 1998; Moser et al., 1998; Nakazawa et al., 2002). At the experimental level, Hebbian pairing of afferents and postsynaptic activity of neurons, as modeled by long-term potentiation/depression paradigms, has been suggested to be the key mechanism underlying synaptic weight

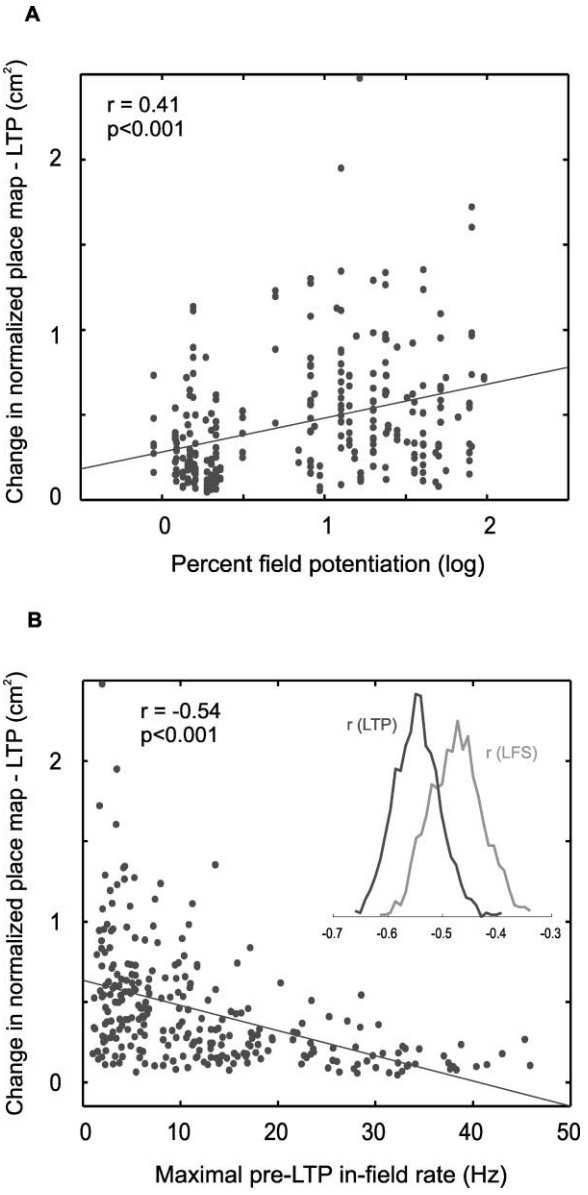

Figure 7. Synaptic Plasticity- and Firing Rate-Dependent Changes in Place Fields of Pyramidal Cells after LTP

(A) Correlation between absolute change in slope of field potentials after LTP and shift in place fields (change in normalized place maps) for neurons recorded with the same tetrode.

(B) Correlation between pre-LTP maximal in-field firing rate and magnitude of LTP-induced shifts in place fields. Inset: distributions of correlation coefficients, calculated from data points obtained after bootstrap resampling of the data in (B).

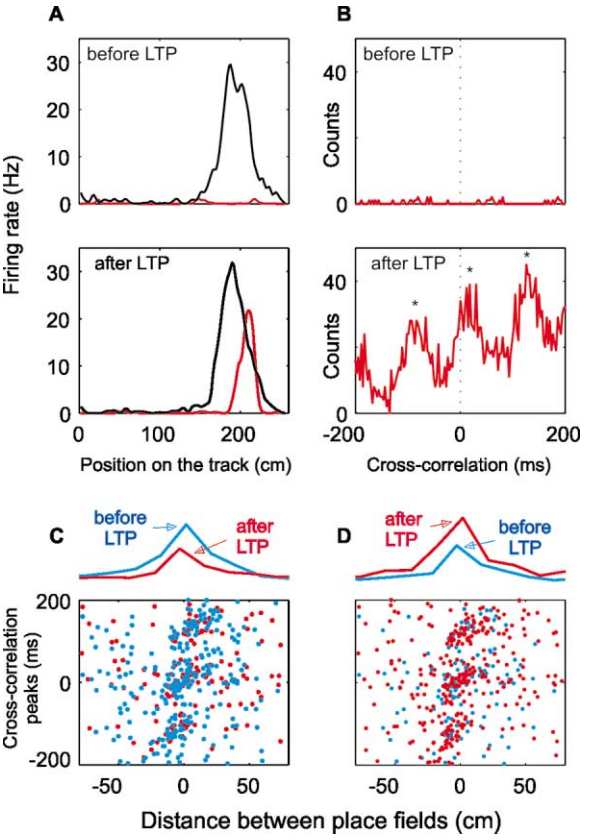

Figure 8. LTP Affects Representation of the Familiar Environment, but Does Not Alter Place Representation Rules

(A) Place fields for two simultaneously recorded units before and after LTP. Note emergence of a new place field (red), which overlaps with the unchanged place field (black).

(B) Crosscorrelation between the two neurons (reference, black neuron). Note theta frequency modulation of the crosscorrelogram after LTP (stars mark peaks).

(C) Relationship between spatial distance of place field peaks and temporal peaks of the crosscorrelograms (marked with stars for the pair in B) for all neuron pairs. Note high density of dots corresponding to three theta cycles and approximately 30 cm distance. The densities of dots are shown by the same color line histograms above, separately for before (blue) and after (red) LTP. Red dots, subgroup of pairs unchanged by LTP.

(D) Same layout as in (C) for pairs after LTP. Red, significant pairs after LTP; blue, subset of the post-LTP group that had significant correlations before LTP as well (no-change pairs).

changes (Levy and Steward, 1979; Markram et al., 1997; Magee and Johnston, 1997). Our findings provide a link between these two lines of research. Induction of long-term changes of VHC-evoked responses was associated with a "remapping" of the hippocampal representation of the environment, including creation of new place cells and abolishment of preexisting place fields, supporting the view that place features of pyramidal cells emerge within hippocampal circuits (McNaughton et al., 1996; Lever et al., 2002). LTP-induced effects were context dependent since place fields associated with one direction of movement were often selectively modified without affecting the neuron's place representation when moving in the opposite direction. These observations indicate that single neurons may be part of several representations (O'Keefe and Nadel, 1978; Markus et al., 1995; Wood et al., 1999, 2000) and inputs from these representations can be modified selectively. The same neuron can thus be part of different neuronal ensembles that may be activated by different combinations of inputs.

The changes in place field representation occurred without affecting (1) the theta cycle compression of distances between place fields, (2) the size and shape of place fields, (3) the power of theta, (4) the incidence of

sharp wave bursts, or (5) the global firing rate of the network. These findings suggest that LTP led to rearrangement of place representation in the hippocampus without altering the encoding "rules" of the network.

Because electrical stimulation might activate subcortical neurons connected with the hippocampus, one could argue that such indirect effects were responsible for the altered place representation after LTP. However, the demonstration of a reliable relationship between the magnitude of place field changes and the magnitude of change in the evoked field responses, as induced by LTP, supports the interpretation that an LTP-related process, rather than some nonspecific changes, was responsible for biasing place field activity. In addition, most units were selectively affected only during a given direction of movement, and units with large place field changes and units with nonsignificant changes could be recorded by the same tetrode. These observations also eliminate the possibility that changes due to discrete electrode drift in the brain were responsible for our findings.

The preservation of global firing rates after the LTP train is surprising since increase in the excitability of the affected pathways by LTP is expected to increase the firing rates of the target cells. Nevertheless, no changes were observed at the population level either in the sleeping animal or in the behaving animal engaged in the foraging task, even when only the subpopulation of changed cells was considered. One potential explanation of these findings is that the LTP-potentiated synapses at sites with the strongest convergence of the stimulated afferents were compensated for by a decrease in synaptic weights elsewhere (Lynch et al., 1977; Royer and Pare, 2003). Alternatively, the potentiated neurons could decrease the firing rate of the surrounding neurons by interneuron-mediated recurrent inhibition. A third possibility is that intrinsic mechanisms compensated the altered magnitude of afferent inputs, although such "rescaling" mechanisms operate on a significantly longer time scale (Turrigiano et al., 1998) than observed here. Importantly, similar preservation of global firing rates with altered individual firing patterns were observed in rats exposed to a new environment (Hirase et al., 2001), indicating that similar processes may underlie both LTP- and novel environment-related remapping. Altogether, the findings suggest that an LTP-like mechanism has the potential for abolishing and creating new functional connections in behavioral learning.

An implicit interpretation of the present findings is that arbitrary alteration of synaptic connectivity within the hippocampus should affect spatial memory. If all synaptic connections were rearranged by artificial means, such as LTP, the hippocampal representation of the same environment is expected to be entirely different. Behavioral experiments testing this hypothesis have produced conflicting results. Repeated hippocampal LTP, in an attempt to "saturate" all excitatory synapses, failed to affect spatial memory in most cases (Castro et al., 1989; Korol et al., 1993; Cain et al., 1993; McNamara et al., 1993; Jeffery and Morris, 1993). However, in those experiments the same pathways were tetanized repeatedly. It is therefore possible that only a subset of afferents and synapses were affected, leaving a large portion of the hippocampal network unaltered (Barnes et al., 1994), as was also the case in our present experiments. An explicit prediction of our observations is that if the majority of hippocampal synapses are affected, this should be associated with compromised spatial performance. Indeed, when LTP was induced in a large proportion of hippocampal afferents by several closely spaced stimulation electrodes, spatial memory in a water-maze task was impaired (Moser et al., 1998; Brun et al., 2001).

Experimental Procedures

Surgery, Recording, Stimulation, and Behavior

Seven adult male Sprague-Dawley rats (300–450 g) were implanted with eight independently movable tetrodes (3–4 mm posterior to bregma and 1.5–3.5 mm from the midline) and equipped with a single LED for position tracking (at 40 Hz with 0.8 cm spatial resolution) following NIH guidelines. Bipolar stimulating electrodes were placed in the contralateral ventral hippocampal commissure (VHC). While all seven rats were recorded during sleep, four rats were trained to run on an elevated rectangle-shaped linear track (8.5 cm wide, 70 $\times$ 60 cm sides, 30 cm above the ground) located inside a wooden box with 60 cm high walls. The rats ran clockwise or counterclockwise to retrieve bits of chocolate wafers from two fixed opposite corners. During recording sessions, the rats were placed on the track for approximately 20 min and then returned to the home cage for rest. Rest-sleep in the home cage and 20 min run sessions on the linear track were alternated several times. At the beginning of a sleep episode in the home cage, evoked responses were elicited by low-frequency stimulation (LFS) pulses (0.1 ms) delivered at 0.1 Hz (10 to 20 pulses) to VHC after the first, third, and fourth run sessions. LTP was induced by two 200 Hz trains of 10 pulses, separated by 2 s, after the second run session, and also in the home cage during sleep. Tetanic stimulation intensities were adjusted individually to evoke 25%–50% of the maximum population spike amplitude in the CA1 pyramidal layer before LTP (range, 100–200 μA). The VHC arises from CA3 pyramidal neurons. The axons travel in the ventral portion of the fimbria-fornix, and the fibers from left and right hippocampi are mixed. Thus, stimulation directly and orthodromically activates the contralateral CA3 and CA1 regions by discharging fibers of passage from the ipsilateral CA3. In addition, the stimulation backfires the contralateral CA3, whose collaterals now indirectly but also orthodromically activate CA1 (and CA3 by the recurrent collaterals). Independent of the stimulation site, there is a mixture of direct and indirect activation of the contralateral CA3 and CA1 areas (Buzsaki and Eidelberg, 1982). The effect of LTP on place cell firing was compared with that of LFS applied after the first run session. After the recording sessions, the electrodes were moved to isolate new sets of cells and a few days later a new session was recorded. After the completion of the experiments, the brains were perfused, fixed, sectioned, and stained with cresyl violet to identify all stimulation and recording electrode tracks.

Data Analysis

For the assessment of LTP, the middle 1–1.5 ms of the EPSP slope (between field onset and population spike onset) was determined before and after the tetanic trains at each recording location (Figures 1A and 1B). Single hippocampal pyramidal cells and interneurons were identified and isolated using a semiautomatic cluster cutting method (Wilson and McNaughton, 1993; Csicsvari et al., 1999; Harris et al., 2000). Stability of the neuron was assessed by spike wave shape changes: the principal component values of the spike were plotted against time for the entire recording period. In addition, the stability of two-dimensional projections of the unit clusters was examined by comparing the position of unit clusters corresponding to each session (Figure 2). Units with large progressive shifts or sudden changes were excluded from the analyses. With these criteria, 3 to 6 single units were obtained per tetrode. Action potentials associated with immobility and sharp-wave/ripple epochs on the track were excluded from the analysis. A total of 464 CA1 and CA3 units in seven rats met the stability criteria. Of these, 332 were recorded in the four rats tested in the spatial task. Of the 332 units, 146 pyramidal cells had place fields prior to the induction of LTP.

Burst events were composed by spikes with no more than 6 ms interspike interval (Harris et al., 2001). Place fields were computed by a smoothing-based method (Harris et al., 2001), where the estimated firing rate at a point $\mathbf{x}$ was computed as:

$$f(\mathbf{x}) = \frac{1}{\Delta t} \frac{\sum_t n_t w(|\mathbf{x} - \mathbf{x}_t|)}{\sum_t w(|\mathbf{x} - \mathbf{x}_t|)}.$$

Here, n_t is the number of spikes fired in a given time bin, $\mathbf{x}_t$ is the two-dimensional position of the rat in that time bin, and Δt is the time bin size. The smoothing function $w(d) = \exp(-d^2/2\lambda^2)$ is a Gaussian with a width parameter $\lambda = 5$ cm. The similarity of two place fields $f_1(\mathbf{x})$ and $f_2(\mathbf{x})$ was assessed by the L_1 distance between place maps, weighted by the geometric mean occupancy probability across the two sessions $\int\int |f_1(\mathbf{x}) - f_2(\mathbf{x})| \sqrt{p_1(\mathbf{x}) p_2(\mathbf{x})} d^2\mathbf{x}$. The weighting term ensured that the results were not biased by areas the rat visited infrequently, where rate calculation is inaccurate. In order to compare the spatial distribution of neuronal firing independent of overall changes in firing rate, normalized place fields were computed as $f'(\mathbf{x}) = f(\mathbf{x}) / \int\int f(\mathbf{x}) d^2\mathbf{x}$, and again compared with the same metric.

Place fields were defined as areas with localized increase in firing rate above 1 Hz for at least 10 contiguous pixels (20 cm). After "linearization" of the squared track into one dimension, place field borders were defined as the points where the firing rate became less than 10% of the peak firing rate for at least 10 cm. The width of the place field was defined as the distance (in cm) between the two borders of the place field. In neurons with multiple place fields, only the field corresponding to the maximum firing rate was considered for further analysis. The summed instantaneous firing rate between the borders of each place field (Hz·cm) represented the integrated place field size. The shape of the place field was evaluated by calculating its skewness (the ratio between the third moment of the place field rate distribution and the cube of the standard deviation [Mehta et al., 2000]). Crosscorrelations between neurons pairs were calculated in a 400 ms window, with 3 ms bin size. Crosscorrelograms with <0.8 count/ms were discarded. Several peaks were detected in each crosscorrelogram (marked with stars on Figure 8B). In case two or more peaks were detected in a 50 ms window, only the largest value was included in the analysis. Distances between place fields of two neurons were determined by calculating the distance travelled by the rat between the pixels with the peak firing rates of the respective place fields (Figure 8A).

Acknowledgments

We thank A. Sirota for technical help and E. Moser and D. Paré for comments on an earlier version of the manuscript. Supported by grants from NIH.

Received: April 10, 2003
Revised: June 9, 2003
Accepted: July 11, 2003
Published: August 27, 2003

References

Barnes, C.A., Jung, M.W., McNaughton, B.L., Korol, D.L., Andreasson, K., and Worley, P.F. (1994). LTP saturation and spatial learning disruption: effects of task variables and saturation levels. J. Neurosci. *14*, 5793–5806.

Bliss, T.V., and Collingridge, G.L. (1993). A synaptic model of memory: long-term potentiation in the hippocampus. Nature *361*, 31–39.

Bliss, T.V., and Lomo, T. (1973). Long-lasting potentiation of synaptic transmission in the dentate area of the anaesthetized rabbit following stimulation of the perforant path. J. Physiol. *232*, 331–356.

Brun, V.H., Ytterbo, K., Morris, R.G., Moser, M.B., and Moser, E.I. (2001). Retrograde amnesia for spatial memory induced by NMDA receptor-mediated long-term potentiation. J. Neurosci. *21*, 356–362.

Buzsaki, G., and Eidelberg, E. (1982). Convergence of associational and commissural pathways on CA1 pyramidal cells of the rat hippocampus. Brain Res. *237*, 283–295.

Cain, D.P., Hargreaves, E.L., Boon, F., and Dennison, Z. (1993). An examination of the relations between hippocampal long-term potentiation, kindling, afterdischarge, and place learning in the water maze. Hippocampus *3*, 153–163.

Castro, C.A., Silbert, L.H., McNaughton, B.L., and Barnes, C.A. (1989). Recovery of spatial learning deficits after decay of electrically induced synaptic enhancement in the hippocampus. Nature *342*, 545–548.

Chavez-Noriega, L.E., Halliwell, J.V., and Bliss, T.V. (1990). A decrease in firing threshold observed after induction of the EPSP-spike (E-S) component of long-term potentiation in rat hippocampal slices. Exp. Brain Res. *79*, 633–641.

Csicsvari, J., Hirase, H., Czurko, A., Mamiya, A., and Buzsaki, G. (1999). Oscillatory coupling of hippocampal pyramidal cells and interneurons in the behaving rat. J. Neurosci. *19*, 274–287.

Deadwyler, S.A., Gribkoff, V., Cotman, C., and Lynch, G. (1976). Long-lasting changes in the spontaneous activity of hippocampal neurons following stimulation of the entorhinal cortex. Brain Res. Bull. *1*, 1–7.

Fregnac, Y., Shulz, D., Thorpe, S., and Bienenstock, E. (1988). A cellular analogue of visual cortical plasticity. Nature *333*, 367–370.

Harris, K.D., Henze, D.A., Csicsvari, J., Hirase, H., and Buzsaki, G. (2000). Accuracy of tetrode spike separation as determined by simultaneous intracellular and extracellular measurements. J. Neurophysiol. *84*, 401–414.

Harris, K.D., Hirase, H., Leinekugel, X., Henze, D.A., and Buzsaki, G. (2001). Temporal interaction between single spikes and complex spike bursts in hippocampal pyramidal cells. Neuron *32*, 141–149.

Hirase, H., Leinekugel, X., Czurko, A., Csicsvari, J., and Buzsaki, G. (2001). Firing rates of hippocampal neurons are preserved during subsequent sleep episodes and modified by novel awake experience. Proc. Natl. Acad. Sci. USA *98*, 9386–9390.

Jeffery, K.J., and Morris, R.G. (1993). Cumulative long-term potentiation in the rat dentate gyrus correlates with, but does not modify, performance in the water maze. Hippocampus *3*, 133–140.

Kandel, E.R., and Squire, L.R. (2000). Neuroscience: breaking down scientific barriers to the study of brain and mind. Science *290*, 1113–1120.

Kentros, C., Hargreaves, E., Hawkins, R.D., Kandel, E.R., Shapiro, M., and Muller, R.V. (1998). Abolition of long-term stability of new hippocampal place cell maps by NMDA receptor blockade. Science *280*, 2121–2126.

Kimura, A., and Pavlides, C. (2000). Long-term potentiation/depotentiation are accompanied by complex changes in spontaneous unit activity in the hippocampus. J. Neurophysiol. *84*, 1894–1906.

Korol, D.L., Abel, T.W., Church, L.T., Barnes, C.A., and McNaughton, B.L. (1993). Hippocampal synaptic enhancement and spatial learning in the Morris swim task. Hippocampus *3*, 127–132.

Lever, C., Wills, T., Cacucci, F., Burgess, N., and O'Keefe, J. (2002). Long-term plasticity in hippocampal place-cell representation of environmental geometry. Nature *416*, 90–94.

Levy, W.B., and Steward, O. (1979). Synapses as associative memory elements in the hippocampal formation. Brain Res. *175*, 233–245.

Lynch, G.S., Dunwiddie, T., and Gribkoff, V. (1977). Heterosynaptic depression: a postsynaptic correlate of long-term potentiation. Nature *266*, 737–739.

Magee, J.C., and Johnston, D. (1997). A synaptically controlled, associative signal for Hebbian plasticity in hippocampal neurons. Science *275*, 209–213.

Malenka, R.C., and Nicoll, R.A. (1999). Long-term potentiation—a decade of progress? Science *285*, 1870–1874.

Markram, H., Lubke, J., Frotscher, M., and Sakmann, B. (1997). Regulation of synaptic efficacy by coincidence of postsynaptic APs and EPSPs. Science *275*, 213–215.

Markus, E.J., Qin, Y.L., Leonard, B., Skaggs, W.E., McNaughton, B.L., and Barnes, C.A. (1995). Interactions between location and task affect the spatial and directional firing of hippocampal neurons. J. Neurosci. *15*, 7079–7094.

Martin, P.D., and Shapiro, M.L. (2000). Disparate effects of long-

term potentiation on evoked potentials and single CA1 neurons in the hippocampus of anesthetized rats. Hippocampus *10*, 207–212.

Martin, S.J., Grimwood, P.D., and Morris, R.G. (2000). Synaptic plasticity and memory: an evaluation of the hypothesis. Annu. Rev. Neurosci. *23*, 649–711.

McNamara, R.K., Kirkby, R.D., dePape, G.E., Skelton, R.W., and Corcoran, M.E. (1993). Differential effects of kindling and kindled seizures on place learning in the Morris water maze. Hippocampus *3*, 149–152.

McNaughton, B.L., Barnes, C.A., and O'Keefe, J. (1983). The contributions of position, direction, and velocity to single unit activity in the hippocampus of freely-moving rats. Exp. Brain Res. *52*, 41–49.

McNaughton, B.L., Barnes, C.A., Gerrard, J.L., Gothard, K., Jung, M.W., Knierim, J.J., Kudrimoti, H., Qin, Y., Skaggs, W.E., Suster, M., and Weaver, K.L. (1996). Deciphering the hippocampal polyglot: the hippocampus as a path integration system. J. Exp. Biol. *199*, 173–185.

Mehta, M.R., Quirk, M.C., and Wilson, M.A. (2000). Experience-dependent asymmetric shape of hippocampal receptive fields. Neuron *25*, 707–715.

Morris, R.G., Anderson, E., Lynch, G.S., and Baudry, M. (1986). Selective impairment of learning and blockade of long-term potentiation by an N-methyl-D-aspartate receptor antagonist, AP5. Nature *319*, 774–776.

Moser, E.I., Krobert, K.A., Moser, M.B., and Morris, R.G. (1998). Impaired spatial learning after saturation of long-term potentiation. Science *281*, 2038–2042.

Muller, R.U., Stead, M., and Pach, J. (1996). The hippocampus as a cognitive graph. J. Gen. Physiol. *107*, 663–694.

Nakazawa, K., Quirk, M.C., Chitwood, R.A., Watanabe, M., Yeckel, M.F., Sun, L.D., Kato, A., Carr, C.A., Johnston, D., Wilson, M.A., and Tonegawa, S. (2002). Requirement for hippocampal CA3 NMDA receptors in associative memory recall. Science *297*, 211–218.

O'Keefe, J., and Nadel, L. (1978). The Hippocampus as a Cognitive Map (Oxford: Oxford University Press).

Royer, S., and Pare, D. (2003). Conservation of total synaptic weight through balanced synaptic depression and potentiation. Nature *422*, 518–522.

Silva, A.J., Paylor, R., Wehner, J.M., and Tonegawa, S. (1992). Impaired spatial learning in alpha-calcium-calmodulin kinase II mutant mice. Science *257*, 206–211.

Skaggs, W.E., McNaughton, B.L., Wilson, M.A., and Barnes, C.A. (1996). Theta phase precession in hippocampal neuronal populations and the compression of temporal sequences. Hippocampus *6*, 149–172.

Taube, J.S., and Schwartzkroin, P.A. (1988). Mechanisms of long-term potentiation: EPSP/spike dissociation, intradendritic recordings, and glutamate sensitivity. J. Neurosci. *8*, 1632–1644.

Thompson, L.T., and Best, P.J. (1990). Long-term stability of the place-field activity of single units recorded from the dorsal hippocampus of freely behaving rats. Brain Res. *509*, 299–308.

Turrigiano, G.G., Leslie, K.R., Desai, N.S., Rutherford, L.C., and Nelson, S.B. (1998). Activity-dependent scaling of quantal amplitude in neocortical neurons. Nature *391*, 892–896.

Wilson, M.A., and McNaughton, B.L. (1993). Dynamics of the hippocampal ensemble code for space. Science *261*, 1055–1058.

Wood, E.R., Dudchenko, P.A., and Eichenbaum, H. (1999). The global record of memory in hippocampal neuronal activity. Nature *397*, 613–616.

Wood, E.R., Dudchenko, P.A., Robitsek, R.J., and Eichenbaum, H. (2000). Hippocampal neurons encode information about different types of memory episodes occurring in the same location. Neuron *27*, 623–633.